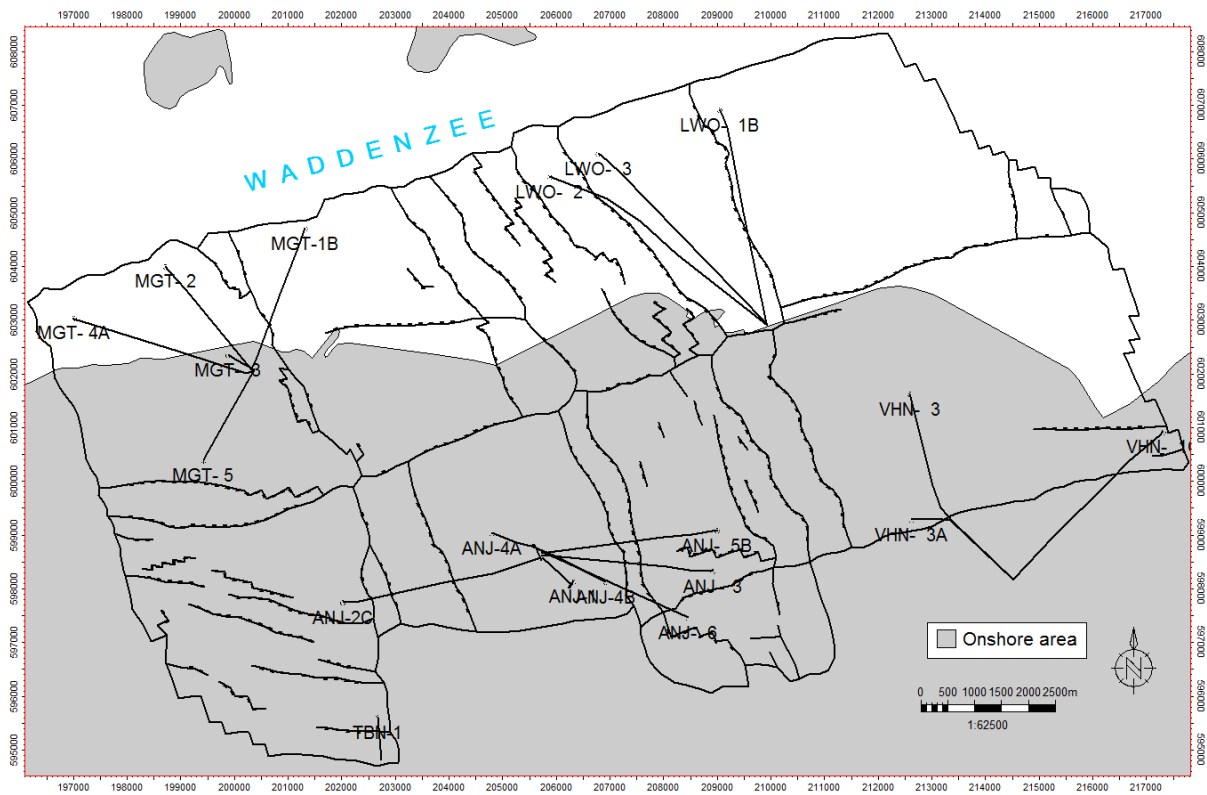


Subsurface Technical Report

Dynamic Reservoir Modelling of Waddenzee Fields for Subsidence

Meet & Regel 2016



Date: February, 2017

Document Number: EP201703201178

NEDERLANDSE AARDOLIE MAATSCHAPPIJ B.V. ASSEN

TABLE OF CONTENTS

1	KORTE SAMENVATTING (NL)	4
2	SUMMARY	5
2.1	INTRODUCTION.....	5
2.2	MODEL OBJECTIVE AND APPROACH	5
2.3	MAIN CHANGES COMPARED TO M&R2015.....	7
2.4	M&R2016 CONCLUSION	7
3	INTRODUCTION	9
4	MODEL DESCRIPTION & OVERVIEW	10
4.1	GEOLOGICAL OVERVIEW	10
4.1.1	<i>Depositional model</i>	10
4.1.2	<i>Porosity, permeability and thickness trends</i>	11
4.1.3	<i>Slochteren reservoir units</i>	11
4.2	MODEL INPUT.....	12
4.2.1	<i>Rock compressibility</i>	12
4.2.2	<i>Hydrocarbon volumes in place</i>	12
4.2.3	<i>Absolute Permeability</i>	13
4.2.4	<i>Capillary pressure</i>	15
4.2.5	<i>PVT properties</i>	15
4.2.6	<i>Initialisation</i>	16
4.2.7	<i>Wells</i>	16
4.3	HISTORY MATCHING DATA.....	17
4.3.1	<i>Historical production</i>	17
4.3.2	<i>Bottom-hole pressure measurements</i>	17
4.3.3	<i>Production logging data (PLT)</i>	18
4.3.4	<i>Pulsed neutron log data</i>	18
4.3.5	<i>Water production</i>	18
4.3.6	<i>Tubing head pressure data</i>	19
4.4	AQUIFER MOBILITY	19
4.5	UPSCALING.....	21
4.6	DEFINING SUBSURFACE REALISATIONS	21
4.6.1	<i>Pre-M&R2014 method</i>	21
4.6.2	<i>M&R 2014 method</i>	22
4.6.3	<i>M&R 2015-2016 method</i>	22
4.7	FORECASTING.....	23
4.8	TRANSLATION INTO SUBSIDENCE REALISATIONS	24
5	UNCERTAINTY MANAGEMENT	25
5.1	UNCERTAINTIES	25
5.1.1	<i>GIIP</i>	25
5.1.2	<i>Absolute permeability</i>	26
5.1.3	<i>Relative permeability</i>	26
5.1.4	<i>Vertical permeability</i>	27
5.1.5	<i>Vertical heterogeneity</i>	28
5.1.6	<i>Faulting</i>	28
5.1.7	<i>Water encroachment behaviour</i>	28
5.2	ASSISTED HISTORY MATCHING WORKFLOW	28
6	DYNAMIC MODELLING	29
6.1	FIELD MODELS AND HISTORY MATCHING	29
6.1.1	<i>Anjum</i>	29
6.1.2	<i>Ezumazijl</i>	35
6.1.3	<i>Lauwersoog Central</i>	41
6.1.4	<i>Lauwersoog-Oost</i>	45
6.1.5	<i>Lauwersoog West</i>	50
6.1.6	<i>Metslawier</i>	56
6.1.7	<i>Moddergat</i>	64

6.1.8	<i>Nes</i>	69
6.1.9	<i>Vierhuizen</i>	80
6.2	FORECASTING.....	83
6.2.1	<i>Forecasting Assumptions</i>	83
6.2.2	<i>Forecasting results</i>	83
6.2.3	<i>Subsidence scenarios</i>	88
6.2.4	<i>General forecasting conclusion</i>	89
REFERENCES		91
FIGURES		92
TABLES		95
APPENDIX A: IMPOSED FORECASTS BY WELL		96

1 KORTE SAMENVATTING (NL)

Dit modellering rapport bevat een gedetailleerde beschrijving van de geologische computermodellen en numerieke rekenmodellen die gebruikt zijn voor het onderzoeken van het gedrag van de gasvelden rond de Waddenzee.

De druk in een gasveld daalt door gasproductie. De modellen in dit rapport maken prognoses van deze veranderende druk in de zandlagen op 3000m onder het aardoppervlak. Het rapport beschrijft de prognoses op basis van de meest recente metingen en de laatste inzichten en vergelijkt de uitkomsten met prognoses uit voorgaande jaren. De uitkomsten van de hier beschreven modellen, worden gebruikt als input voor geomechanische modellen die uiteindelijk de diepe bodemdaling in de Waddenzee voorspellen.

Het aardgas is opgeslagen in zandafzettingen op ongeveer 3000 meter diepte. De geologie van deze zandafzettingen en de eigenschappen van de gashoudende lagen worden uiteengezet in paragraaf 3.1 en 3.2. Hier worden de eigenschappen beschreven die bepalend zijn voor de verlaging en de verdeling van de druk als het gas uit de lagen geproduceerd wordt. Paragraaf 3.3 geeft een beschrijving van de meetgegevens waaraan de uitkomsten van de modellen kunnen worden vergeleken en paragraaf 3.6 beschrijft de uiteenlopende scenario's die zijn gebruikt om de spreiding van de mogelijke uitkomsten van de prognose afdoende te beschrijven.

De Meet & Regel Cyclus van de gasvelden rond de Waddenzee wordt door de audit commissie gebruikt om erop toe te zien dat de inklinking van de bodem onder de Waddenzee binnen de gestelde normen blijft. De reservoir modellen bevatten parameters die niet exact bekend zijn. Hoofdstuk 4 beschrijft de onzekerheden in de belangrijkste parameters en geeft aan hoe deze onzekerheden zijn meegenomen in de berekeningen.

Om een betrouwbare voorspelling te kunnen maken van de toekomst moet een computer model allereerst in staat zijn om de historische meetgegevens goed te beschrijven. Het proces om een model aan te passen en te kalibreren om dit voor elkaar te krijgen wordt in het jargon van een Reservoir Engineer, "History Matching" genoemd. Dit proces dat voor ieder gas reservoir individueel wordt uitgevoerd en de maatregelen die nodig waren om het model te kalibreren wordt beschreven in paragraaf 5.1 en in de volgende paragraaf 5.2 wordt met het gekalibreerde model vervolgens een prognose van de toekomst gemaakt.

De conclusie uit de meest recente prognoses is dat de voorspelling van de drukdaling zeer goed overeenkomt met de prognoses van de vorige Meet&Regel Cyclus. Een uitzondering is het Nes gasveld waarin 2 nieuwe gasputten zijn geboord. De metingen in deze putten lieten zien dat de drukdaling veel lager was dan verwacht. De modellen zijn aangepast om deze nieuwe gegevens te reflecteren.

2 SUMMARY

2.1 Introduction

The Waddenzee dry gas fields are located in the environmentally sensitive Waddenzee area. To limit the environment impact, subsidence induced by gas production is closely monitored and modelled as part of the yearly *Meet&Regel* cycle. This document describes in detail the reservoir modelling performed as part of the *Meet&Regel 2016* cycle step 3: verify prognosis.

Static and dynamic reservoir models are improved and updated with the latest data for input in the Winningsplan and the *Meet&Regel* cycle, the aim is to continuously improve the subsidence modelling. Top structure maps were updated in 2012 using the data acquired during drilling of MGT-3 infill well in the Nes field and the updated time depth conversion in other fields. This update of the static reservoir model led to a reconstruction of the dynamic models for M&R2013. In 2015 the static model was updated for Lauwersoog-Oost and Moddergat fields based on new structural and property modelling. In 2016 well results of newly drilled MGT-4A and MGT-5 were used to update the Nes field static model.

Production and pressure data are updated annually and included in the dynamic models, the history match of the dynamic models is updated with the most recent data. The outcome of these models is then used to assess subsidence predictions on an annual basis.

This document describes the workflow and details of the dynamic reservoir models updated for the *Meet&Regel* cycle of 2016 (M&R2016) and also includes the comparison and changes compared to the *Meet&Regel* cycle of 2015 (M&R2015).

2.2 Model objective and approach

The main objective of the reservoir modelling exercise is to generate the range of inputs into the subsidence calculations. Production of gas causes pressure decline in the reservoir. For each of the Waddenzee fields the reservoir models predict how the pressure will vary over time for each location in the field. The models aim to generate a realistic range of outcomes for the pressure drop in the each field. The input range for the subsidence calculations covers a realistic range of outcomes for the pressure. A base case indicating the best estimate, a low pressure depletion case and a high pressure depletion case.

In recent years, it has become evident that the depletion of laterally extensive water bearing layers has a large impact on subsidence of the surface. The mobility of aquifers is thus seen as primary uncertainty for subsidence predictions throughout the fields. To make sure the entire range of possibilities is captured, the aquifer mobility has been varied to extreme cases: an (almost) fully immobile aquifer (low subsidence case) and fully mobile aquifer (high subsidence case). The actual mobility is most likely somewhere in between: an aquifer that is impaired in mobility by the presence of (paleo-residual) gas in the water leg (base subsidence case).

In the M&R cycles of 2012 and 2013¹, cases distinguished between a mobile aquifer and an immobile aquifer. A stochastic approach was used for history matching. Models with a reasonable history match were scanned for high, low and base model GIIP case.

After M&R 2013 it became clear that, in general, the mobility of the aquifer was of much bigger relevance to the subsidence than the variation of high, low and base case dynamic GIIP, since with more and more production data, the uncertainty in dynamic GIIP becomes less and less. It was therefore chosen not to use the dynamic GIIP uncertainty any longer and focus solely on two history matches: an immobile aquifer realisation and a mobile aquifer realisation.

More recent data and understanding shows that the two history matches provided in M&R2014 did not sufficiently cover the base case subsidence scenario. Hence the M&R2015 approach included a new base case definition with an impaired aquifer (including presence of paleo-residual gas) described above.

The M&R2016 method follows this same approach. The fields Nes and Vierhuizen somewhat deviate from this approach. Nes' aquifer has been measured with post-production RFTs in new wells, which means that aquifer mobility is no longer the key uncertainty. For Vierhuizen, no immobile aquifer realisation could be generated, since it could not be matched with dynamic data.

For subsidence forecasting, the future yearly gas production as per this year's Business Plan (2016) has been applied to the models, similar to the assumption used for M&R2015, where Business Plan 2015 numbers were applied.

A summary of the M&R2016 realisations are given in Table 1, Table 2 and Table 3.

Table 1. Overview of dynamic realisations (all fields except Nes and Vierhuizen).

	Base structure	Immobile aquifer	Gas saturation below FWL	Mobile aquifer	Base dynamic GIIP	Business Plan 2016 profile
1 – Low pressure drop	x	x			x	x
2 – Base pressure drop	x		x		x	x
3 – High pressure drop	x			x	x	x

Table 2. Overview of dynamic realisations (Nes).

	Base structure	Low vertical permeability	Base vertical permeability	High vertical permeability	Base dynamic GIIP	Business Plan 2016 profile
1 – Low pressure drop	x	x			x	x
2 – Base pressure drop	x		x		x	x
3 – High pressure drop	x			x	x	x

¹ M&R cycle 2012 (2013) refers to the work that was done during 2012 (2013) and was presented in Q1 2013 (2014).

Table 3. Overview of dynamic realisations (Vierhuizen).

	<i>Base structure</i>	<i>Immobile aquifer</i>	<i>Gas saturation below FWL</i>	<i>Mobile aquifer</i>	<i>Base dynamic GIIP</i>	<i>Business Plan 2016 profile</i>
<i>1 – Low/Base pressure drop</i>	x		x		x	x
<i>2 – High pressure drop</i>	x			x	x	x

2.3 Main changes compared to M&R2015

The following changes have been implemented in the reservoir models.

- The static model for Nes has been revised after MGT-4A and MGT-5 wells were drilled in Q4 2015 and Q1 2016 respectively.
 - o Formation tops have changed to match to the new wells.
 - o Field porosity and absolute permeability have increased to match both well logs as well as dynamic data.
 - o The gas saturation height function has been modified (increasing average gas saturation), to match dynamic data, giving more weight to MGT-3 S_g observations.
- Nes RFT measurements revealed that the ROSLU2 holds over 240 bar. This has led to a revision of the key uncertainty for the low-base-high subsidence models for Nes. In M&R2015, the transmissibility of the ROSLU2 was seen as key uncertainty to overall reservoir pressure drop. In M&R2016, vertical permeability is marked as key uncertainty. With the ROSLU2 acting as pressure barrier, the forecast pressure drop in the Nes (bottom-)aquifer has significantly reduced.
- Brine properties were somewhat modified, after a revision of salinity in the models from 100 000 ppm to 260 000 ppm. This affected both density and viscosity. The effect on history matches and pressure forecast has been proved marginal.
- Production forecasting profiles have been modified, following BP'16 update. A longer production duration (until 2035) has been assumed for MGT-1,-2,-3 and ANJ-4 as a consequence of system-lifetime-extension caused by possible new well TRN-2. An extension of VHN-1 production to 2019 has also been incorporated. Furthermore, the latest estimate on Nes Infill production (MGT-4 and MGT-5) was incorporated, which is significantly less than forecast in M&R2015.

2.4 M&R2016 Conclusion

Some general conclusions can be made from the modelling work done for M&R 2016.

The Nes field's pressure decline forecast has shown a large revision, after new well results came in from MGT-4A and MGT-5. Forecast pressure drop is significantly less than was reported in M&R2015, since RFTs in these wells have revealed that the ROSLU2 shale layer is not/poorly transmissible.

The other fields show minor changes to M&R2015. Any changes are mainly related to updated production forecast assumptions.

The uncertainty approach, with aquifer mobility as main uncertainty, is fit-for purpose. With few wells in the fields, reservoir pressure in aquifers are poorly known. Extremes (fully

immobile, fully mobile aquifer) are modelled to ensure a wide enough range of forecast pressure.

3 INTRODUCTION

The Waddenzee area consists of nine fields on the shore face of northern Friesland. Anjum, Ezumazijl and Metslawier are the three fields not lying under the Waddenzee, which are used mainly for subsidence calibration. These fields commenced production in 1997. Lauwersoog Central, East and West, Moddergat, Nes are situated partly or entirely beneath the Waddenzee, gas production in these fields may therefore potentially cause subsidence to the Waddenzee. These fields started production in 2007. The fields are depicted in Figure 1.

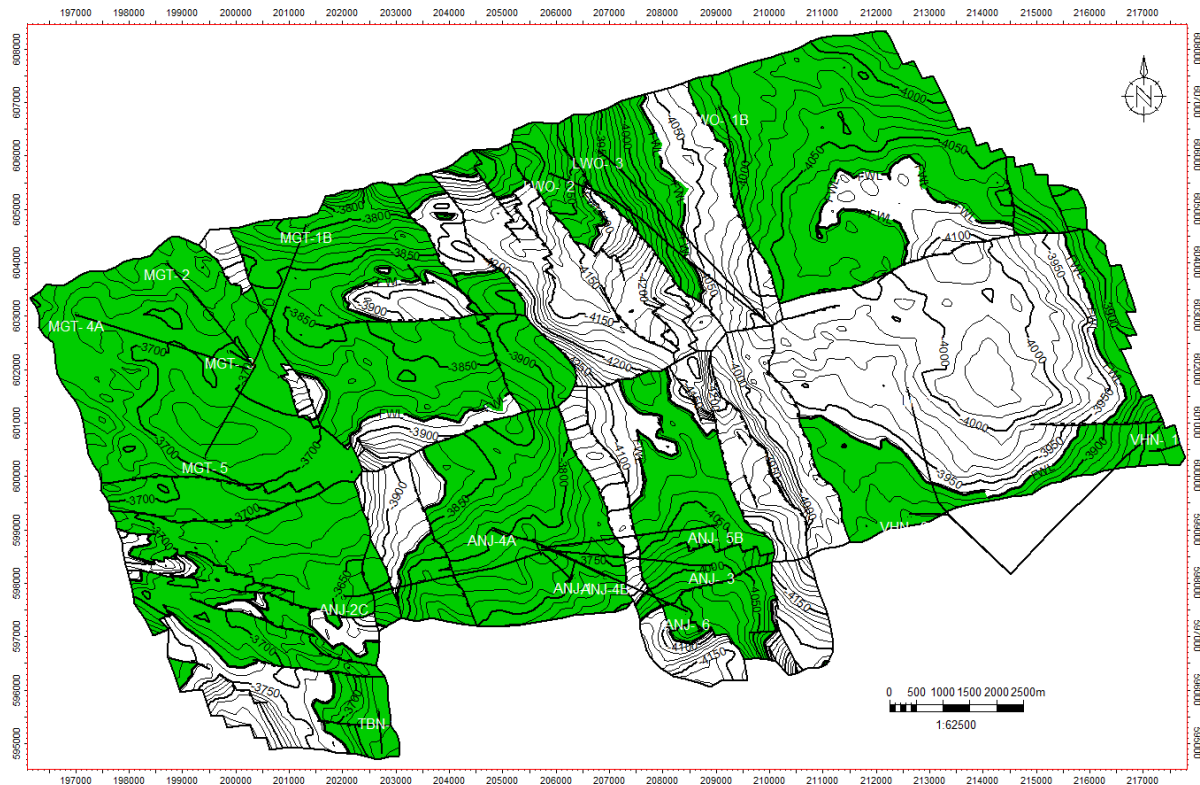


Figure 1 Map of the Waddenzee area

This document describes the workflow and details of the dynamic models updated for the M&R2016 and also includes the comparison and changes compared to the M&R2015. Chapter 4 describes the setup of the model. It includes the model input, the input data for history matching, the main uncertainty to subsidence (aquifer mobility), the way different realisations are defined and the forecasting method. Chapter 5 describes the main uncertainties and how they are taken into account. Chapter 6 discusses the individual dynamic models in greater detail and discusses the results and its implications.

4 MODEL DESCRIPTION & OVERVIEW

Dynamic reservoir models have been built in MoReS, which is a Shell proprietary reservoir simulation software. This software is able to perform multiphase 3D simulations. This is particularly important to capture vertical and lateral heterogeneity, as well as two-phase (gas-water) behaviour.

4.1 Geological overview

The model grid and reservoir properties are imported from a static geological model, created using *Petrel* software. Geological interpretation and understanding is important when building this geological model. This subsection discusses the geological overview of the Waddenzee field area.

4.1.1 Depositional model

Climate and creation of accommodation space are two factors that affect the distribution of sediments in the reservoirs of the northern Netherlands. Climatic changes were interpreted to range from extreme arid to humid conditions whilst the creation of accommodation space was dependent on subsidence and the rate of sedimentation. An increased rate in subsidence results in ephemeral (intermittent) ponds/lakes while a reduced rate in subsidence results in dryer more arid environments. A more variable driver to deposition are the north-easterly Aeolian processes that transport fine-grained sediments to the land and the south-westerly wind direction which transports and deflates sand grains towards the ancient lake margins.

Super-imposed on the large-scale trends in reservoir quality are more local east to west trends in porosity. These trends are postulated to be a response to the presence of paleo-lows and paleo-highs. The Lauwerszee Trough marks a paleogeographic low with lower N/G and porosity values extending to the east due to preferential southward incursion of wetter, lacustrine facies. Furthermore, there is a slight reduction in porosity with depth. The fault boundary separating the Moddergat and Lauwersoog blocks marks a change in reservoir quality.

Unlike Ameland, trends in mineralogical composition between chlorite and kaolinite also don't vary across the Waddenzee fields. All wells are chlorite prone. The chlorite is a grain coating clay which helps to preserve reservoir quality by reducing compaction and preventing nucleation of other cements. Similar chlorite cements occur in the Rotliegend of northern Germany, interpreted as forming in a belt parallel to the shoreline of the desert lake, with Mg-rich fluids expelled from compacting basin shales forming chlorite from early precursor clays (Hillier et al., 1996). In the study area the chlorite is also interpreted as forming a belt parallel to the facies belts on the margin of the desert lake. Furthermore, a belt of anhydrite cementation can be traced from wells in Lauwersoog to Nes. The anhydrite is abundantly developed in certain stratigraphic layers significantly reducing porosity. The anhydrite is dominantly early and is interpreted as representing periods of sabkha development on the margins of the desert lake, with cementation from evaporitic groundwaters.

For modelling purposes, porosity distributions were designed to reflect influences on reservoir quality described above, that then link to permeability distribution. The realisations reflect changes in porosity from west to east although no hard trends have been included in the *Petrel* models perse. Where porosity reduction with depth is observed, these trends are included in the *Petrel* models.

4.1.2 Porosity, permeability and thickness trends

Overall, vertical heterogeneity of the Waddenzee reservoirs is greater than lateral variations of reservoir quality reflecting changes in the level of the water table with respect to the depositional surface over time. Within the sand-rich intervals, evidence for high porosity and permeability streaks (HPS) is observed at the core level (typically 10-50cm thick). These are attributed to grain flow deposits that result in improved reservoir quality in aeolian dune settings. These features have 2-3 orders of magnitude of higher permeability than the background and can occur in ROSLU Unit's 1, 3, 4, and 6. Spatially, it was recognised that HPS have a wider spread in the east of Wadden. In this area thin high porosity/permeability streaks provide the major flow contribution during production. Although sometimes below log resolution, they require representation in the reservoir model to effectively capture key considerations that impact subsidence modelling such as differential depletion.

To capture the required heterogeneity due to interbedding and associated cementation (e.g. anhydrite), model layering is refined sufficiently but is balanced against the need to reduce simulation time. The result is a more accurate representation of reservoir property distribution (e.g. porosity) and porosity ranges per unit.

Furthermore, the lack of resolution in porosity and permeability logs compared to in-situ corrected core data over the core interval results in an underestimation of the rock's heterogeneity. Even though the resolution at which the core plugs have been taken from the core is not much greater than the resolution of log porosity, they do not suffer from averaging effects that result from limited vertical resolution of a density tool. An approach chosen to accommodate for this was to upscale both core plug data and wireline data and replace wireline data where cored intervals existed. As most core was taken in key flowing units, a better approximation of magnitude of permeability contrast is achieved, compared to just averages calculated using a perm curve that varies in line with the porosity log; capture of high porosity/permeability streaks for differential depletion sensitivity.

4.1.3 Slochteren reservoir units

A change to wetter conditions, discussed above, can result in a widespread transgression of a playa lake margin across the area and an increase in water-lain sedimentation. These events result in barriers and baffles to flow represented by transgressive surfaces.

Cored intervals of Units 2, 4, 5, and 6 revealed correlatable shale horizons across the Waddenzee field (e.g. up to 10 km distances between wells). These transgressions were used as a sensitivity for vertical communication between units in the dynamic model, with Unit 5 further divided into 2 intra-units. Unit 2 shale is due to a regional "drowning" resulting in a development of a playa lake across the area (including Ameland) and a major barrier to flow. For example, LWO-3 encountered a ROSLU1 that was 1.9 bar lower in pressure than in ROSLU2-6 resulting in a different fluid contact. The most likely explanation is that ROSLU2 is sealing and ROSLU1 forms a separate accumulation within the majority of fields in the Waddenzee area. The other incursions are reflected by shale breaks between Unit 5A and 5B and Unit 5B and Unit 6 within the each field.

4.2 Model input

4.2.1 Rock compressibility

Rock compressibility is a relatively minor energy term, but may have impact on the water influx. For the model rock compressibility was based on the compaction coefficients initially provided by the Geomechanics discipline. The rock compressibility was calculated by dividing the compaction coefficient by the average porosity in the field. These are given in Table 4.

Table 4 Rock compressibility per field

Field	C_R (10^{-5} PU*bar ⁻¹)	Average porosity (-)	C_R (10^{-5} bar ⁻¹)
Anjum	0.89	0.14	6.4
Ezumazijl	0.69	0.11	6.5
Lauwersoog-Central	0.69	0.09	7.5
Lauwersoog-Oost	0.69	0.10	7.1
Lauwersoog-West	0.69	0.10	7.0
Metslawier	0.98	0.15	6.7
Moddergat	0.87	0.12	7.5
Nes	1.00	0.13	8.0
Vierhuizen	0.69	0.12	5.7

Rock compressibility method has not changed since M&R2015. Although the reported values have slightly changed, since average porosity values were slightly modified during modelling updates, whilst the reported values had not. Any changes have had negligible effect on the pressure history match.

4.2.2 Hydrocarbon volumes in place

The structure of the reservoir of the Waddenzee and Anjum fields was last fully updated in 2012, following the MGT-3 drilling results, where the top reservoir came in deeper than expected by 22m TVDNAP. This led to changes in (static) volumes in place. For Anjum, the static GIIP was updated based on the observed dynamic volume.

However, since then some separate updates have been made:

1. Lauwersoog-Oost: A new depth map was used in 2015. There is no significant GIIP change, although the popups in the east of the field are excluded, to give a better comparison with dynamic GIIPs. A modification of porosity-depth trend was also applied.
2. Moddergat: Depth map was updated in preparation from the Moddergat (south) infill opportunity in 2015, decreasing GIIP significantly. Furthermore, the MGT-SE blocks are excluded, and the NES-North block included conform what is currently believed to be in connection with the MGT-1B well. A modification of porosity-depth trend was also applied.
3. Nes: In 2016 the static model of Nes has been modified. This is a result of the data obtained during the drilling of the wells MGT-4A and MGT-5. Top structure was calibrated to the well tops and the log readings were implemented to update reservoir properties. Also, based on dynamic insights, the saturation-height-function was updated, to increase the gas saturation. This is described further in Section 4.2.4.

Table 5 Static gas initially in place (GIIP) above FWL

Field	Base Case GIIP M&R2015 (BNCM)	Base Case GIIP M&R2016 (BNCM)	Main reason for change
Anjum	16.6	16.6	
Ezumazijl	2.1	2.1	
Lauwersoog-Central	1.2	1.2	
Lauwersoog-Oost	5.1	5.1	
Lauwersoog-West	3.4	3.4	
Metslawier	5.2	5.2	
Moddergat	6.8	6.8	
Nes	18.9	16.7	Deeper top structure after MGT-4A and MGT-5 well results.

4.2.3 Absolute Permeability

Permeability is largely based on the porosity-permeability correlation established in 2004 (Ref 1). After the drilling and coring of MGT-3 updates were made on the porosity-permeability correlations for some fields. Horizontal and vertical permeability are used as a matching parameter in the history matching process.

The permeability of the aquifer is used as a separate parameter in order to capture the uncertainty in the depletion of the water bearing layers. Core data show that the permeability in the water leg can be a factor 2-4 smaller than those in the gas leg (Ref 1) or even a factor 10 smaller (Figure 2, Ref 2). See also Section 4.4 .

Modifications have been made to the permeability model for Moddergat and Lauwersoog Oost. For Moddergat and Lauwersoog an updated permeability log was created based on flow zone indicators. For Moddergat, the FZI log was used in combination with the actual stress corrected core porosities and permeabilities to populate the inter-well space. Specifically, the inter-well space was co-kriged with porosity as a the guiding secondary variable to control the permeability distribution based on the core data. This had a significant impact by reducing connectivity across the field. For Lauwersoog-Oost, a similar modelling approach was followed however the core data was not used directly. The effect was marginal.

A change was made for M&R2016 to the absolute permeability model of the Nes field. The well logging results of MGT-4A and MGT-5, combined with RFT data suggesting good connectivity, led to an increase of the permeability of the field. This has been depicted in Figure 2 in the form of a histogram and in Figure 3 in the form of the porosity-permeability relationship.

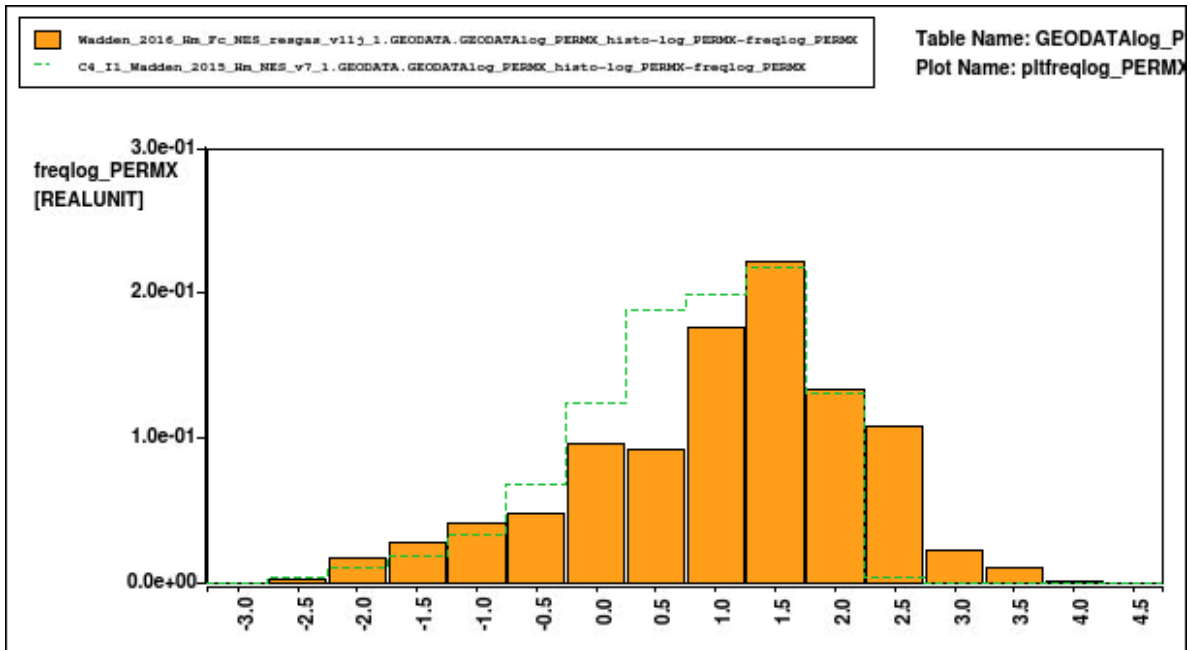


Figure 2 Histogram of Nes permeability (M&R2016: Orange filled, M&R2015: green dotted line)

The Uncertainty in permeability is high, to honour the historic data, permeability multipliers have been used on a field by field basis to achieve an acceptable history match, the multipliers are specified in Section 6.1 .

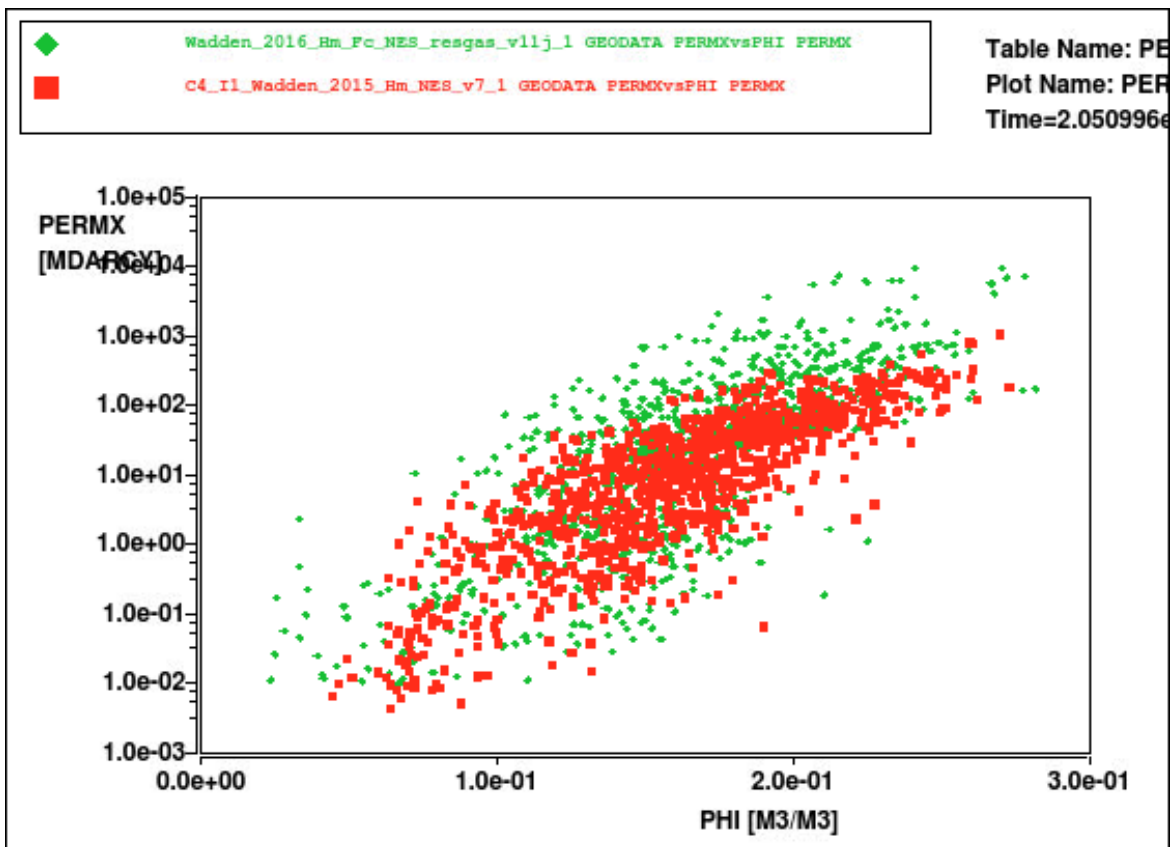


Figure 3 Porosity-Permeability relationship (M&R 2016: green, M&R2015: red)

4.2.4 Capillary pressure

Capillary pressure is calculated from the saturation height function as described in the petrophysical study from 2004 (Ref 1).

Some modifications have been made for Moddergat and Lauwersoog East fields:

- **Moddergat**² - Saturation Height functions have been re-generated for the Moddergat and Nes Fields. The new functions are Lambda-functions, based on log derived gas saturations. The reason for generating new functions is was a slight mismatch between log derived saturations and SHF saturations in Unit 1 in the Upper Slochteren reservoir. To improve the match, the irreducible water saturation (B) was increased from 0.05 to 0.075. This increase in B resulted in a GIIP reduction of 0.5 BCM. The irreducible water saturation in the lower units in the Upper Slochteren, remained unchanged at 0.1.
- **Lauwersoog fields**³ - Saturation Height functions have been assessed for the three Lauwersoog Fields. The new functions are simple Lambda-functions, based on log derived gas saturations. Reason for generating new functions was a slight mismatch between log derived saturations and SHF saturations, in Unit 1 in the Upper Slochteren reservoir. To improve this fit, the irreducible water saturation (B) was increased from 0.05 to 0.075. In the lower units of the Upper Slochteren, the irreducible water saturation remained unchanged at 0.1. This increase in B in Unit 1, resulted in a GIIP reduction of approximately 0.2 BCM in each of the three LWO fields.
- **Nes** - Gas saturation is thought to be higher for Nes than was modelled prior to M&R2016. This was done to ensure a good history match with dynamic (pressure and production) data in this field. The updated saturation height function is based solely on the MGT-3 well.

4.2.5 PVT properties

For gas fields, the PVT property model exists of viscosity and expansion factor. Expansion factors per field differ depending on pressure, temperature, and gas composition. The correlations used in the simulator are established from PVT reports on gas samples. Viscosity is usually not measured, but correlations from literature predict gas viscosity reasonably accurately. Here, Lee and Gonzalez correlation was used.

For dry gas fields, dynamic behaviour is rather insensitive to PVT parameters, hence no uncertainty ranges are specified: the properties are fixed.

An update since M&R2015 was done on the salinity of the water (brine) in the models. Prior to M&R2015, a salinity of 100 000 ppm was used. This has been modified to 260 000 ppm as this better represented the available water sample data. The change in salinity changes the water viscosity and density in the dynamic simulations. The water density has changed from

² This modification will also be applied to future models or Nes. For now, only applied in the model update of Moddergat.

³ This modification has only been applied to Lauwersoog East in M&R2015. In future models, this change will be applied to all Lauwersoog fields.

$\sim 1.0 \text{ g/cm}^3$ to $\sim 1.1 \text{ g/cm}^3$. Also the compressibility was changed from $4.2 \cdot 10^{-5}$ to $2.5 \cdot 10^{-5} \text{ bar}^{-1}$ and viscosity from 0.26 to 0.40 cP, following p139-141 of Ref 33.

4.2.6 Initialisation

All fields are hydrostatically initialised with initial pressure at datum depth. All other pressures and saturations are calculated by the simulator from the given free water level (FWL) and capillary pressure curves.

The initialisation process has changed since M&R2015 since the latest models include residual gas below FWL. Initialisation is done in two steps, and in between a residual gas saturation is added to the aquifer:

- (1) **First** capillary pressure curves are created conventionally, adding gas and water saturations to the gas reservoir resulting in a 100% water saturation below FWL.
- (2) After this initialisation, a **residual gas saturation is included** in water bearing cells where $S_w > (1 - S_{PRG})$, where S_{PRG} is the Paleo Residual Gas Saturation.
- (3) After this, the model is **initialised for a second time**, using the “PSAT” method. This maintains a non-zero gas saturation below FWL.

4.2.7 Wells

The well trajectories are imported from the static reservoir model (Petrel). Perforation intervals are obtained from the corporate database (Discovery/DREAM). Using recompletion tables, the perforations can be opened and closed at specific times during their history. Lift tables are generated with Prosper software and assigned to their respective wells. These are also included in the history matching run in order to check the well inflow performance over time.

Since M&R2015, the well trajectories of the new wells MGT-4A and MGT-5 and their lift tables have been included to the Nes model.

Table 6 gives an overview of all wells in the Waddenzee area.

Table 6. Overview wells in Waddenzee area.

Well	Field	Status 1/1/2016
ANJ-1	Anjum	Suspended
ANJ-2C	Metslawier	Suspended
ANJ-3	Ezumazijl	(Unreliably) producing , regularly sands in.
ANJ-4B	Anjum	Producing
LWO-1B	Lauwersoog-Oost	Producing
LWO-2	Lauwersoog-C	Intermittently producing
LWO-3	Lauwersoog-West	Producing
MGT-1B	Moddergat	Producing
MGT-2	Nes	Producing
MGT-3	Nes	Producing
MGT-4A	Nes	Suspended (obstruction in well, unable to remove plug an perforate reservoir)
MGT-5	Nes	Producing
VHN-1C	Vierhuizen East	Producing

4.3 History matching data

Historical data used to history match the reservoir behaviour are summarized below and comments are provided on their importance for history matching.

4.3.1 Historical production

Historical production for the M&R2016 models have included monthly production up to and including October 2016. Two methods for implementing production data were used.

Anjum, Metslawier, Vierhuizen East:

For these fields, the model is constrained by historical production with monthly time steps. This means that short shutdowns are not captured; only long shutdowns are accurately represented. This means that the BHP cannot always be used to history match the closed-in pressure measurements. For history matching, a permeability averaged reservoir pressure is calculated. This calculates the equivalent shut-in pressure (for fixed shut-in times) while the well is flowing, by averaging reservoir pressures over grid cells depending on the permeability that is connected. This means that adding or closing in perforations can have significant impact on the pressure observed. This is also observed in reality, for example ANJ-3. A permeability averaged pressure is considered to give a good representation of the pressure that would be measured by a pressure gauge in the well.

Ezumazijl, Lauwersoog Central, - West, - East, Nes, Moddergat

A more detailed approach is used for these fields, by refining the historical production time steps around pressure points, taking shut-in times to nearest day into account. This method is more suitable for matching the Bottom Hole Pressures (BHP) in fields with large permeability contrasts.

Effectively, both simulated reservoir pressures and simulated BHP are plotted together with the historical pressure points to observe the history match adequately.

4.3.2 Bottom-hole pressure measurements

This is the main source of data used for history matching, since it gives the most reliable representation of the reservoir pressure. One way of obtaining the data is via static pressure gradients (SPG) by lowering a pressure gauge in a well to the level of the perforations during a shut-in period. SPGs are converted to datum depth. In all wells, SPGs are taken at regular intervals. The following measurements were made since M&R2015.

Table 7. SPG measurements since M&R2015.

Well	Field	Date	Pressure at datum
ANJ-3	Ezumazijl	21/9/2016	96.5 bara
MGT-1B	Moddergat	7/4/2016	187.8 bara

Another way of obtaining BHP data is by taking a closed in tubing head pressure measurement (CITHP), with an estimate of the fluid column in the wells this can then be converted to a BHP. This is somewhat less accurate, but still can give appropriate results for history matching. The following measurements and interpretations were made since M&R2015.

Table 8. Converted CITHPs since M&R2015.

Well	Field	Date	Pressure at datum
ANJ-4B	Anjum	15/6/2016	51.2 bara

LWO-2	Lauwersoog-C	8/4/2016	188.4 bara
LWO-1B	Lauwersoog-Oost	8/4/2016	172.7 bara
LWO-3	Lauwersoog-West	8/4/2016	165.5 bara
MGT-2	Nes	8/4/2016	232.7 bara
MGT-3	Nes	8/4/2016	229.3 bara
MGT-5	Nes	8/11/2016	216.2 bara

A third way of measuring pressure downhole is via Repeat Formation Testing (RFTs). This is done for new wells in open hole, before the well is completed. Last year, new data from the two new wells were obtained.

Table 9. RFT measurements since M&R2015.

Well	Field	Date	Pressure at datum
MGT-4A	Nes	8/12/2015	454-478 in waterleg of ROSLU3-4
MGT-5	Nes	13/2/2016	188.4 bara in ROSLU1, ~483 bara in ROSLU3-4

4.3.3 Production logging data (PLT)

In some wells production logging tools have been run. These tools are lowered in a flowing well and measure the inflow rate as function of depth. PLTs are used to get a match on permeability contrasts in the field. No new measurements were done since M&R2015.

4.3.4 Pulsed neutron log data

Pulsed neutron logs are used to determine water saturation changes in the reservoir and can hence monitor aquifer encroachment. These were not run in this area and therefore are not used for history matching.

4.3.5 Water production

Liquid production is only accurately measured and reconciled at system level. Individual well water gas ratios have been estimated from WaCo tank level changes and changes in the amount of liquid produced historically. As the only reliable way to look at the water production is at system level, the uncertainties are relatively large. This data is therefore not strictly used for history matching, but may sometimes act as a guide to observe the order of magnitude of water production in the model compared to reality.

The main parameters that impact the water production are the residual gas and water relative permeability end point. The first determines the timing of water break through, while the latter mainly impacts the amount of water produced at all times.

No new WGR estimates were provided in 2016.

As extra soft data point, in 1-9-2015 a consolidated MGT-LWO Liquid Gas Ratio (LGR) was found to be $21 \text{ s m}^3/\text{E6N m}^3$. With Condensate Gas Ratio (CGR) around 8, this makes a Water Gas Ratio (WGR) of $13 \text{ s m}^3/\text{E6N m}^3$. Since this figure cannot be back-allocated to a well, it is not included in the data. However it does show that in 2015, the WGR of the large producers MGT-1, -2, -3 cannot exceed this figure by a great amount.

Water production is usually a combination of *condensed* water and *formation* water. Only the latter is modelled in the MoReS simulator. Using the Wehe-McKetta correlation, an estimate of the condensed water to gas ratio can be given, depending on reservoir temperature,

pressure and salinity. The salinity used for all fields is 260 000 ppm, in line with the value reported in Section 4.2.5. The condensed WGR number (pressure, hence time dependent) is added to the formation WGR to give a total WGR, which is matched to the data points.

4.3.6 Tubing head pressure data

During the history matching process, gas rates are used as a constraint. In order to assess the well inflow performance, the tubing head pressure data is used. When the inflow and lift table are correct, one would expect to reproduce the tubing head pressure. Near wellbore effects and water influx may however cause deviations. Therefore, THP data is generally matched qualitatively, but is considered of secondary importance compared to downhole pressure measurements.

Tubing head pressures are continuously measured. The pressures have been updated until 30/11/2016 for M&R2016.

4.4 Aquifer mobility

The main uncertainty for subsidence modelling is the depletion of water bearing sections of the reservoir. Depletion of the water bearing layers cannot be accurately determined from material balance analysis, due to the low compressibility of water.

Industry data suggests that the aquifer is less permeable than the gas leg. The theory for this is twofold: firstly, the permeability of the water zone can be lower due to clay particles existing in the aquifer (see Figure 4). Secondly, there is evidence for existing trapped gas below the free-water-level, this is residual gas from the time the gas travelled through the water to fill the gas reservoir, which negatively impacts effective permeability of the water and will sustain a higher pressure in the waterleg (Ref 2). Also the subsidence behaviour south of the Ameland field and north of the Nes field suggests a slow aquifer response, implying a less permeable aquifer.

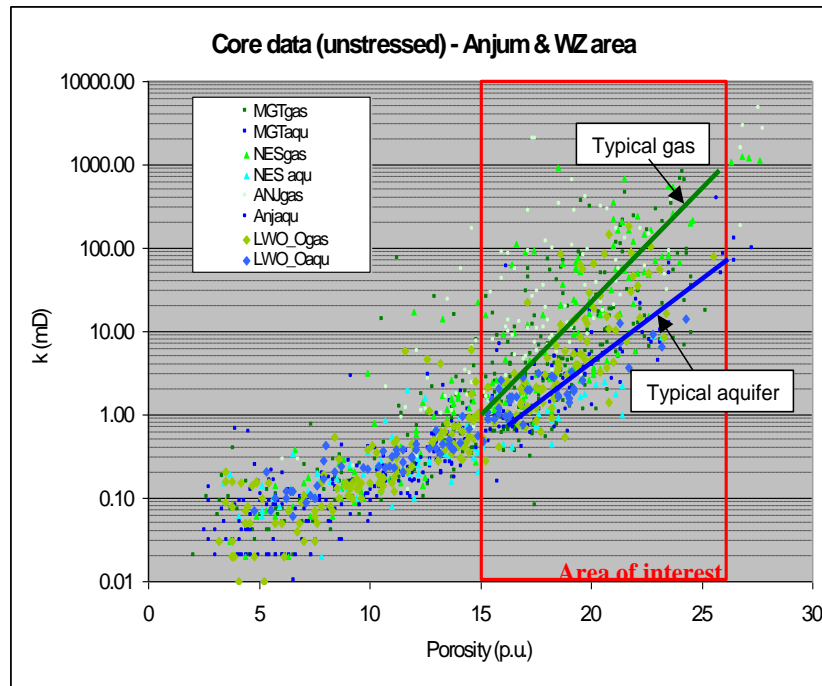


Figure 4 Core plug permeability data for gas and aquifer leg.

To sufficiently capture all the uncertainties, three cases have been generated: the low pressure drop realisation (all aquifer permeabilities 10^{-4} times the gas permeability), the base pressure drop realisation (with paleo-residual gas modelled in the aquifer and only a small reduction of absolute permeability in the waterleg) and the high aquifer mobility (aquifer permeability equalling that of the gas leg).

In M&R2016, a slightly different method was used to model and initialise paleo-residual gas. This is described in Section 4.2.6 (see also Ref 4). The expected gas saturations below FWL are depicted in Table 10.

Table 10: Average of gas saturation measurements in aquifer and the weighted average resulting in expected field averages for residual gas saturation below FWL (encircled in green). This saturation was used as a starting point and was only modified if an insufficient history match could be made.

Well	Average Gas bFWL	Weights for averaging								
		Anjum	Ezumaziji	Metslawier	Lauwersoog E	Lauwersoog C	Lauwersoog W	Moddergat	Nes	Vierhuizen
ANJ- 2C	0.061	2		3					1	
ANJ- 3	0.1743	1	3							
ANJ- 5B	0.1698	1	1							
LWO- 1B	0.2313				3		1			1
LWO- 2	0.2808					3	1	1		
LWO- 3	0.19				1	1	2			
MGT- 1B	0.1895					1		2	1	
MGT- 2	0.1738							1	2	
MGT- 3	0.1875			1				1	2	
VHN- 1C	0.137				1					3

VHN- 3A	0.1511				1		1			3
	Res Gas bFWL	0.12	0.17	0.09	0.20	0.24	0.21	0.20	0.16	0.16
	High	0.28	0.28	0.28	0.28	0.28	0.28	0.28	0.28	0.28
	Low	0.06	0.06	0.06	0.06	0.06	0.06	0.06	0.06	0.06

Some precaution is required when examining these models, since by adding saturation below the free water level, trapped gas is existent throughout the entire aquifer, changing the GIIP, which are then no longer comparable to P/Z and static GIIP. Model GIIP numbers presented in this document refer to GIIP *above the FWL*. This ensures that a better comparison is possible between model GIIPs and static or P/Z GIIPs.

4.5 Upscaling

The model is upscaled one-to-one. Vertical permeability is set at 0.1* horizontal permeability by default, which resembles the microscopic permeability contrast between flow along and across the bedding. The history matching sensitivity parameter on the vertical permeability is used as an additional modification of vertical permeability, to account for extra macroscopic vertical flow barriers.

4.6 Defining subsurface realisations

4.6.1 Pre-M&R2014 method

Since history matching is an inverse problem, often many realisations can give a reasonable history match. Before M&R2014, multiple scenarios were taken using a probabilistic method. A low, base and high case scenario would be extracted from a cloud of realisations with an acceptable root-mean-square (rms) error. A P90, P50 and P10 dynamic GIIP realisation would then be constructed. This exercise would be done for a mobile aquifer and an immobile aquifer case (as described in Section 4.2.3), giving six realisations. Since the immobile aquifer cases generally gave the better pressure history match, as well as the better subsidence match, the P50 immobile aquifer case would be seen as the deterministic base case used for other reservoir engineering purposes. This model would generally also be further optimised in detail to create a good working model. The other five models represented probabilistic scenarios to capture the uncertainty range, but did not have the granularity of detailed correctness to be used as deterministic case.

Table 11. Overview of dynamic realizations. Cases 1-6 apply to all fields. The high structure cases were applied to Moddergat and Nes only.

	Base structure	High structure	Immobile aquifer	Mobile aquifer	Low dynamic GIIP	Base dynamic GIIP	High dynamic GIIP
1	x		x		x		
2	x		x			x	
3	x		x				x
4	x			x	x		
5	x			x		x	
6	x			x			x
7		x	x		x		
8		x	x			x	
9		x	x				x
10		x		x	x		
11		x		x		x	
12		x		x			x

4.6.2 M&R 2014 method.

As of M&R2014, it has become clear that the uncertainty with the largest impact on modelling subsidence is the mobility of the aquifer. The other uncertainties are of lesser significance and generally give a similar result for subsidence. It was therefore decided to eliminate the uncertainty of the other parameters and focus solely on the difference between immobile and mobile aquifer cases, see Table 12.

Table 12. Overview of dynamic realizations. Cases 1-2 apply to all fields. The high structure cases were applied to Moddergat and Nes only.

	Base structure	High structure	Immobile aquifer	Mobile aquifer	Base dynamic GIIP
1	x		x		x
2	x			x	x
3		x	x		x
4		x		x	x

Since the amount of realisations is smaller, there can be more focus on getting a usable deterministic mobile aquifer case. By default the old base case dynamic GIIP realisations are used where the match is acceptable. The immobile aquifer cases gave very good results and required little revision. For the mobile aquifer case, which is seen as a sensitivity and a high subsidence case, it was attempted to, except for the aquifer permeability, change the immobile (base case) model as little as possible for optimum transparency of the two cases. In the high and the low case, where possible, the transmissibility of existing faults was increased as much as possible, since this will increase the prediction of subsidence.

Although high structure realisations were made, they were in the end not used in the subsidence predictions. The high, base and low cases were deemed to give the maximum realistic range of subsidence uncertainty.

4.6.3 M&R 2015-2016 method.

After RFT measurements in the water-leg in MGT-3 and especially after observing late subsidence above an aquifer due south of the Ameland field, evidence is mounting that the expectation case should be somewhere in between the extreme cases of Table 12. This intermediate solution was generated by modelling residual gas in the aquifer as described in Section 4.4. Furthermore it was decided to drop the models based on a high-structure realisations. These realisations were not used during M&R2015, and dynamic data now

clearly shows that these models no longer resemble reality. An overview of the different realisations is given in Table 13, Table 14 and Table 15.

Table 13. Overview of dynamic realizations during M&R 2016 for all Waddenzee fields except Nes and Vierhuizen.

	Base structure	Immobile aquifer	Paleo-residual gas below FWL	Mobile aquifer	Base dynamic GIIP
1 – Low pressure drop	x	x			x
2 – Base pressure drop	x		x		x
3 – High pressure drop	x			x	x

For Vierhuizen, the immobile aquifer realisation is discarded (Table 14), which is further discussed in Section 6.1.9.1.

Table 14. Overview of dynamic realizations during M&R 2016 for Vierhuizen

	Base structure	Immobile aquifer	Paleo-residual gas below FWL	Mobile aquifer	Base dynamic GIIP
1 – Base pressure drop	x		x		x
2 – High pressure drop	x			x	x

The Nes field, with two new wells MGT-4A,-5 drilled since the M&R 2015 documentation, has changed in approach. MGT-3,-4A,-5 have RFT measurements in the water leg, post production. The aquifer pressure is now well-known and is no longer the key uncertainty to pressure depletion in this field. For Nes, vertical permeability is captured as largest uncertainty to average pressure depletion. The reasoning behind this is described further in Section 6.1.8.2.

Table 15 Overview of dynamic realizations during M&R 2015 for Nes.

	Base structure	Low vertical permeability	Base vertical permeability	High vertical permeability	Base dynamic GIIP	Paleo-residual gas below FWL
1 – Low pressure drop	x	x			x	x
2 – Base pressure drop	x		x		x	x
3 – High pressure drop	x			x	x	x

4.7 Forecasting

Pre-M&R2015, multiple forecasting scenarios were constructed: a base profile and an accelerated profile. The former was based on the production as given in the Winningsplan Wadden 2011, in the latter these yearly production figures were increased by 20% until the UR was reached, after which the forecast stopped. This to ensure that the total bandwidth given in the Winningsplan (+/- 20%) is accounted for.

In M&R2015, a different approach was taken. The main reason for this is that the Winningsplan 2011 numbers by then were outdated. Therefore, from 2015 onwards, only the

Business Plan production forecasts are used. These comprise of the sum of the no-further-activity (NFA) profiles and some expected forecasts from firm infill opportunities to the Anjum system (Ternaard infill well, Lauwersoog East infill well, Moddergat infill well).

After the history matches are obtained, the model is ready for forecasting. The production profiles from Business Plan 2016 are taken and imposed on the wells.

The key changes to Business Plan 2015 are as follows. A longer production duration (until 2035) has been assumed for MGT-1,-2,-3 and ANJ-4 as a consequence of system-lifetime-extension caused by possible new well TRN-2. An extension of VHN-1 production to 2019 has also been incorporated. Furthermore, latest estimate on Nes Infill production (MGT-4 and MGT-5) was incorporated, which is significantly less than forecast in M&R2015.

Any changes to Business Plan 2016 will be covered in Chapter 6.

4.8 Translation into subsidence realisations

The Anjum, Ezumazijl and Metslawier fields (or Anjum fields) are mature fields and their subsidence has been thoroughly monitored. These fields therefore act as a calibration for the compaction coefficients of the neighbouring Waddenzee fields: Nes, Moddergat, the Lauwersoog fields and Vierhuizen.

An immobile aquifer results in higher aquifer pressures than is the case for a depleting aquifer. In order to match the observed subsidence, compaction coefficients will be higher for an immobile aquifer than for a depleting aquifer. It is the combination of different reservoir realisations for the Anjum fields versus the Waddenzee fields that form a deterministic subsidence scenario.

The results of the reservoir modelling work are combined with geomechanical parameters and calibrated to actual subsidence data. The way the separate reservoir model realisations are implemented in subsidence scenarios is described in Section 6.2.3.

5 UNCERTAINTY MANAGEMENT

Many of the parameters that are used as input into dynamic models have uncertainty. This section describes which uncertainties have been considered and how they have been implemented in the different realisations.

As described in Section 4.6.3, aquifer mobility has been used as the main uncertainty parameter, defining the low, base and high subsidence cases for each field (except for Nes, where vertical permeability was used). However, there are more dynamic properties with uncertainty ranges. The three distinct cases often required optimisation to generate a good history match. This was done by modifying the parameters described in Section 5.1 .

Uncertainty ranges have not been modified for M&R2014, except for relative permeability, described in Section 5.1.3.

5.1 Uncertainties

5.1.1 GIIP

In the Static domain, the main uncertainty parameters are GIIP and permeability. GIIP Different static parameters (Top structure, FWL, Net-over-gross, porosity and water saturation) determine the gas initially in place (GIIP). All these parameters have uncertainty in the mean and the distribution around the mean, as the parameter varies across the reservoir, especially away from the wells. Since the amount of wells in the Waddenzee area is rather limited, uncertainties can be significant. Taking all these into account separately is a laborious exercise and will not give a great deal of insight. It is therefore chosen to capture the GIIP uncertainty as a whole by changing only (1) the net pore volume (NPV), by a factor 0.9-1.1 from base case, and (2) the free water level (range dependent on field by field). When modifying the NPV by a large amount, the GIIP distribution might be distorted too much from reality. Therefore a high-structure case was also captured for the Nes and Moddergat fields to observe whether these matches were more plausible than the base-structure realisation.

Table 16 Gas initially in place, BNCM

Field	Low	Base	High
Anjum	11.2	16.6	17.6
Ezumazijl	1.2	2.1	1.9
Lauwersoog-Central	0.70	1.2	1.30
Lauwersoog-Oost	3.1	5.1	9.2
Lauwersoog-West	2.6	3.4	4.2
Metslawier	3.4	5.2	6.4
Moddergat	5.3	6.8	10.6
Nes	N/A ⁴	16.7	N/A

⁴ Since the new wells MGT-4A and MGT-5 were drilled, no new static probabilistic runs were performed.

5.1.2 Absolute permeability

Permeability is distributed by applying a porosity-permeability relation that applies to well or field. A large number of wells in the Waddenzee area have been cored and analysed. The porosity and permeability relation around the wells are therefore well established (Ref 1). But uncertainties, especially away from the wells, can be large.

Field-wide horizontal and vertical permeability multipliers have been used as sensitivity parameters. These sensitivity parameters are defined logarithmically, because of their exponential impact on pressure response. When applying this to assisted history matching (see Section 5.2) it makes the proxy more efficient. Uncertainty range generally varies between -0.5 and 0.5 in the log domain (or between a factor 0.3 and 3.0 of the multiplier).

5.1.3 Relative permeability

The relative permeability ranges that are used are as follows since M&R 2015 (see Ref 55).

Table 17 Relative permeability uncertainty range

Meet&Regel 2015, 2016			
Quantity	Low	Base	High
krw @ Sgr	0.01	0.1	0.3
ResGas = $S_{gr}/(1-S_{wc})$	0.15	0.30	0.45
krg @ Swc	0.84	0.84	0.84
Swc	<i>from capcurves – porosity dependent</i>		
Corey water	3	4.0	6
Corey gas	1	2.0	5

The specific values used may differ for every field (or realisation), specified in Section 6.1 .

Relative permeability has a significant impact on the water influx. The two most important parameters are residual gas saturation and the water permeability when the gas saturation has reduced to residual saturation. The first determines the point of water breakthrough. At higher values of the residual gas saturation, the water will more quickly bypass the gas towards the well. The water relative permeability at residual gas saturation mainly determines the rate of water production and influx. Core experiments on ANJ-1 are available (Ref 6) and show that (Figure 5) the residual gas correlates with the initial water saturation. This was taken along in defining the relative permeability model. The core experiments also show that (Figure 6) the water relative permeability endpoint is between 0.3 and 0.01.

The gas relative permeability end point is not varied, since modifying the absolute permeability has a similar effect.

Base case values for relative permeability are used as a starting point. The values are typical matching parameters: they are modified so as to ensure an optimum match, but are not seen as the key uncertainty to subsidence prediction.

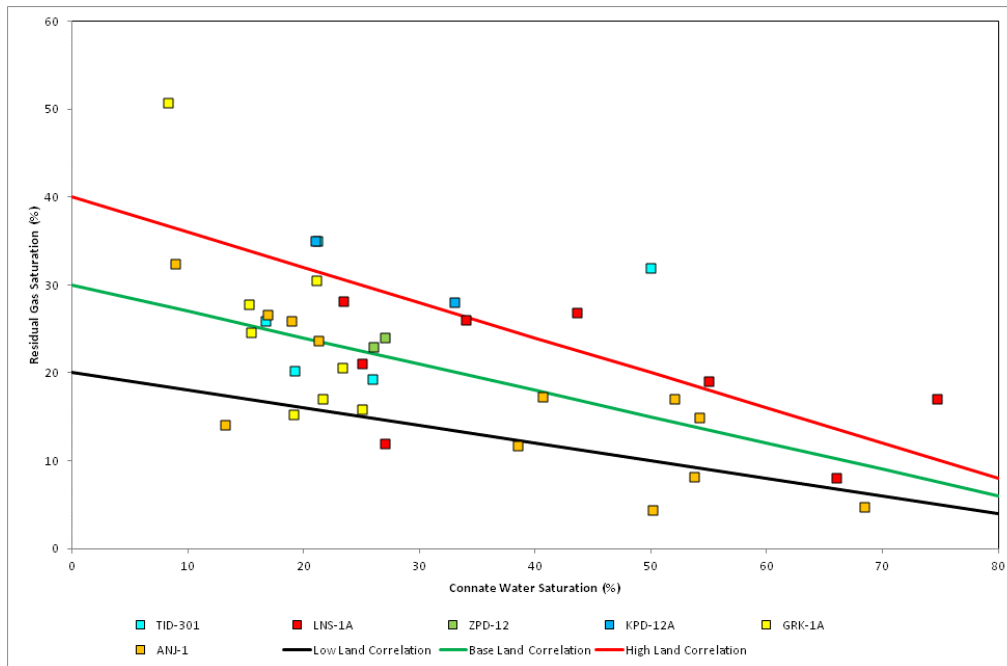


Figure 5 Residual gas saturation as a function of the connate water saturation

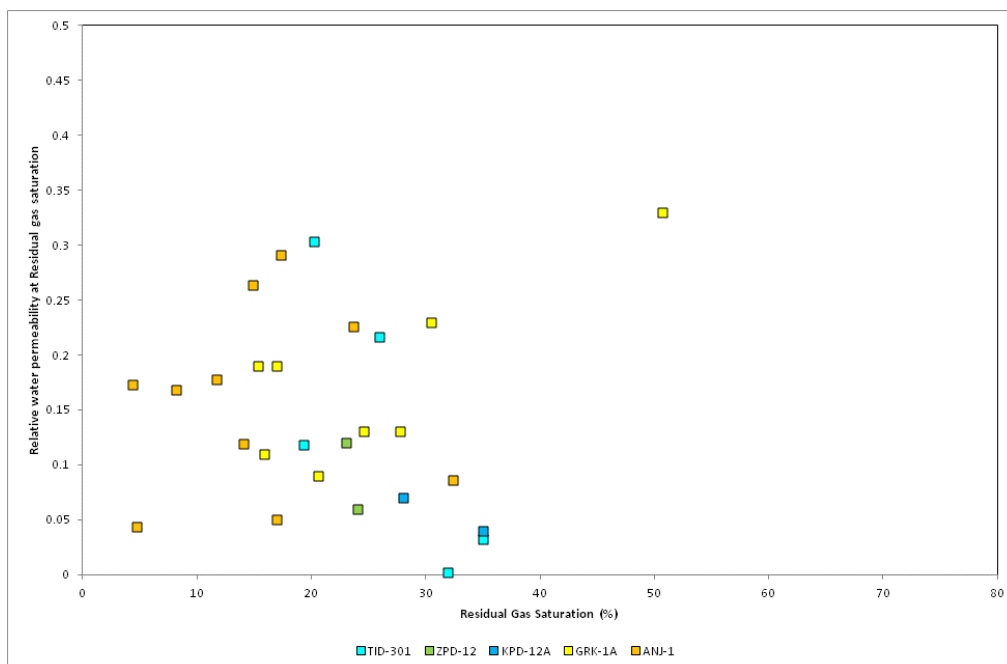


Figure 6 Relative water permeability at residual gas saturation as a function of the residual gas saturation.

5.1.4 Vertical permeability

Vertical permeability is often a poorly known quantity and is often very much dependent on vertical grid refinement, especially in vertically heterogeneous reservoirs. During the import of the static models to the dynamic simulator, as mentioned in Section 4.5, by default the vertical permeability k_v is set to 0.1 times the value of the horizontal permeability k_h . This represents a first guess for the “microscopic” k_v/k_h ratio, observed in core plugs. However, considering that vertical layers in the dynamic models (~1m) are much larger than core plugs (~5 cm), heterogeneities of the scale between these two dimensions are not captured. To overcome this, an extra k_v -multiplier is used, of which the value is poorly known beforehand

and hence is used as matching parameter. Typical values range from maximum 1 to minimum $\sim 10^{-3}$ (Ref 4).

5.1.5 Vertical heterogeneity

High porosity sand streaks have been observed. Because of their small size, these are difficult to detect and model. These layers can have high impact on inflow performance and water inflow. Only for Lauwersoog East and Lauwersoog West this uncertainty has been added, by having the freedom of multipliers on the low and high perm zones separately.

5.1.6 Faulting

Few intra-field faults have been observed. Only in Ezumazijl and possibly Moddergat faults are identified that have large sealing potential. The fault seal multiplier is, similar to the permeability multiplier, applied as a logarithmic sensitivity parameter.

5.1.7 Water encroachment behaviour

The parameters that have most impact on this behaviour apart from the static uncertainties in dip, free-water level and high permeable streaks, are residual gas and water relative permeability end point. These have been used as dynamic uncertainty parameters.

Residual gas saturation has an important effect on water behaviour: first, by increasing the saturation at which the gas phase will cease being mobile, more gas can be bypassed by the water resulting in early water breakthrough. Second, residual gas expands which results in an extra drive on the water.

5.2 Assisted history matching workflow

In order to assess the uncertainties with respect to the fields, a history matching workflow is set up in the SUM++ tool. This workflow is used to assist in assessing the impact of uncertainties on the history match. Since M&R2014, the results of this workflow are not directly implemented as a final history matched realisation, but simply used as a tool to quicken history matching and gain model insight.

SUM++ is a Shell propriety assisted history matching tool that manages the in- and output of several runs in order to create a polynomial approximation (the so-called 'proxy') of the input-output relation. This proxy is then used to explore the uncertainty parameter space.

The number of uncertainty parameters and the number of matching points determines the complexity of the proxy. Often this does not improve the predictive quality of the proxy. This is because most parameters counterbalance, and therefore the proxy behaviour is dominated by the most sensitive parameters. The best matches that are obtained from the assisted history matching workflow are therefore only meaningful for these most sensitive parameters.

Runs can be exported to Spotfire software, in order to explore cross-correlations by filtering the data. From the remaining subset of data, an insight can be given on to which solution the model converges.

6 DYNAMIC MODELLING

In this chapter, the history matches and production/pressure forecasts are discussed on a field-by-field basis.

6.1 Field models and history matching

The history matching results, uncertainties and opportunities are discussed per field. Also, a comparison is made between the models used for M&R2015 and M&R2016. For each field, a table is given with the most important variable values used each model.

6.1.1 Anjum

The Anjum field is located in the central onshore part of the Noord Friesland Concession (Lauwerszee Trough, NE-Netherlands). It was discovered in 1992 by ANJ-1, finding (virgin) pressure at 563 bara, which is strongly overpressured at a datum depth of 3850mTVNAP. In 1996-97 ANJ-4 was drilled as a horizontal production well. Both wells were drilled from the Anjum location and are producing since 1997 to the on-site Anjum facilities. At the time of drafting the report, more than 88% of the static and dynamic GIIP has been recovered.

The Rotliegend formation in the Anjum field consists of the Ten Boer Claystone Member (ROCLT), the Upper Slochteren Sandstone Member (ROSLU), the Ameland Claystone Member (ROCLA) and the Lower Slochteren Sandstone Member (ROSL). Only the ROSLU and the ROSLL contain sandstone of reservoir quality. They consist of aeolian and fluvial/lacustrine sediments deposited in a desert environment. The thickness of the ROSLU in ANJ-1 is 106.0 m. The Anjum gas field consists of two fault blocks. The main block is situated in the East, and the small block in the West contains only about 1% of the total GIIP. Detailed geology is described in the Geology section above.

The Anjum field (Figure 7) contains two wells, ANJ-1 and ANJ-4B. Dynamic data suggests that they are draining the same volume (Figure 8).

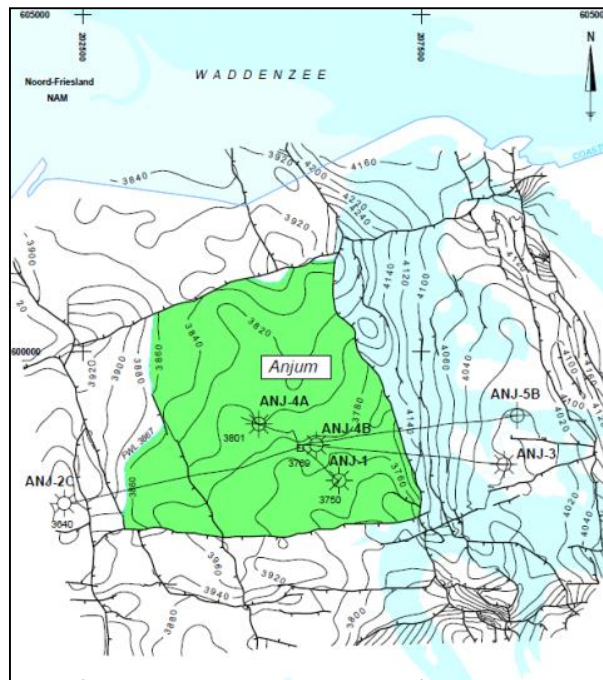


Figure 7 ARPR top ROSL map of Anjum field

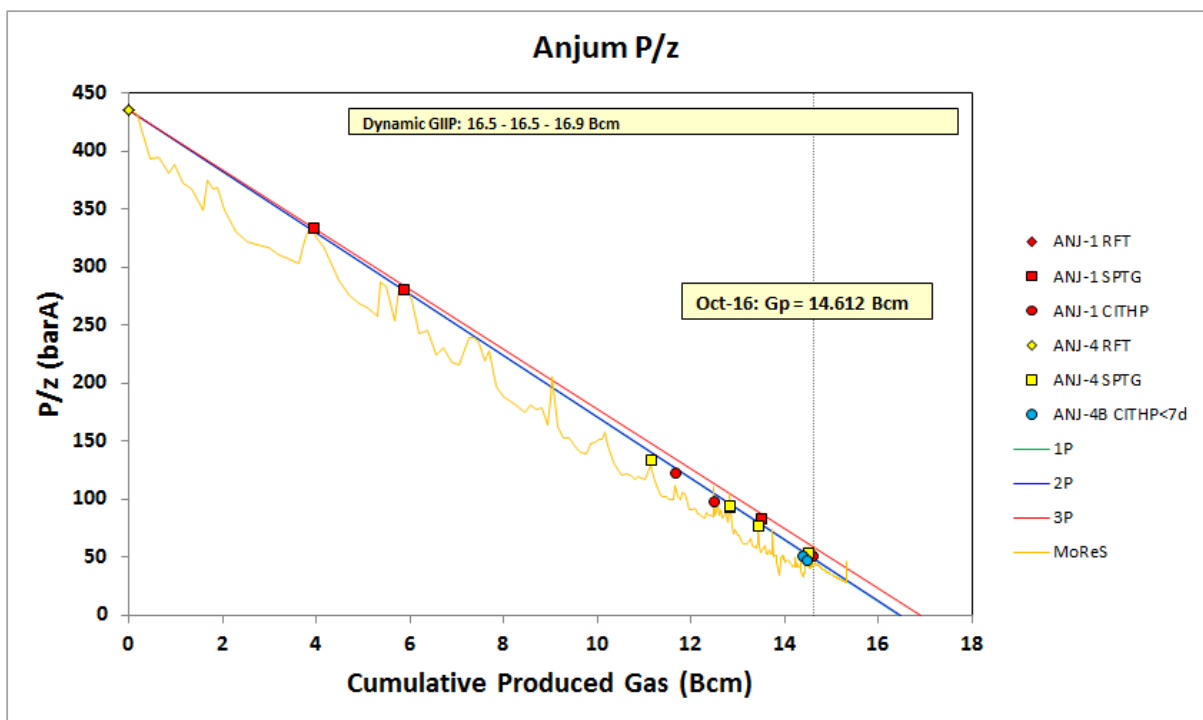


Figure 8 P/z plot Anjum-1 and Anjum-4 combined

ANJ-1 is more or less vertical and has ceased production in 2012 to a high hold-up depth (HUD). The high HUD is most likely related to sand production from Unit 2⁵, that has been perforated in 2006. Unit 2 has high porosity/permeability streaks embedded in shale layers. Restoring the well with a straddle over the high porosity units and a workover to replace the tubing was deemed not economic, since the other well, ANJ-4 is situated in the same hydraulic unit.

⁵ Unit 2 is a shale layer within the Rotliegend Upper Slochteren (ROSLU) that is deemed laterally extensive throughout the entire Waddenzee area. Flow is known to be significantly baffled if not sealing between the Unit 1 on top of it and Unit 3-6 below.

ANJ-4B is a more or less horizontal well, which is currently the only producer of the Anjum field. Unit 2 has not been perforated in this well. Since 2015, this well has been periodically water soaked to avoid salt scaling in the well. The result was a not only a higher uptime, but also improved inflow of the well.

6.1.1.1 Reservoir model

As is shown in Figure 9 and Figure 10, a good history match was achieved on downhole pressure.

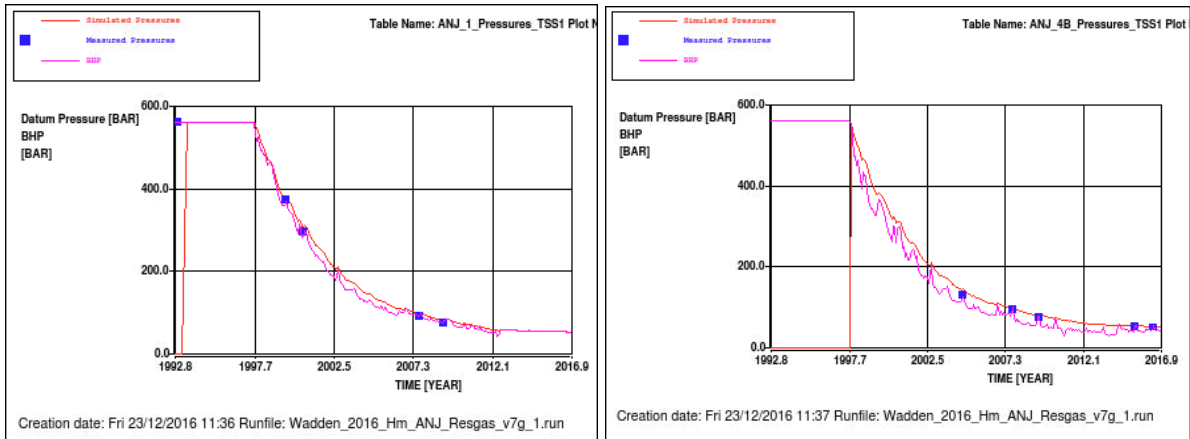


Figure 9 Simulated pressure (red line), simulated BHP (violet line) and measured down hole pressure (blue squares) for base case. Left: ANJ-1, Right: ANJ-4B.

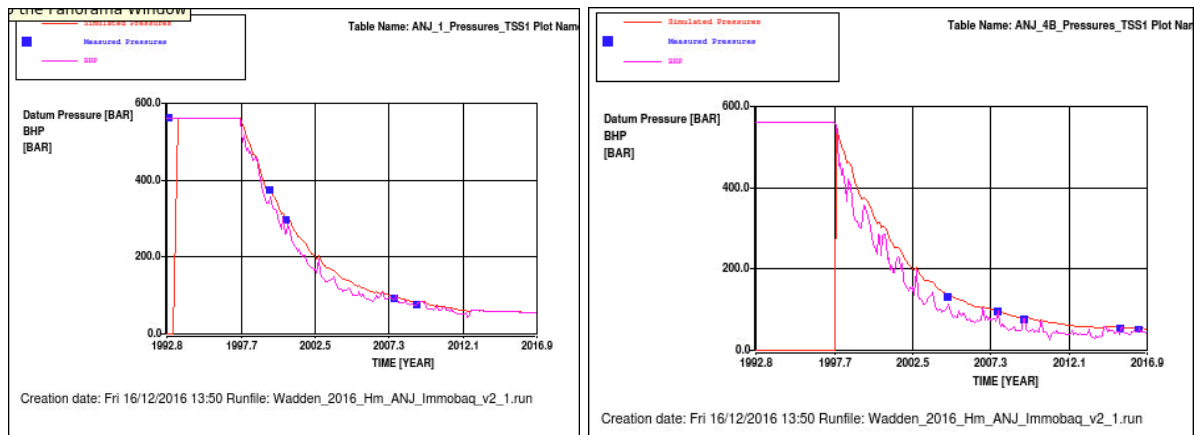


Figure 10 Simulated pressure (red line), simulated BHP (violet line) and measured down hole pressure (blue squares) for low case. Left: ANJ-1, Right: ANJ-4B.

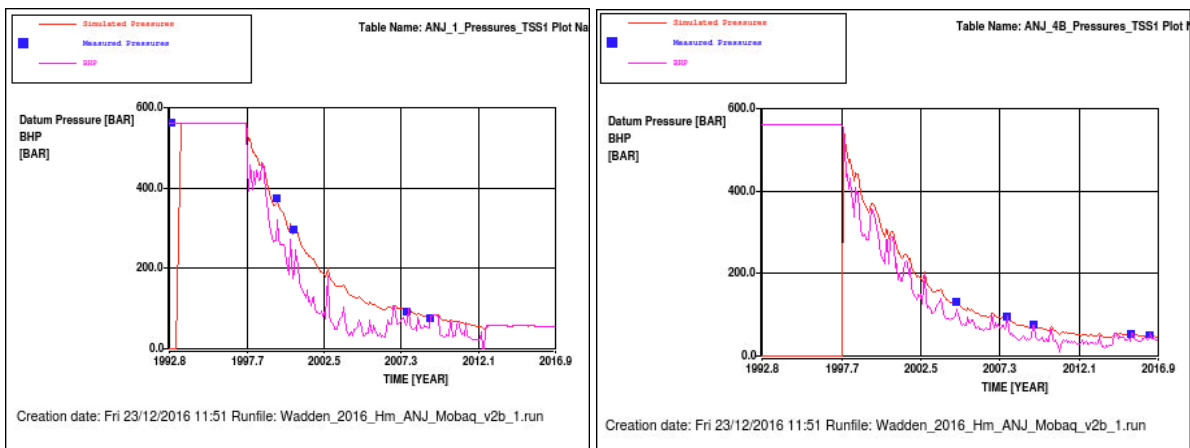


Figure 11 Simulated pressure (red line), simulated BHP (violet line) and measured down hole pressure (blue squares) for high case. Left: ANJ-1, Right: ANJ-4B.

The match on tubing-head pressures in ANJ-4B is shown in Figure 12. It is clear that the historical inflow performance is well matched.

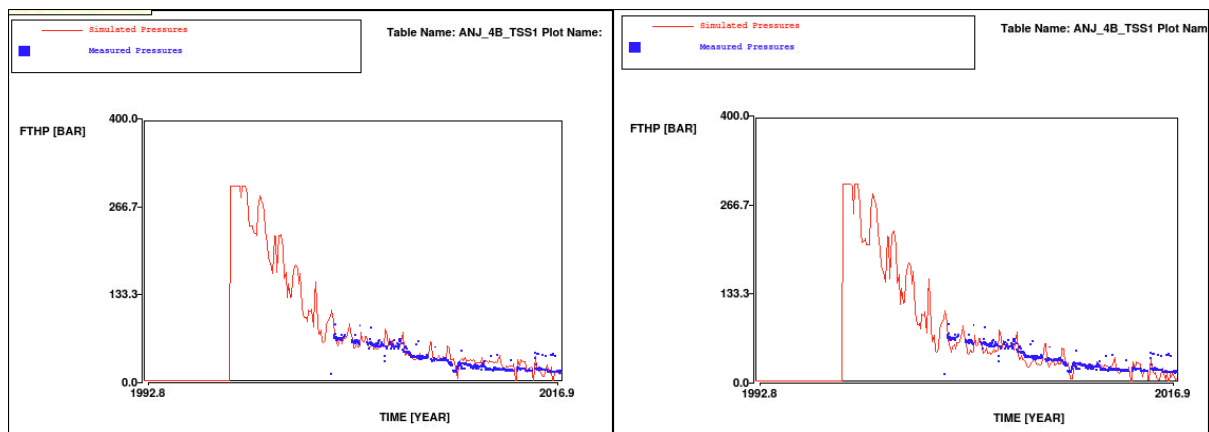
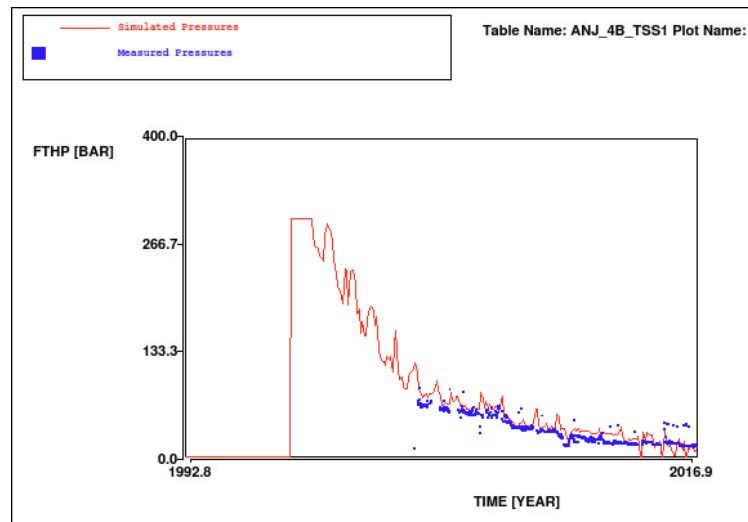


Figure 12 Simulated (red line) and measured (blue squares) FTHP data in ANJ-4B. Top: base case. Left: low case. Right: high case.

In ANJ-1, a PLT has been run in 1997 and the match is shown in Figure 13. A decent match was obtained. It indicates that in the bottom a high permeable layer has not been fully captured. Considering that the inflow performance in ANJ-4B has been captured well, this is not considered an issue.

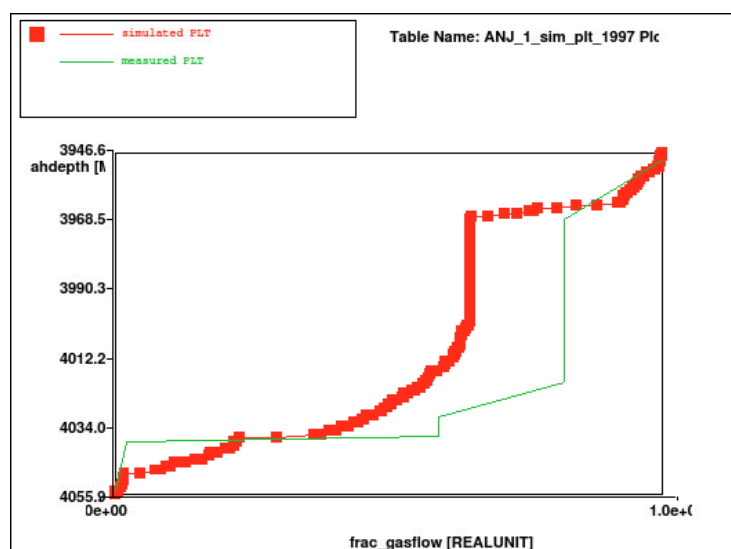


Figure 13 Simulated (red line + squares) and measured (green line) PLT in ANJ-1. Base case model.

The Anjum field has a good history match. The history matching parameters used are shown in Table 18.

Table 18 History matching parameters used for the Meet & Regel cycle for Anjum.

Parameter	Static base	Low M&R2016 ⁶	Mid M&R2016 ⁷	High M&R2016 ⁸	Low M&R2015 ⁹	Mid M&R2015 ⁹	High M&R2015 ⁹
Residual gas sat. below FWL	0.12	0	0.06	0	0	0.06	0
GBV multiplier	1.0	1.00	0.97	0.99	0.98	0.96	0.97
k_h multiplier	1	0.49	0.79	0.13	0.49	0.56	0.13
k_v multiplier	NA	0.032	0.014	0.20	0.032	0.014	0.20
FWL (m TVNAP)	3867±3	3868	3868	3868	3870	3870	3870
k_h multiplier aquifer	1	1. 10⁻⁴	0.1	1	1. 10⁻⁴	0.1	1
k_v multiplier aquifer	1	1. 10⁻⁴	0.1	1	1. 10⁻⁴	0.1	1
Fault I_2 transm.	N/A	0.1	0.1	0.91	0.1	0.1	0.91
Residual gas	0.30	0.30	0.15	0.20	0.30	0.15	0.1
$k_w@S_{rg}$	0.1	0.1	0.05	0.1	0.1	0.08	0.1
Skin since water soaks	-	-4	-4	-4	0	0	0

Overall, the values of the dynamic modelling parameters are well within the expected uncertainty range. A permeability multiplier of between 0.13 and 0.79 is acceptable, accounting for heterogeneities within gridblocks. Although the mid case, with the permeability multiplier closest to unity, has the preference.

The base-case model has a paleo-residual-gas saturation somewhat lower than expected. Inserting the expected value of 12% strongly overestimated the pressure support from the

⁶ Input deck: Wadden_2016_ANJ_Immobaq_v2.INP

⁷ Input deck: Wadden_2016_ANJ_Resgas_v7g.INP

⁸ Input deck: Wadden_2016_ANJ_Mobaq_v2b.INP

⁹ Input deck: Wadden_2015_ANJ_MRN_v2.INP

aquifer. Adjusting relative permeability parameters did not have the desired effect. Hence the value was decreased to 6%. This figure is not unreasonable: the aquifer of Anjum has not been logged, hence the estimate was based on analogue wells. One important analogue well, ANJ2C in the Metslawier field, measured only 6% gas saturation below FWL.

The intra-field fault, running in N-S direction, appears not to be sealing. A slight baffle (0.1) is modelled in the base case (immobile aquifer) model, but this is not substantial. The static GIIP has already been updated (increased) due to dynamic input. A sealing fault will imply an even higher GIIP, which appears unlikely.

6.1.1.2 Meet & Regel cycle 2015 vs 2016 model comparison

Some changes have been made to the 2015 models as can be seen in Table 18. The free-water level was adjusted somewhat to align better with its base case value. This was compensated with a Gross Block Volume (GBV) revision approaching unity and a slight modification of the water permeability end-point. Secondly, due to the improved inflow performance since periodic water soaks have started in 2015, a negative skin was applied to the well. Also the lateral permeability was somewhat modified to match later life well performance.

6.1.1.3 Water production

Water production for the base case realisation has been nicely matched (Figure 14).

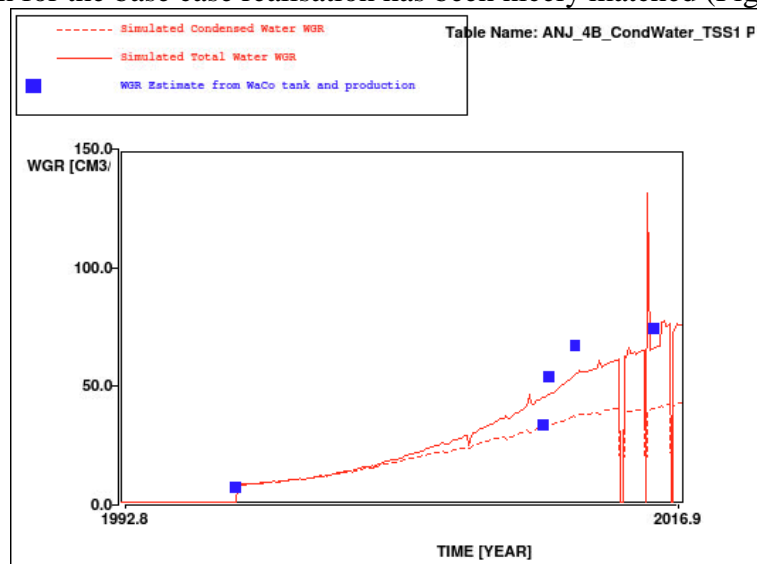


Figure 14 Simulated total WGR (red solid line), simulated condensed WGR (red dashed line) and estimated WGR from production and WaCo tank observations (blue squares) for ANJ-4B. Base case realisation.

6.1.2 Ezumazijl

The Ezumazijl field forms part of the deepest graben trend in the Lauwerszee Trough. It was discovered by ANJ-3 in 1998, finding virgin pressures at 493 bara. Ezumazijl was brought on-stream in February 1999, with ANJ-3 hooked-up to the on-site Anjum facilities. The field is fully covered by a 3D Pre-SDM seismic dataset.

Ezumazijl is a down-thrown Rotliegend fault block. ANJ-3 encountered approximately 121 m of gas bearing sandstone in the Rotliegend Upper Slochteren, which consists of aeolian and fluvial/lacustrine sediments deposited in a desert environment.

The field consists of the Ezumazijl main block and a smaller block to the Southeast. Two faults run to the south and to the north of the well ANJ-3 and separate the main field into a northern, a central and a southern lobe. A material balance analysis indicates the faults act as

a seal or at least a baffle to gas flow, however some uncertainty remains and will be addressed through material balance analysis after prolonged production.

Ezumazijl field (Figure 15) contains three wells, ANJ-3, ANJ-5B and ANJ-6, of which only ANJ-3 is producing. Its P/z plot can be found in Figure 16. ANJ-5B was drilled in the northern flank of the field and found initial pressures. Due to the small and low saturation gas column, it was decided to abandon ANJ-5 (Ref 7). In 2014, the southern block was drilled by the ANJ-6 wells and found a mere 20m of gas column, with poorer reservoir quality than expected. The pressure acquired was around 480 bara, which is almost virgin, indicating poor connectivity between the ANJ-6 well and the producing ANJ-3.

The Ezumazijl field is relatively tight: slow pressure build-ups have been observed. Flow is dominated by unit 2 that has the highest permeability.

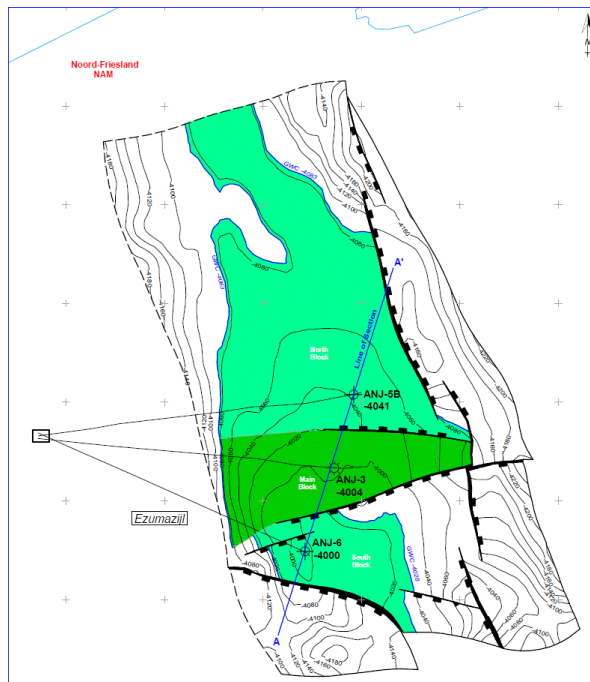


Figure 15 Ezumazijl ARPR top ROSL map

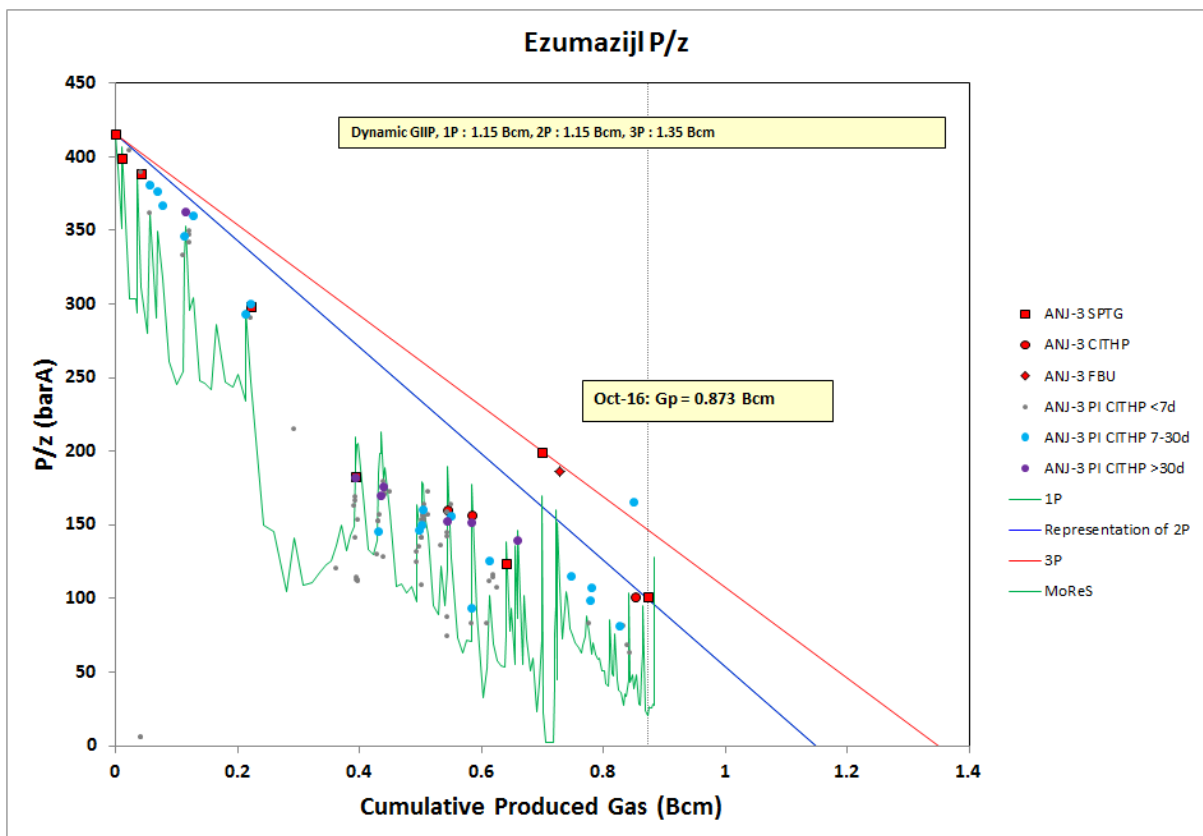


Figure 16 P/z plot ANJ-3

6.1.2.1 Reservoir model

Downhole pressures in Ezumazijl are matched as shown in Figure 17.

In order to achieve a match, both the fault between ANJ-3 and ANJ-5B, and the fault south of ANJ-3 needed to be practically closed to act as baffles. The high initial pressure of ANJ-6 (south of ANJ-3) backs this observation. The other history matching parameters used for the different models are shown in Table 19.

Since the drilling of Anjum-6 in 2014, there has not been a static model update. However, since the faults were closed anyway, no changes were needed to get a correct model representation.

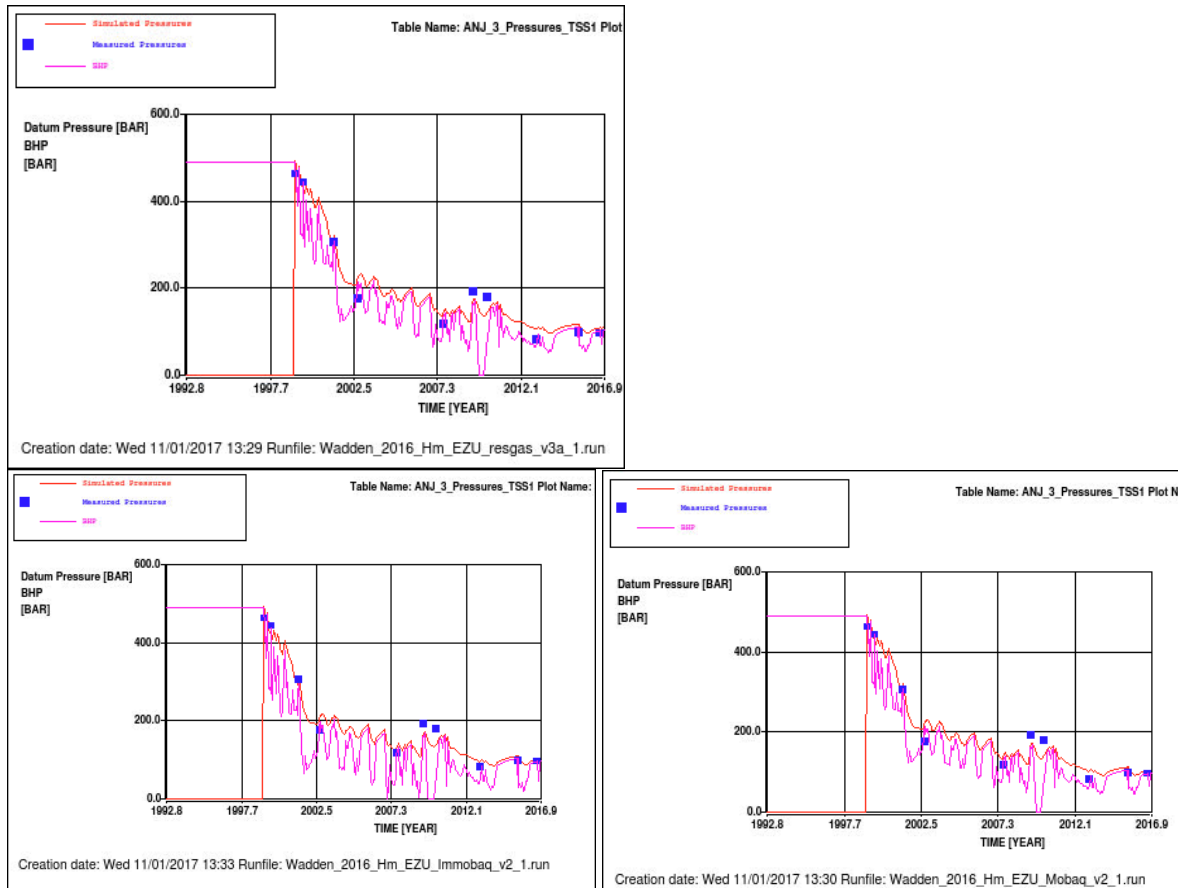


Figure 17 Simulated pressure (red line), simulated BHP (violet line) and measured (blue squares) downhole pressure data in ANJ-3. Top: base case. Left: low case. Right: high case.

The historic pressures show that around 2009, higher pressures were seen than before. It is currently believed that the higher pressures observed in the well are related to more tight layers in the reservoir. Due to sand production from the high permeable streaks, part of the high permeability perforations were closed off. That resulted in pressures in the well to be dominated by more tight, higher pressure layers. After clean-out and reperforation of high permeable layers, pressures returned to original trend.

Historical well performance has been decently matched as is shown in Figure 18.

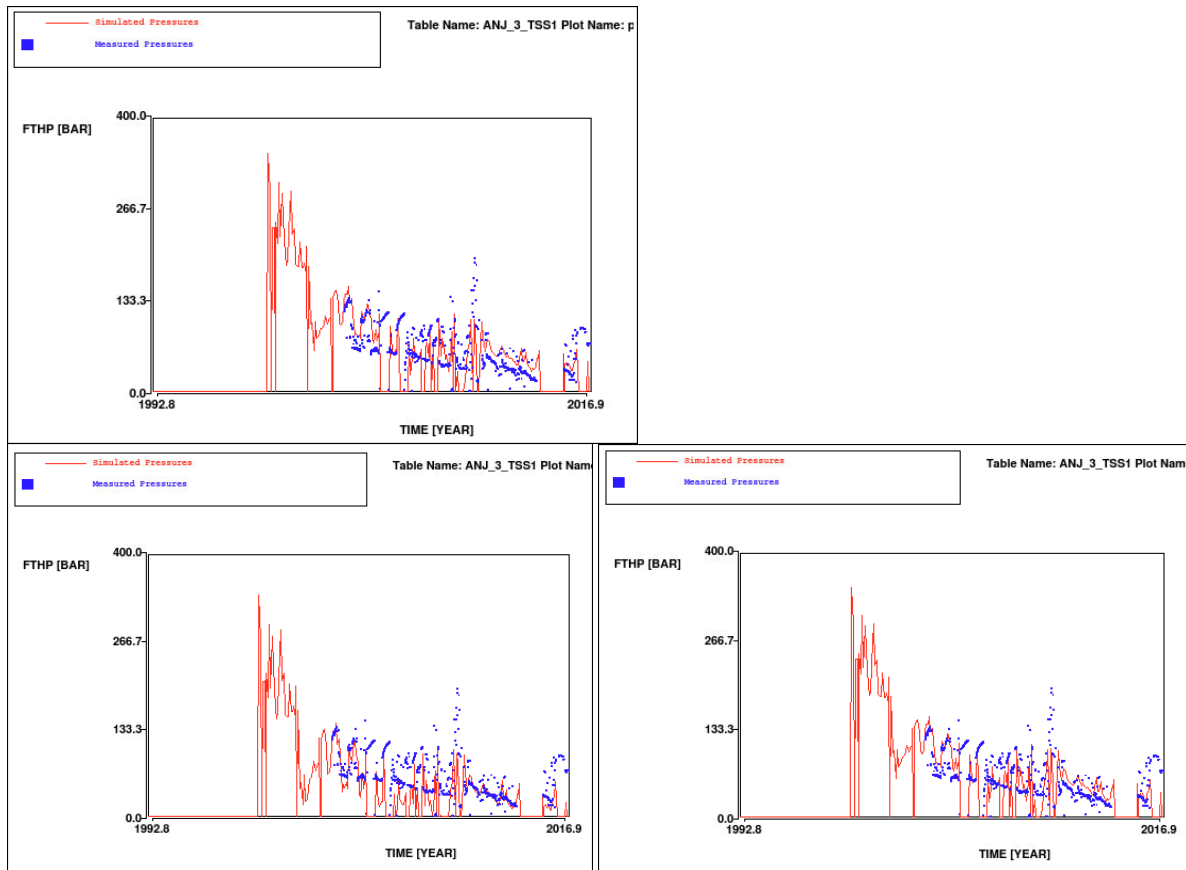


Figure 18 Simulated (red line) and measured (blue squares) flowing tubing head pressures in ANJ-3. Top: Base case. Left: Low case. Right: High case.

The reservoir has quite some permeability contrast, but this is well matched as is shown by the PLT match in Figure 19.

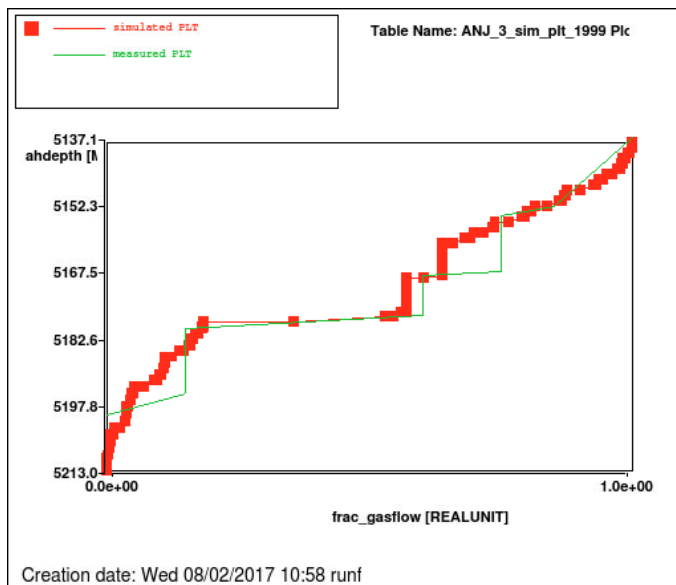


Figure 19 Simulated (red line + squares) and measured (green line) PLT in ANJ-3

An overview of matching parameters can be found in Table 19.

Table 19 History matching parameters used for the Meet & Regel cycle for Ezumazijl.

Parameter	Static	Low M&R2016 ¹⁰	Base M&R2016 ¹¹	High M&R2016 ¹²	Low M&R2015 ¹³	Base M&R2015 ¹³	High M&R2015 ¹³
Residual gas below FWL	0.17	0	0.17	0	0	0.17	0
GBV multiplier	1.0	0.93	0.85	0.85	0.93	0.85	0.85
k_h multiplier	1	0.40	0.40	0.40	0.40	0.40	0.40
k_v multiplier	N/A	$1.0 \cdot 10^{-3}$					
GWC (m TVNAP)	4083	4080	4080	4080	4080	4080	4080
Fault Seal N	N/A	10^{-7}	10^{-7}	10^{-7}	10^{-7}	10^{-7}	10^{-7}
Fault Seal S	N/A	10^{-6}	10^{-6}	10^{-6}	10^{-6}	10^{-6}	10^{-6}
k_h multiplier aquifer	N/A	$1.2 \cdot 10^{-4}$	0.1	1	$1.2 \cdot 10^{-4}$	0.1	1
k_v multiplier aquifer	N/A	$1.8 \cdot 10^{-4}$	0.1	1	$1.8 \cdot 10^{-4}$	0.1	1
Residual gas	0.30	0.43	0.20	0.20	0.43	0.20	0.20
$k_w@S_{rg}$	0.1	0.1	0.1	0.1	0.1	0.1	0.1

Since faults have been closed and the aquifer of Ezumazijl is not laterally extensive, vertical permeability has a large impact on the subsidence cases, but since the vertical perm was already set to a minimum (10^{-3}), the GBV multiplier was altered to ensure a good pressure response for the base and high case models.

All in all, average pressure drop and the induced subsidence for Ezumazijl is minimal.

6.1.2.2 Meet & Regel cycle 2015 vs 2016 model comparison

No changes have been made to the model since M&R 2015.

6.1.2.3 Water production

Water production has not been specifically matched on, but the match is good. In ANJ-3 the salt scaling suggest that indeed formation water is being produced. The estimated WGR and modelled WGR are shown in Figure 20.

¹⁰ Input deck: Wadden_2016_EZU_Immobaq_v2.INP

¹¹ Input deck: Wadden_2016_EZU_resgas_v3a.INP

¹² Input deck: Wadden_2016_EZU_Mobaq_v2.INP

¹³ Input deck: Wadden_2015_EZU_MRN_v2.INP

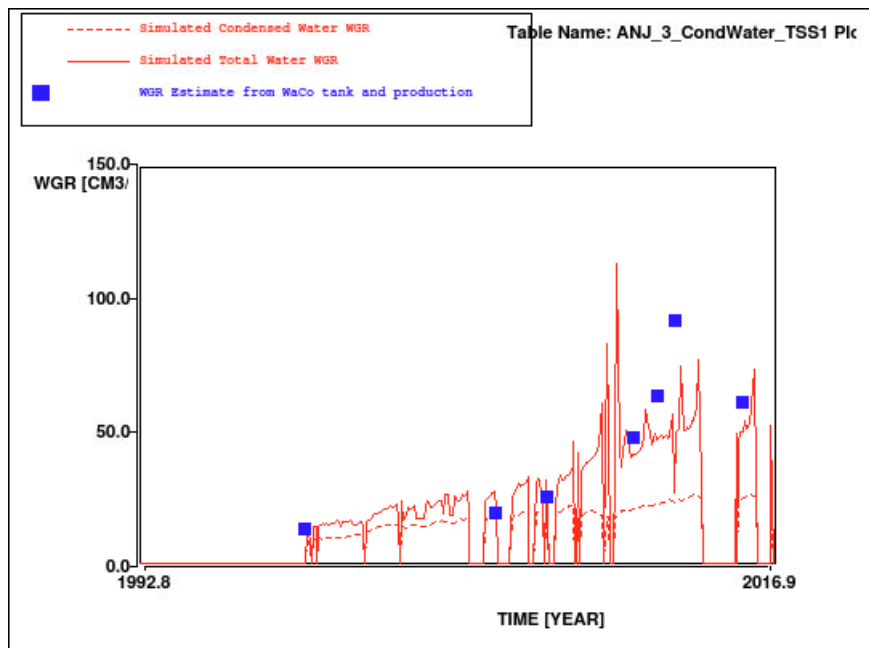


Figure 20. Simulated total WGR (red solid line), simulated condensed WGR (red dashed line) and estimated WGR from production and WaCo tank observations (blue squares) for ANJ-3. Base case realisation.

6.1.3 Lauwersoog Central

Lauwersoog-Central is the most western Lauwersoog block (Figure 21). It was discovered in 1997 by the well LWO-2 and found initial pressure at 500 bara. LWO-2 was brought on stream in 2012. The well is drilled on the low side of the structure.

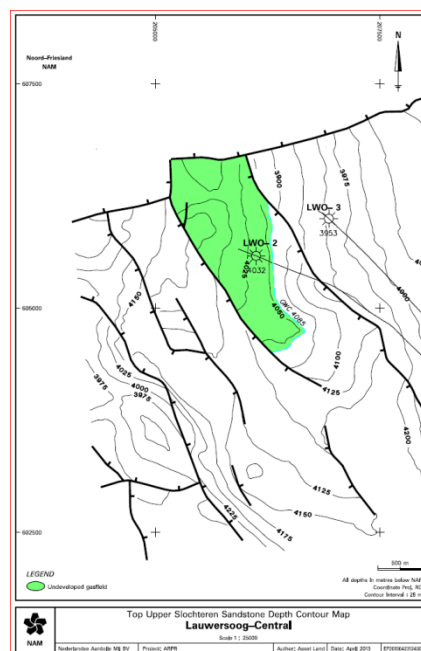


Figure 21 Lauwersoog-Central ARPR top ROSL map

Its P/z plot can be found in Figure 22. LWO-2 is currently producing intermittently.

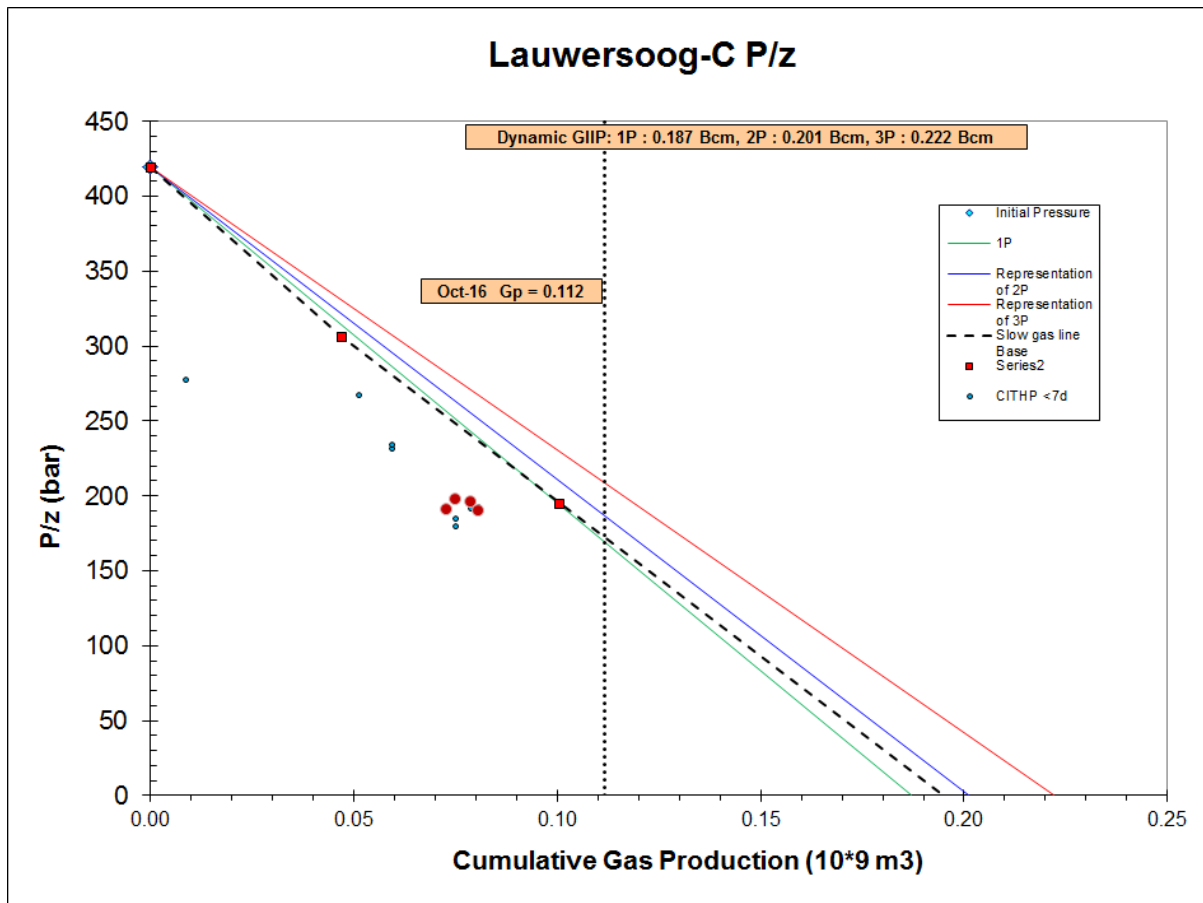


Figure 22 P/z plot for LWO-2.

6.1.3.1 Reservoir model

For the Lauwersoog-Central –East and –West field, as described in Section 4.3.1, the shut-ins are modelled to the nearest day, and therefore BHP can be used for history matching. Since initial production, a fish (an obstruction) has been stuck in the well. Due to this, the well model might not reflect the true pressure drop over the well. Therefore, the flowing THP match is not strictly matched upon. Moreover, the intermittent production of this well causes near-well behaviour and water production to be difficult to model.

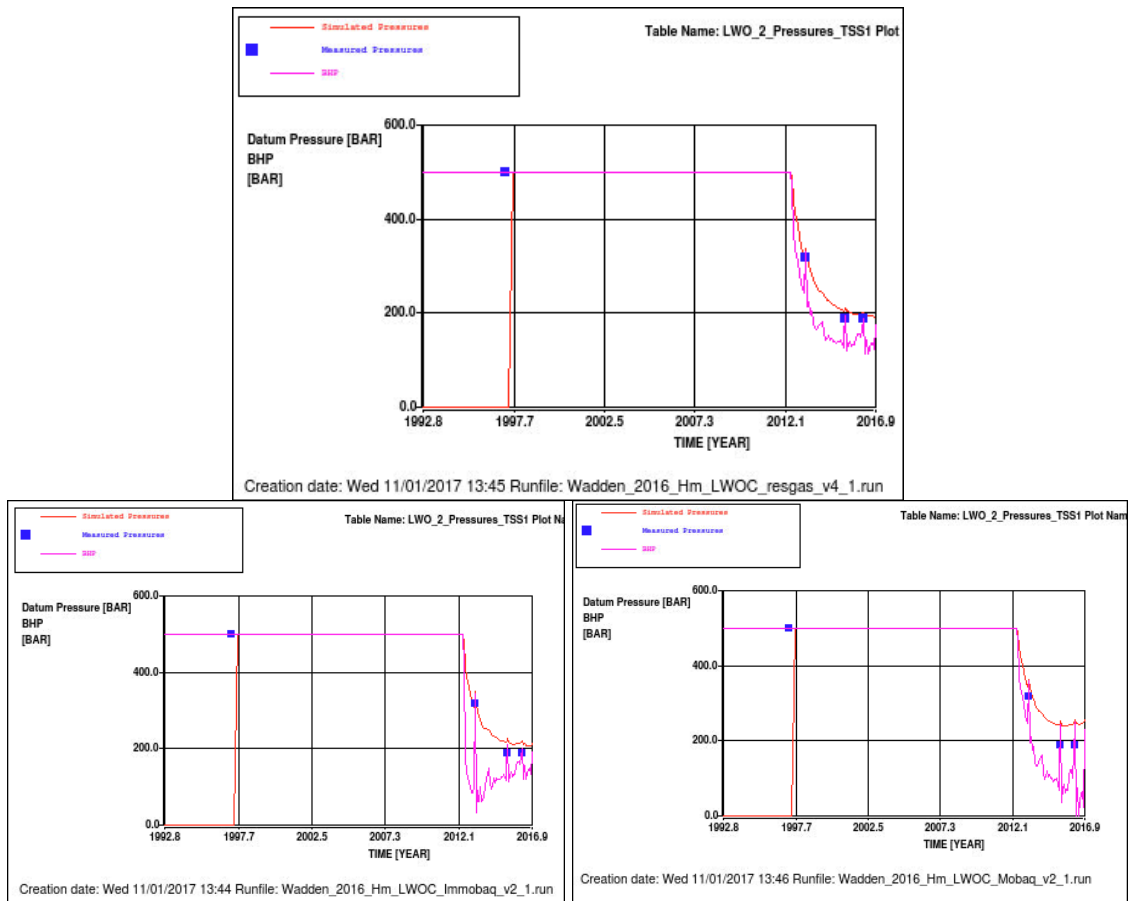


Figure 23 Simulated pressure (red line), simulated BHP (violet line) and measured (blue squares) downhole pressure data in LWO-2. Top: base case. Left: low case. Right: high case.

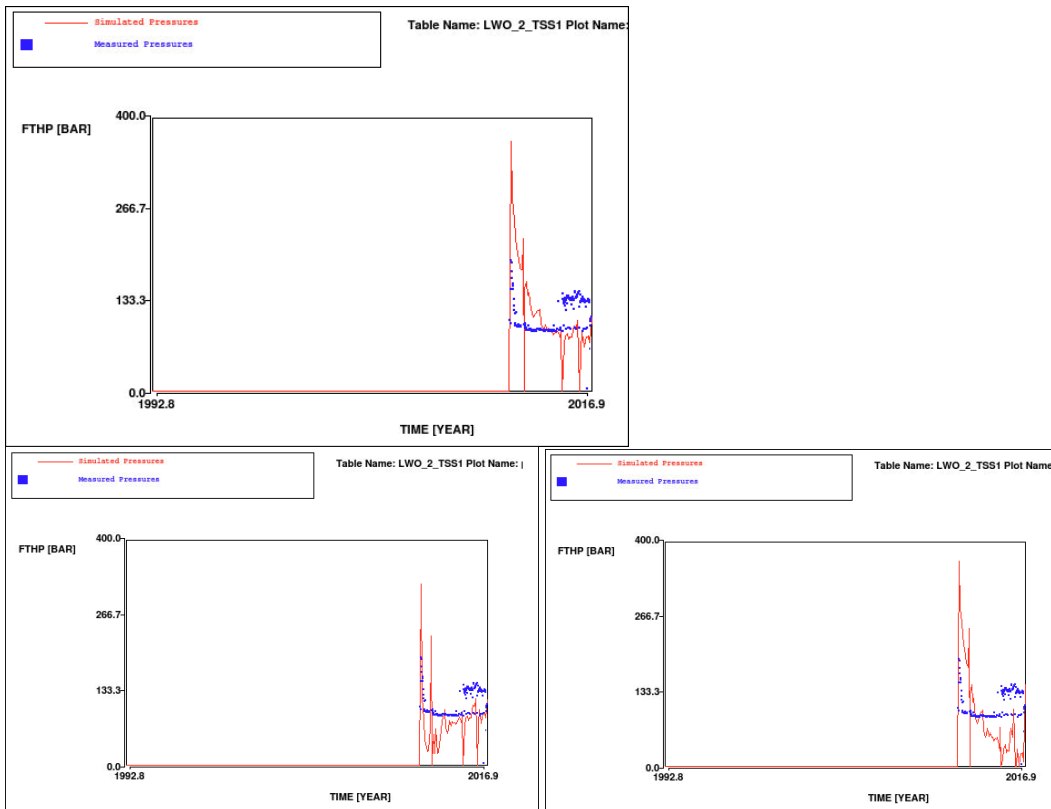


Figure 24 Simulated (red line) and measured (blue squares) flowing tubing head pressures in LWO-2. Top: base case. Left: low case. Right: high case.

From Figure 23 and Figure 24, it can be seen that history match of this field is not ideal. The immobile aquifer realisation (low) and the residual gas saturation realisation (base) give a better match than the mobile aquifer realisation. The mobility of the aquifer mainly causes water encroachment, affecting the relative permeability around the wellbore. To keep an acceptable BHP match, the absolute permeability must increase for the mobile aquifer realisation, which takes its toll on the THP match. This is a good example of a field where dynamic data suggests that the aquifer cannot be as mobile as the gas leg.

In Table 20, the parameter settings are shown that are used to get a match for the field. To get a reasonable match, the GIIP is lowered significantly. Moreover, the k_h is significantly lower than expected, although, probably due to the contrasts in permeability that have not been entirely captured. Also, the FWL is deeper to keep out formation water.

Table 20 History matching parameters used for the Meet & Regel cycle for Lauwersoog C.

Parameter	Static	Low M&R2016 ¹⁴	Base M&R2016 ¹⁵	High M&R2016 ¹⁶	Low M&R2015 ¹⁷	Base M&R2015 ¹⁸	High M&R2015 ¹⁸
Residual gas below FWL	0.24	0	0.24	0	0	0.24	0
GBV multiplier	1	0.86	0.90	0.86	0.86	0.90	0.86
k_h multiplier	1	0.18	1	0.56	0.18	1	0.56
k_v multiplier	N/A	1.6 10⁻⁴	1.5 10⁻⁴	1.6 10⁻⁴	1.6 10⁻⁴	1.5 10⁻⁴	1.6 10⁻⁴
FWL (m TVNAP)	4074	4079	4067	4079	4079	4067	4079
k_h multiplier aquifer	N/A	1.0 10⁻⁴	0.1	1	1.0 10⁻⁴	0.1	1
k_v multiplier aquifer	N/A	1.0 10⁻⁴	0.1	1	1.0 10⁻⁴	0.1	1
Residual gas	0.3	0.25	0.30	0.25	0.25	0.27	0.25
$k_w@S_{rg}$	0.1	0.1	0.09	0.1	0.1	0.09	0.1
LWO-2 Skin	-	1.0	1.0	1.0	0	0	0

The base case model, using residual gas below FWL, is not trivial to match. A lot of problems occur with water approaching the well, which would create large relative permeability effects that are not reflected in the THP data. Therefore absolute permeability is not discounted (multiplier = 1) and GBV multiplier is also higher than for low and high subsidence cases. To still be able to calibrate the model with pressure data, a lower GIIP is created by assuming a shallow contact (4067 versus 4074mTVNAP base case). Considering the small pressure drop in this field (on average only a depletion of under 40 bar for the high

¹⁴ Input deck: Wadden_2016_LWOC_Immobaq_v2.INP

¹⁵ Input deck: Wadden_2016_LWOC_resgas_v4.INP

¹⁶ Input deck: Wadden_2016_LWOC_Mobaq_v2.INP

¹⁷ Input deck: Wadden_2015_LWOC_MRN_v2.INP

¹⁸ Input deck: Wadden_2015_LWOC_MRN_v3.INP

case after forecasting) it was decided to keep this realisation, even though the match is not ideal. Indeed this base case is situated between the low and high case after forecasting (Section 6.2.2.2).

6.1.3.2 Meet & Regel cycle 2015 vs 2016 model comparison

The main change made to M&R2015 is the inclusion of a positive skin, to mimic poorer inflow due to the stuck fish in the well. A minor change is the residual gas saturation of the base case model from 0.27 to 0.30, to optimise for latest production and pressure history.

6.1.3.3 Water production

Lauwersoog-Central has only been producing since 2012. Due to the short history and the relatively low rates, it is difficult to detect formation water. Hence, the water-gas-ratios estimated from the change in WaCo tank level as given in Figure 25, have large uncertainties. However, the proximity of the well to the water because of its downdip position, does give a large risk of water breakthrough. This is also suggested by dynamic simulation.

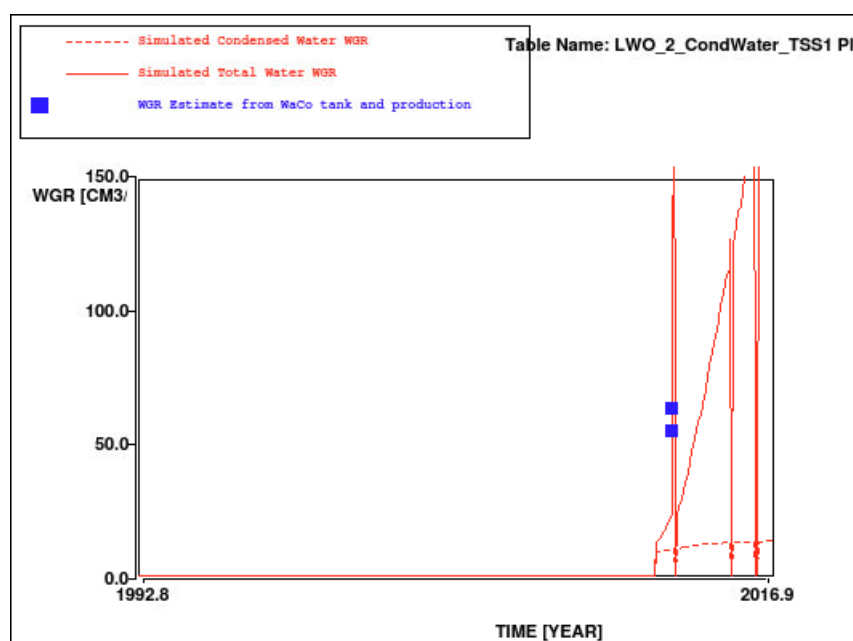


Figure 25 Simulated total WGR (red solid line), simulated condensed WGR (red dashed line) and estimated WGR from production and WaCo tank observations (blue squares) for LWO-2. Base case realisation.

6.1.4 Lauwersoog-Oost

The Lauwersoog-Oost field (Figure 26) lies beneath the Waddenzee at the eastern end of the Noord Friesland concession. It was discovered in 1996 by the well LWO-1 and brought online in November 2008. It found initial pressures at 481 bara. The gas is evacuated to the Anjum facilities. Its P/z plot can be found in Figure 27.

The Lauwersoog Oost gas field is a fault / dip closed structure at Base Zechstein level on the Vierhuizen-Munnekezijl trend. LWO-1 well encountered approximately 78 m of gas bearing Rotliegend Upper Slochteren (ROSLU) reservoir, which consists of aeolian and fluvial/lacustrine sediments deposited in a desert environment. The thickness of the ROSLU in LWO-2 is 113 mTV (gross).

Seismic indicates a saddle structure with the most crestal points on the edges of the structure, although – with only well in the structure – this has not been confirmed by well penetration.

The free water level has been found in the lower units of the structure. It is unknown whether the shallower ROSLU1 layer is sharing its FWL.

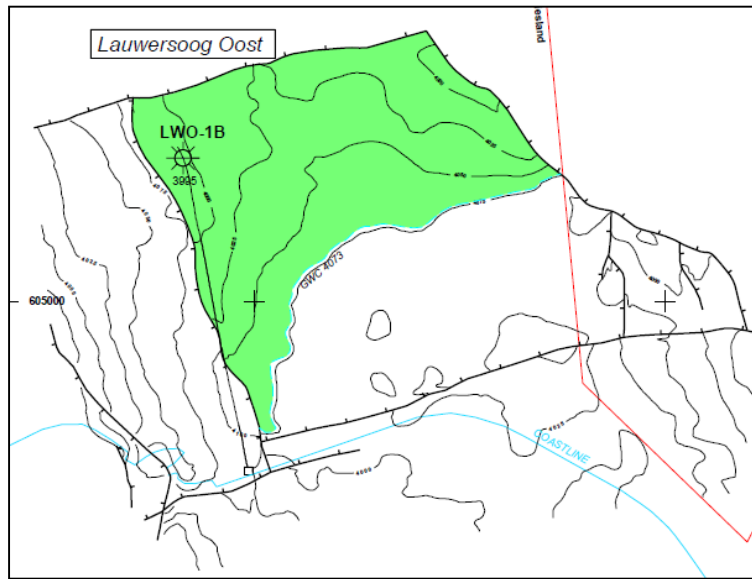


Figure 26 Lauwersoog-Oost ARPR top ROSL map

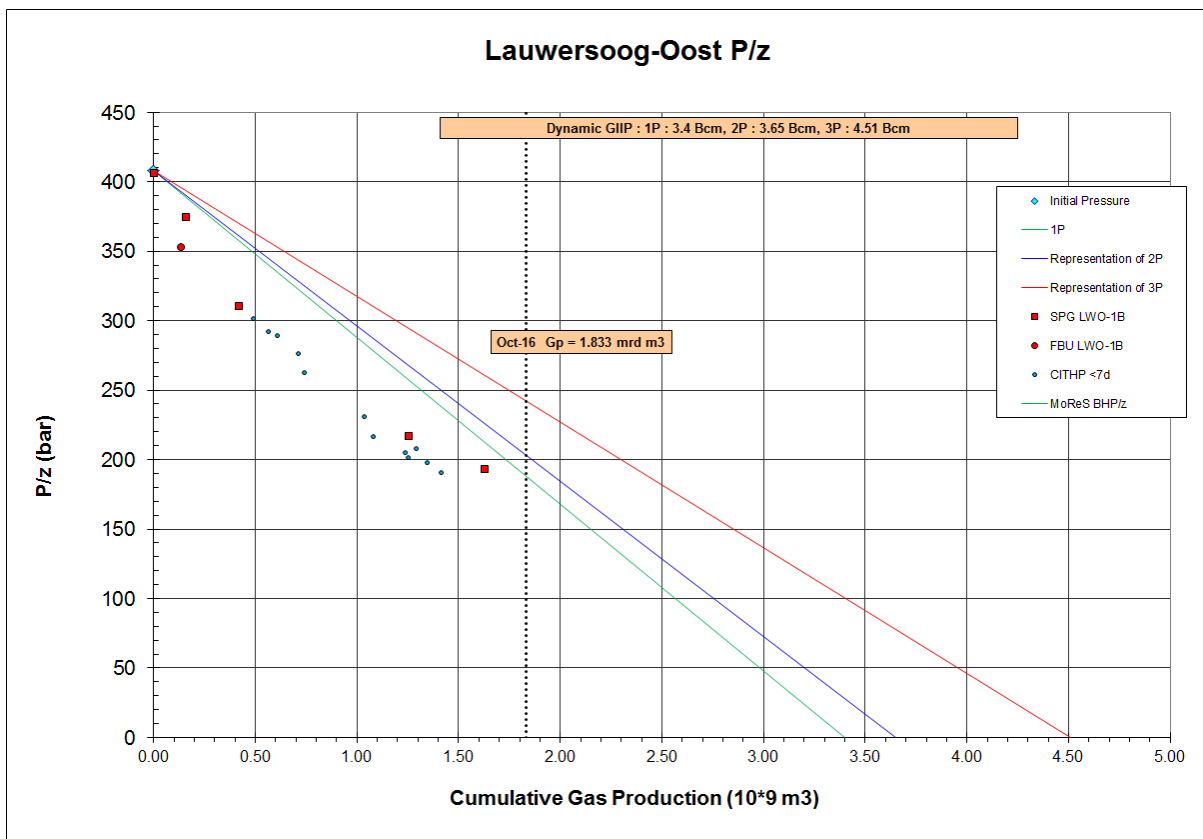


Figure 27 P/z plot for LWO-1B

6.1.4.1 Reservoir model

The material balance for Lauwersoog-Oost indicates that not the entire static volume seems to be connected. However, dynamic 3D simulation volumes are in line with static volumes since no GBV multiplier was needed to match the data (Table 21). Permeability for this field is not infinite and considering the lateral extent of the field, with only one producer, it is believed that an amount of gas on the eastern flank of the structure is effectively not being

drained. Model permeability is in line with static properties. The sensitivity on vertical permeability to the history match indicates that the permeability contrasts are important.

A PLT was done in 1997 (Figure 28), which indicated that the top layers contribute most to the flow. In order to obtain a match in the model, the permeability of the top 14 layers is increased by a factor 5 with respect to the other layers. This is most likely due to a number of high permeable streaks that have not been fully captured. The PLT was repeated in 2014, showing that vertical flow distribution of the model is still reasonably in line with measurements. The portion of production from the lower units is increasing over time, pointing towards differential depletion between the top and bottom units.

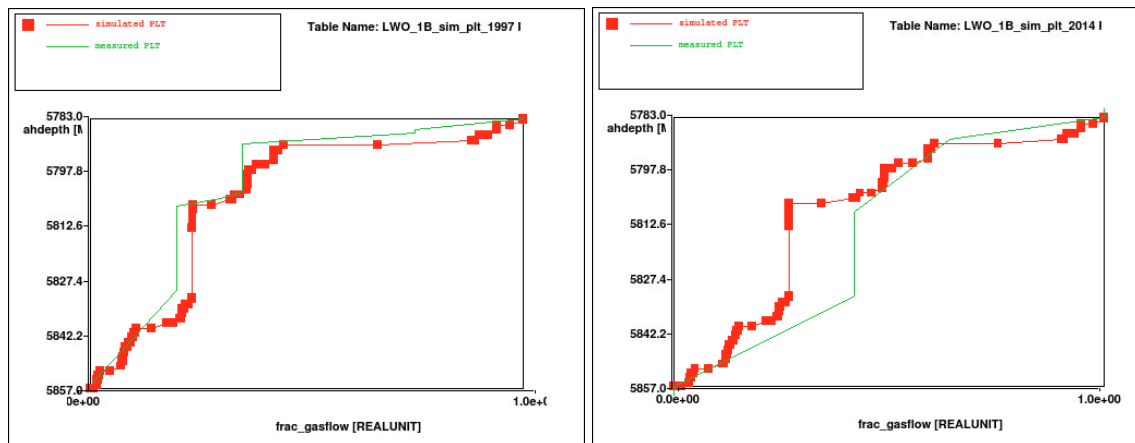


Figure 28 Simulated (red line + squares) and measured (green line) PLT in LWO-1B. Left: 1997, pre-production. Right: 2014. Base case realisation.

The static model was recreated in 2015, during the maturation of the Lauwersoog East infill project. Although properties were updated, the resulting model was marginally different from previous models. Therefore, similar history matches could be created. As part of the update, the popups due east of the field were excluded. In M&R 2014 it was evident that, even with fully open faults and a mobile aquifer, the pressure decline was negligible.

The model was matched on SPG and FTHP data as can be seen in Figure 29 and Figure 30 respectively.

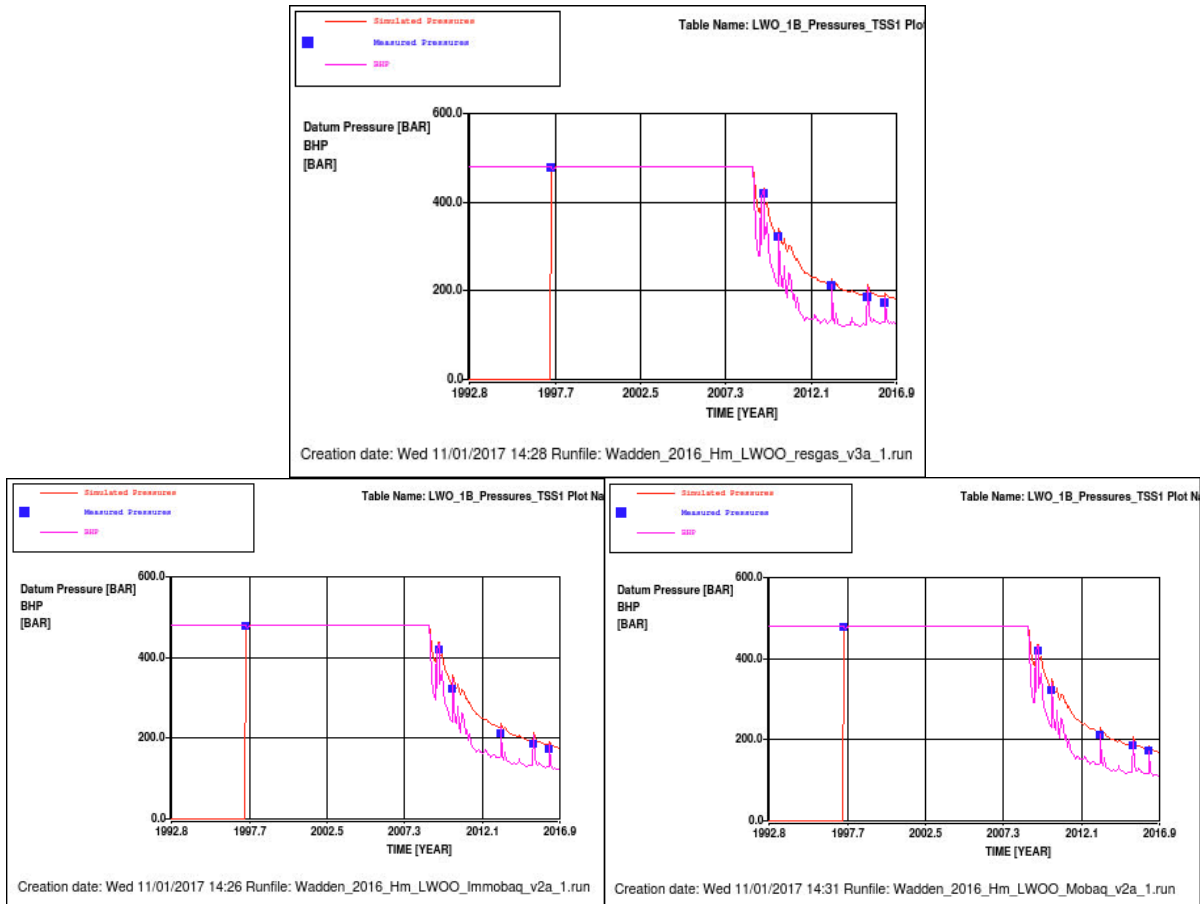
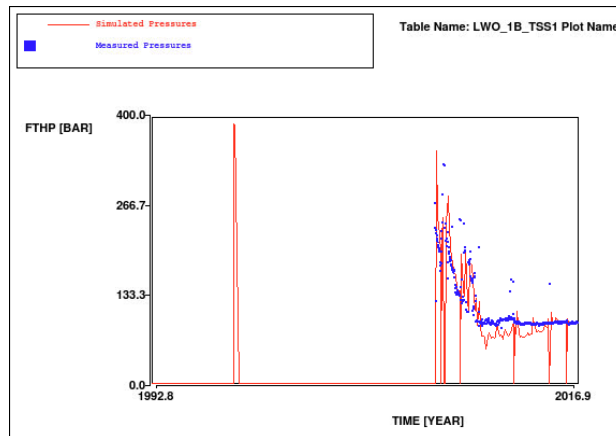


Figure 29 Simulated reservoir pressure (red line), flowing bottom hole pressure (violet line) and measured (blue squares) downhole pressure data in LWO-1B. Top: base case. Left: low case. Right: high case.



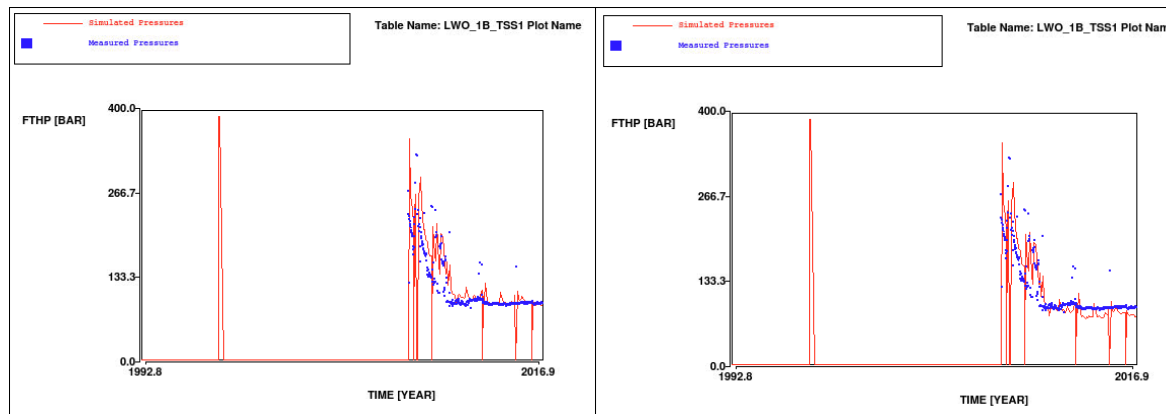


Figure 30 Simulated (red line) and measured (blue squares) flowing tubing head pressures in LWO-1B. Top: base case. Left: low case. Right: high case.

Table 21 shows the parameters used for M&R2015 models. Since the (new) model was modelled first with residual gas in the aquifer (base case), the other two cases have been based on this model. Very little needed to be done the models to keep the fit with dynamic data. For the low case, k_v was increased to counteract some missing pressure support from the (residual gas in the) aquifer. For the high case, the residual gas saturation was slightly lowered to counteract water encroachment that is not seen in the well. This field is a textbook example of a large uncertainty in aquifer pressure, where its behaviour cannot be deduced from measurements around the well.

Table 21 History matching parameters used for the Meet & Regel cycle for Lauwersoog East.

Parameter	Static	Low M&R2016 ¹⁹	Base M&R2016 ²⁰	High M&R2016 ²¹	Low M&R2015 ²²	Base M&R2015 ²²	High M&R2015 ²²
Residual gas sat. below FWL	0.20	0	0.23	0	0	0.23	0
GBV multiplier	1.0	1.0	1.0	1.0	1.0	1.0	1.0
k_h multiplier low perms	1	1.4	1.4	1.4	1.4	1.4	1.4
k_h multiplier high perms	1	4.0	4.0	4.0	4.0	4.0	4.0
k_v multiplier	N/A	0.10	0.006	0.010	0.10	0.010	0.010
FWL (m TVNAP)	4073	4073	4073	4073	4073	4073	4073
k_h multiplier aquifer	N/A	$1.0 \cdot 10^{-4}$	0.1	1.0	$1.0 \cdot 10^{-4}$	0.1	1.0
k_v multiplier aquifer	N/A	$1.0 \cdot 10^{-4}$	0.1	1.0	$1.0 \cdot 10^{-4}$	0.1	1.0
Residual gas	0.3	0.25	0.25	0.20	0.25	0.25	0.20
$k_w@S_{rg}$	0.1	0.1	0.1	0.1	0.1	0.1	0.1

¹⁹ Input deck: Wadden_2016_LWOO_Immobaq_v2a_LWOOE.INP

²⁰ Input deck: Wadden_2016_LWOO_resgas_v3a_LWOOE.INP

²¹ Input deck: Wadden_2016_LWOO_Mobaq_v2a_LWOOE.INP

²² Input deck: Wadden_2015_LWOO_MRN_v2.INP

6.1.4.2 Meet & Regel cycle 2016 vs 2015 model comparison

Negligible changes were made to the Lauwersoog-Oost models since 2015. Only the k_v -parameter of the base case model was slightly modified to align with the most recent FTHP data.

6.1.4.3 Water production

The well LWO-1B has been in production since 2008. The well has not been shut-in on its own and therefore water-gas-ratios determined from WaCo tank level changes are not very accurate (Figure 31) and hence are not matched upon. The model does not expect water breakthrough here yet, but depending on the aquifer behaviour, this might occur in the future.

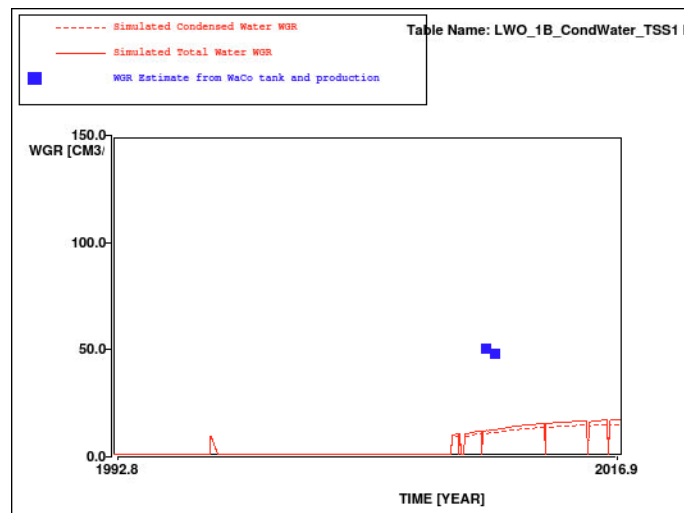


Figure 31 Simulated total WGR (red solid line), simulated condensed WGR (red dashed line) and estimated WGR from production and WaCo tank observations (blue squares) for LWO-1B.

6.1.5 Lauwersoog West

The Rotliegend (ROSLU) Lauwersoog-West field was discovered by the well LWO-3 in 1998, drilled from the Lauwersoog location. It found initial pressure at 484 bara. It is situated in the Eastern part of the Noord Friesland Concession. The field is bounded to the West and East by the Lauwersoog-C and Lauwersoog-Oost gas fields respectively.

The LWO-3 well was perforated in the Upper Slochteren zones and brought on-stream in November 2008, and is evacuated to the Anjum facilities. Its P/z plot can be found in Figure 33.

An RFT was taken for this field and showed a 2 bar pressure difference between the gradient of the top unit and the gradient of the units below. No nearby fields were in production at that time and a (lengthy) production test of LWO-1B (investigated during Lauwersoog East infill work) is assumed not to have been able to cause this depletion. Hence the ROSLU2 shale has a good chance of being fully sealing. The FWL could not be accurately determined because it is located in the Ameland shale layer, but based on saturation and spill point it was estimated at 4055 m TVNAP. With the ROSLU1 having a different pressure gradient, its FWL may well be slightly different.

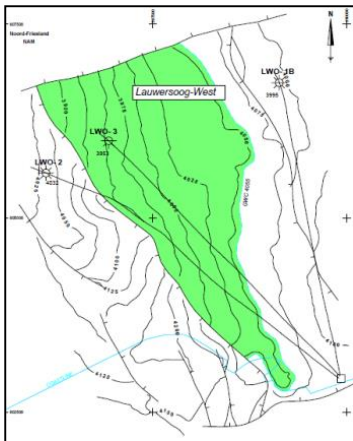


Figure 32 Lauwersoog-West ARPR top ROSL map

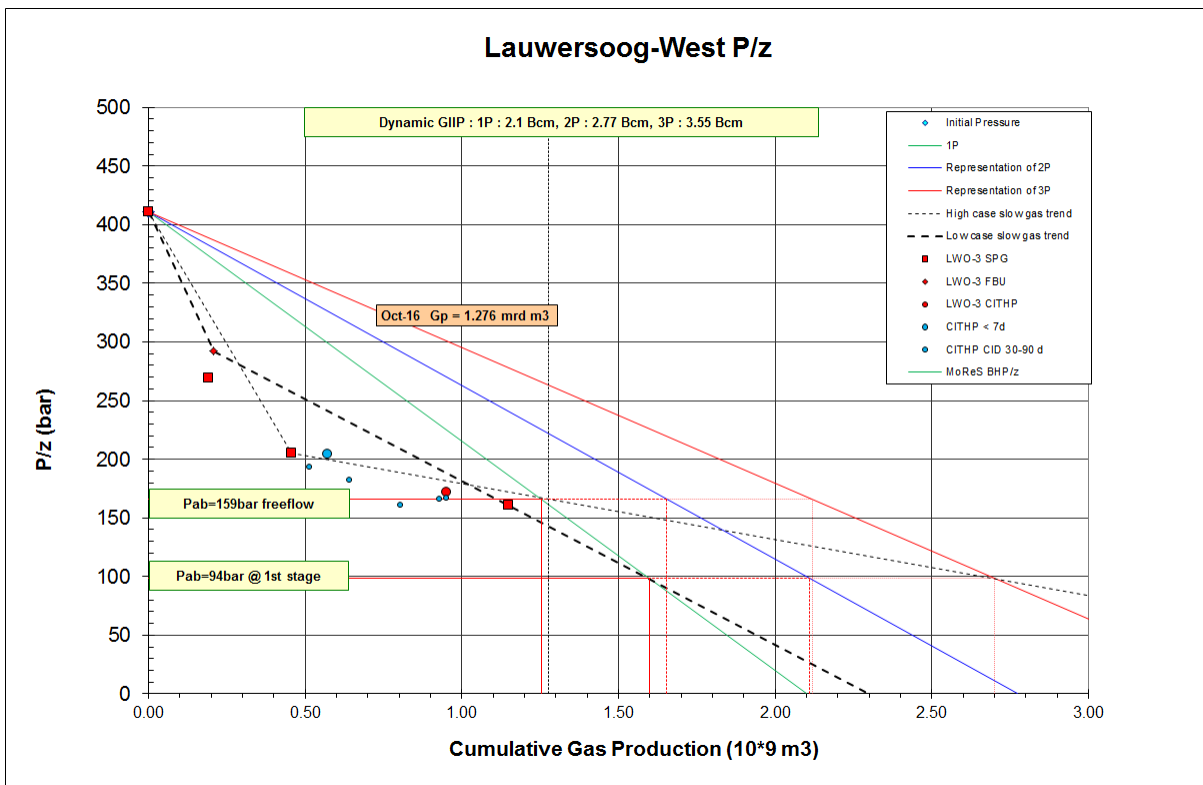


Figure 33 P/z plot LWO-3

6.1.5.1 Reservoir model

Even though the RFT shows two bar pressure differential, this has not been taken into account in initialization. The field has been initialized on a single pressure and FWL as is shown in Figure 34.

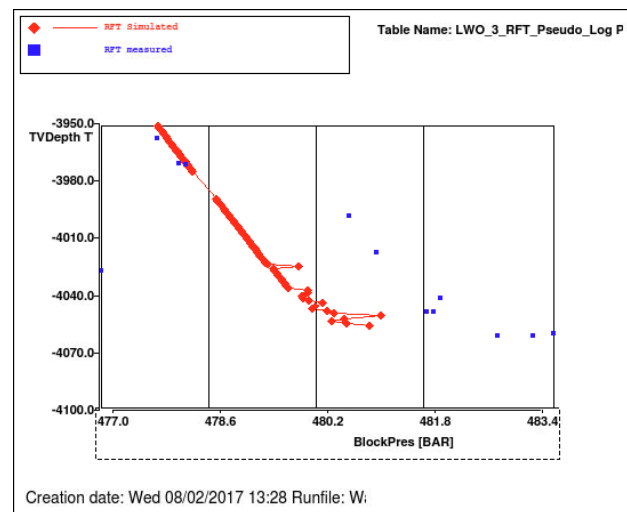


Figure 34 Simulated (red line and squares) and measured RFT pressure data (blue squares) for LWO-3.

The permeability contrast has been captured with a PLT, which has been well matched as can be seen in Figure 35.

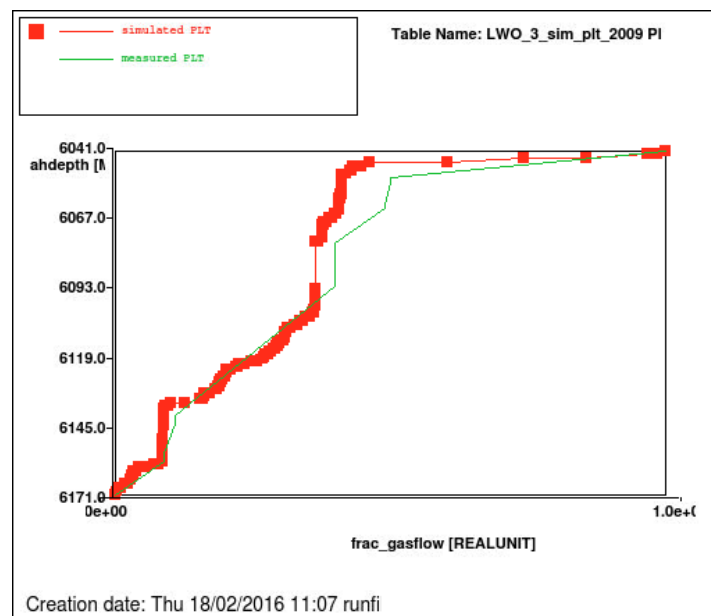


Figure 35 Simulated (red line + squares) and measured (green line) PLT in LWO-3. Base case realisation.

For the Lauwersoog-Central –East and –West field, as described in Section 4.3.1, the shut-ins are modelled to the nearest day, and therefore BHP is used for history matching.

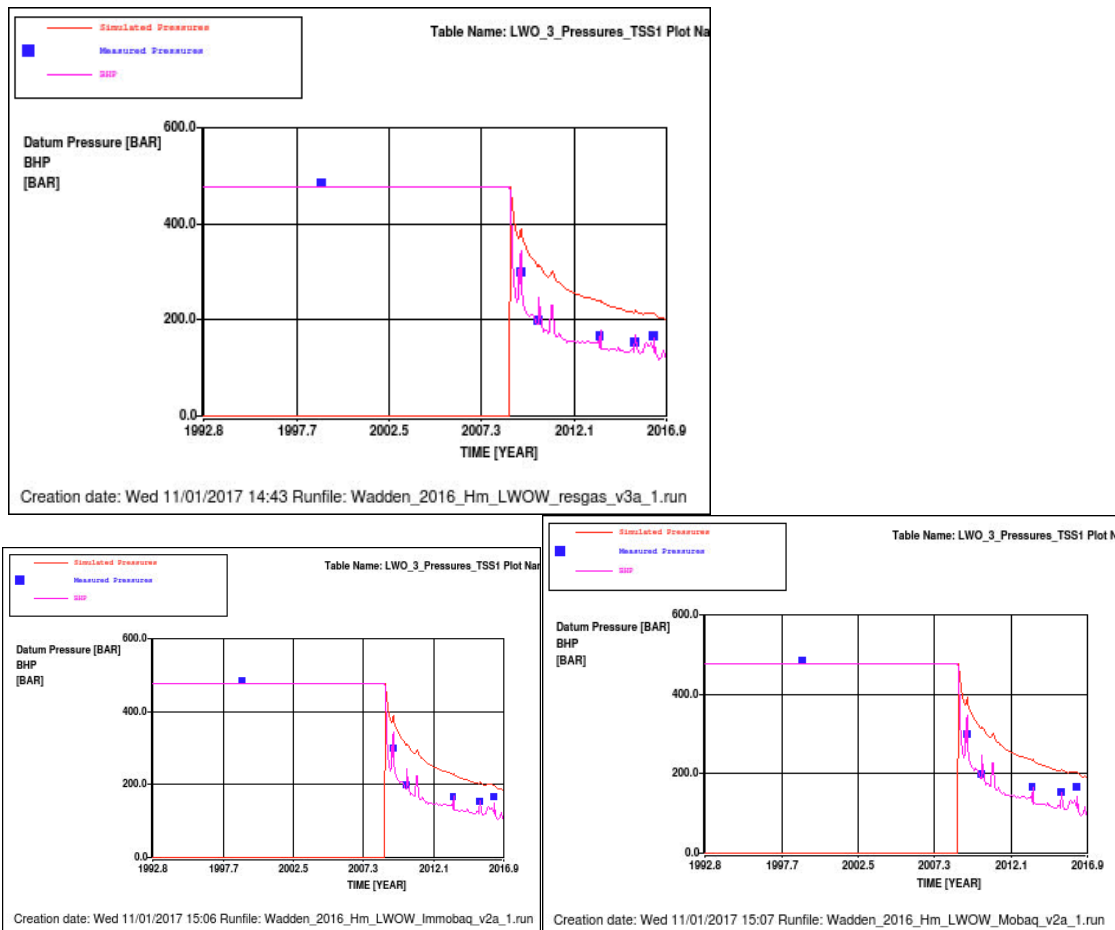


Figure 36 Simulated reservoir pressure (red line), flowing bottom hole pressure (violet line) and measured (blue squares) downhole pressure data in LWO-3. Top: Base case Left: low case. Right: high case.

A north-south fault that is somewhat visible on seismic is included east of LWO-3 to give the model extra flexibility in mimicking slow gas behaviour (Figure 37). North-South faults are abundant in the area and have proven to be sealing or baffling in some cases. However, since M&R2015 it was decided to ignore any baffling potential of this fault, since this could underestimate pressure drop and hence subsidence behind the fault.



Figure 37 Faults in the MoReS simulation model.

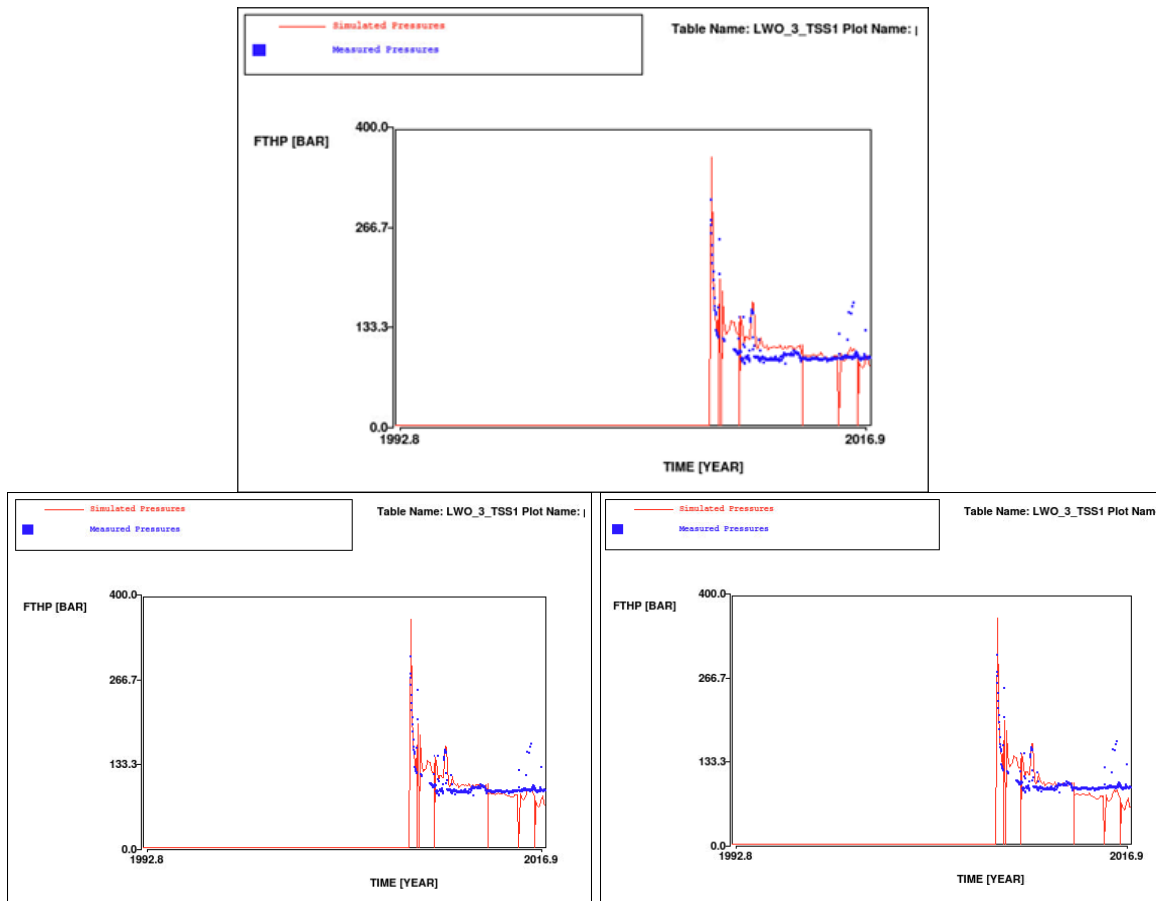


Figure 38 Simulated (red line) and measured (blue squares) flowing tubing head pressures in LWO-3. Top: base case. Left: low case. Right: high case.

Figure 38 shows the THP match with the well. Although the match is good, the response indicates that slightly more late pressure support exists than modelled for the low and high case. This might indicate that some intra-field (fault) baffling might be taking place. However, with (the baffling) of this fault not proved, it chosen to be slightly conservative and assume full connectivity.

For Lauwersoog-West, the main uncertainties are the existence of vertical pressure differentials, depletion of the water bearing layers, the FWL and (slow gas) volumes.

The parameters that are used for matching are shown in Table 22 below. In the Lauwersoog area there is quite some uncertainty around the FWL. But since the mobility of the aquifer is the dominant uncertainty for subsidence, the uncertainty of the free water level is not considered an issue and is kept constant. To model vertical pressure differentials, it is chosen to distinguish between low (<1mD) and high (>1mD) permeability zones when applying permeability multipliers. This is a key ingredient to the slow gas behaviour seen in this well.

Table 22 History matching parameters used for the Meet & Regel cycle for Lauwersoog West

Parameter	Static	Low M&R2016 ²³	Base M&R2016 ²⁴	High M&R2016 ²⁵	Low M&R2015 ²⁶	Base M&R2015 ²⁶ Error! B ookmark not defined.	High M&R2015 ²⁶ Error! B ookmark not defined.
Residual gas sat, below FWL	0.21	0	0.21	0	0	0.21	0
GBV multiplier ²⁷	1	1	1	1.04	1	1	1
k_h multiplier, high k zones	1	0.28	0.28	0.28	0.28	0.28	0.28
k_h multiplier, low k zones	1	0.035	0.035	0.035	0.035	0.035	0.035
k_v multiplier	N/A	0.010	$3.4 \cdot 10^{-3}$	0.010	$3.4 \cdot 10^{-3}$	$3.4 \cdot 10^{-3}$	$3.4 \cdot 10^{-3}$
N-S fault	N/A	1	1	1	1	1	1
GWC (m TVNAP)	4055	4055	4055	4055	4055	4055	4055
k_h multiplier aquifer	N/A	$1 \cdot 10^{-4}$	0.32	1	$1 \cdot 10^{-4}$	0.32	1
k_v multiplier aquifer	N/A	$1 \cdot 10^{-4}$	0.32	1	$1 \cdot 10^{-4}$	0.32	1
Residual gas	0.3	0.25	0.25	0.25	0.25	0.25	0.25
$k_w @ S_{rg}$	0.1	0.1	0.1	0.1	0.1	0.1	0.1

This field is a clear example of the aquifer having little impact on the pressure response at the well, but a large impact on average reservoir pressure. Only aquifer properties have been varied between the three cases, but the impact is large as will become apparent in Section 6.2.2.

6.1.5.2 Meet & Regel cycle 2016 vs 2015 model comparison

Few changes have been made M&R2016. For the low and high cases, the vertical permeability k_v was elevated from 0.0034 to 0.010 since late FTHPs showed some more pressure support. A somewhat higher k_v ensures that more gas from the low-perm zones can access the well. For the high case, also the GBV multiplier was adjusted to account for more

²³ Input deck: Wadden_2016_LWOW_Immobaq_v2a.INP

²⁴ Input deck: Wadden_2016_LWOW_resgas_v3a.INP

²⁵ Input deck: Wadden_2016_LWOW_Mobaq_v2a.INP

²⁶ Input deck: Wadden_2015_LWOW_MRN_v4.INP

²⁷ In M&R2014, a distinction was made between GBV for high and low permeability zones.

late-life pressure support. The extra measure was needed since the mobile aquifer causes permeability deterioration around the well and thus this extra pressure drop must be compensated, in this case by more GIIP.

6.1.5.3 Water production

LWO-3 has been producing since 2008. No specific stops were done on the well that allow for a reliable water-gas-ratio from the WaCo tank levels as can be seen in Figure 39. With the lowering of the FWL in this year's model, formation water production is marginal. There are currently no indications of excessive water production from this well, although with the structure dipping into the water, there is always a risk of future water breakthrough.

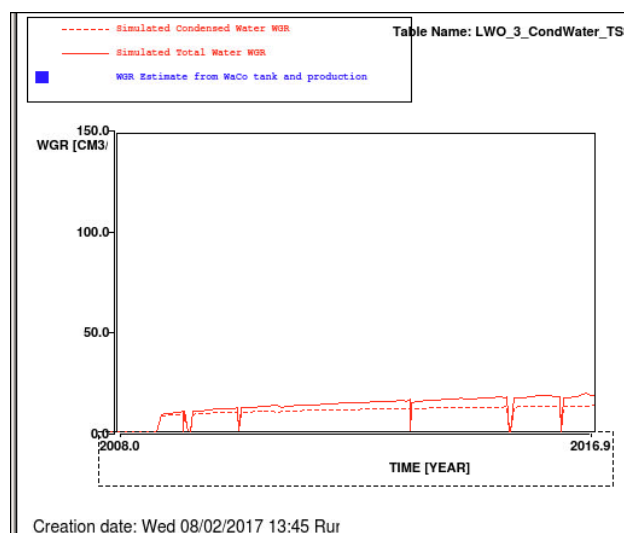


Figure 39 Simulated total WGR (red solid line), simulated condensed WGR (red dashed line) and estimated WGR from production and WaCo tank observations (blue squares) for LWO-3. Base case realisation.

6.1.6 Metslawier

The Metslawier field (Figure 40) is located in the central onshore part of the Noord-Friesland Concession (Lauwerszee Trough, NE-Netherlands), adjacent to the Hantum fault zone. It was discovered in 1994 by ANJ-2, drilled from the Anjum surface location into a crestal position. The field started production in 1997 through the Anjum facilities. Its P/z plot can be found in Figure 41.

The Rotliegend formation in the Metslawier field consists of the Ten Boer Claystone Member (ROCLT), the Upper Slochteren Sandstone Member (ROSLU), the Ameland Claystone Member (ROCLA) and the Lower Slochteren Sandstone Member (ROSL). Only the ROSLU was evaluated as being gas bearing. It consists of Aeolian and fluvial/pond sediments deposited in a desert environment. The thickness of the ROSLU in ANJ-2 is 111 m, of which approximately 88 m TV (gross) is gas bearing.

The ANJ-2C well has been side-tracked 3 times due to lost drill strings that could not be fished. The well was production tested in 1994, but suspended awaiting a workover with Cr-13 tubing. The workover was done in 1997, but during the workover, the original perforations from 1994 were seriously damaged. This is observed in PLT in 1999, which led to re-perforation of the initial perforations in 1999. The well was taken into production in 1997.

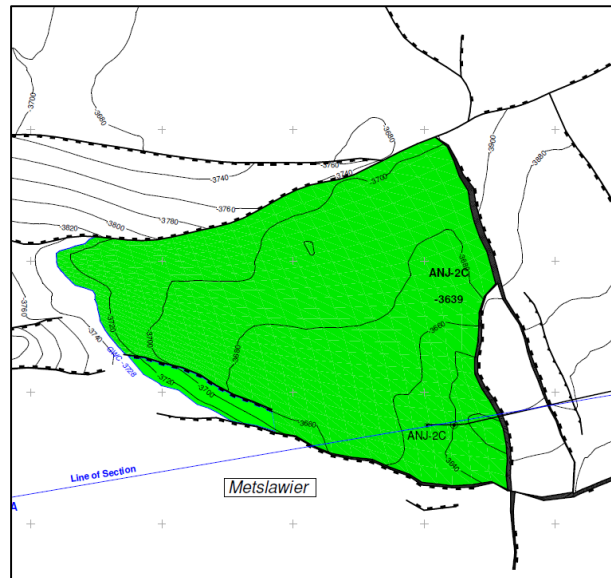


Figure 40 Metslawier ARPR top ROSL map

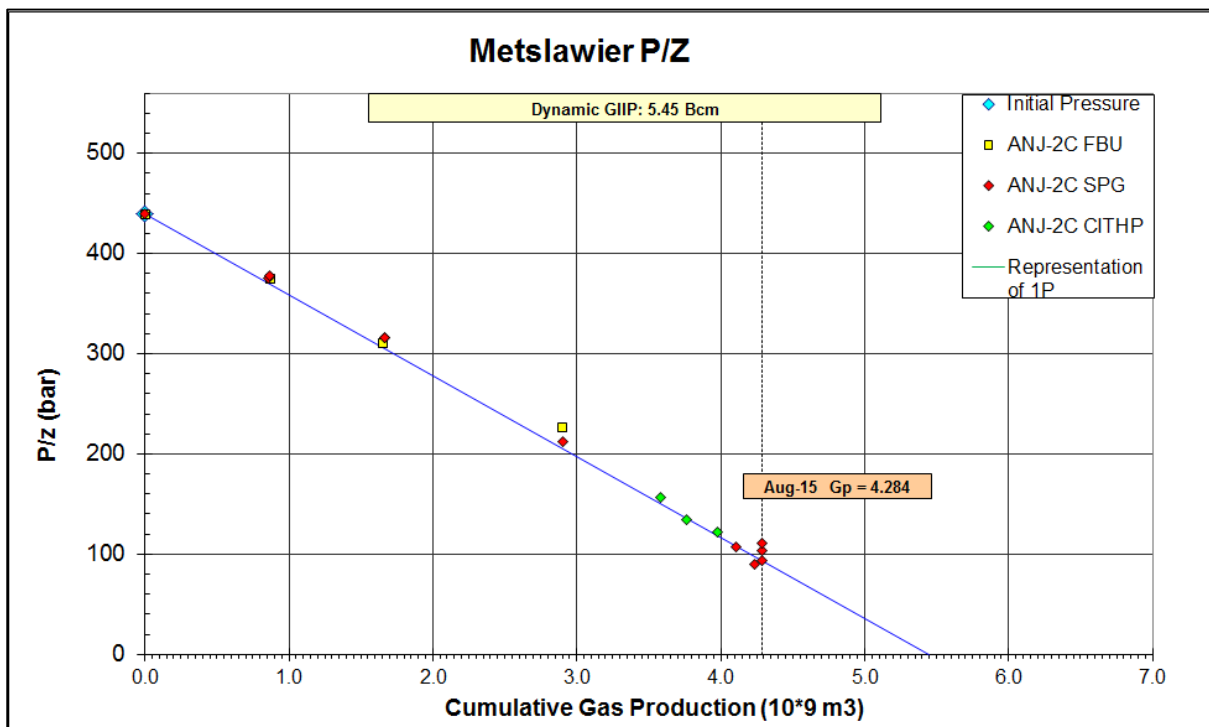


Figure 41 P/z plot for ANJ-2C.

In water samples in 2005, it was found that formation water was being produced. In 2006, the well was produced with foam and in 2009 the well died at 350 000 N m³/d, well above its liquid loading rate for condensed water. Several activities have been done in order to restore the well; the well was perforated in unit 2 in 2011, which had not been perforated before. This did not restore the well (even after nitrogen lifting).

The reservoir pressure measured in downhole pressure measurements has been steadily increasing since 2007, as well as the liquid level in the well. It is believed that formation water has been flowing in from the lower perforations and cross-flowing into the upper layers, creating a water-invaded zone around the well that causes the well not to be able to produce anymore. In a gamma-ray log done in 2012, salt scaling was identified over the

perforations that supports the hypothesis of crossflow. Activities to restore well production were not successful and end 2012 it was decided to stop these activities. The project to drill a side-track was deemed too risky and was cancelled.

Also in 2015, an attempt was made to reopen the well. A plug was set in the ROSLU2 (shale). The well produced briefly into test equipment (surface pressure 3 bara), but flow did not sustain. The WGR observed was ~1000 m³ per mln N m³ – a factor 3 lower than before setting the plug. Also this observation supports the hypothesis described in the previous paragraph.

6.1.6.1 Reservoir model

The Metslawier field has been studied in the previous years in detail for the maturation of the mentioned side-track of ANJ-2. The field has been matched in the previous Waddenzee model of 2010 and reproduced in the current model. In order to reproduce the model, the permeability in unit 1 (see Figure 46), was increased by a factor 2 (1994 perforations in unit 1) – 30 (1997 perforations in unit 1). This was done in order to model the high permeable layers that were included in the previous model and in line with PLT (Figure 42 and Figure 43) and FBU data (Table 23). These high permeable streaks in unit 1 are also observed in MGT-2 PLT, LWO-3 PLT (Figure 35) and ANJ-1 PLT (Figure 13).

Perforation	Perforated	kh model	Modified	FBU 24/11/1994	FBU 3/8/1999	FBU 21/8/2000	FBU 9/8/2002
		mD m	mD m	mD m	mD m	mD m	mD m
P1	1997	3	90		600	1152	1152
P2	1997	14	420				
P3	1994/1999	135	270	578			
P4	2011	870	128				
P5	1994/1999	1511	220				
P6	1997	28					
P7	1999	11					
P8	1999	32					

Table 23 Permeability thickness and modifications compared to permeability thickness obtained from FBU data. Black squares indicate that these zones did not participate in the kh of the FBU.

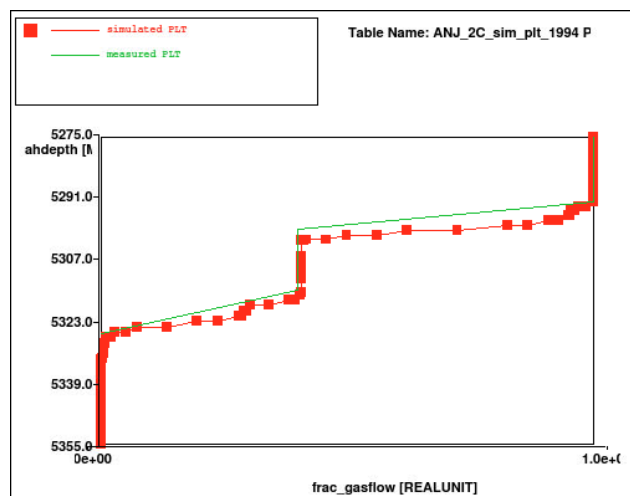


Figure 42 Simulated (red line + squares) and measured (green line) PLT in ANJ-2C with original perforations in 1994. Base case realisation.

The second PLT in 1999 (Figure 43) could only be matched if the original perforations from 1994 were closed, indicating that the original perforations were indeed damaged during the workover as was stated, although the match is still not ideal.

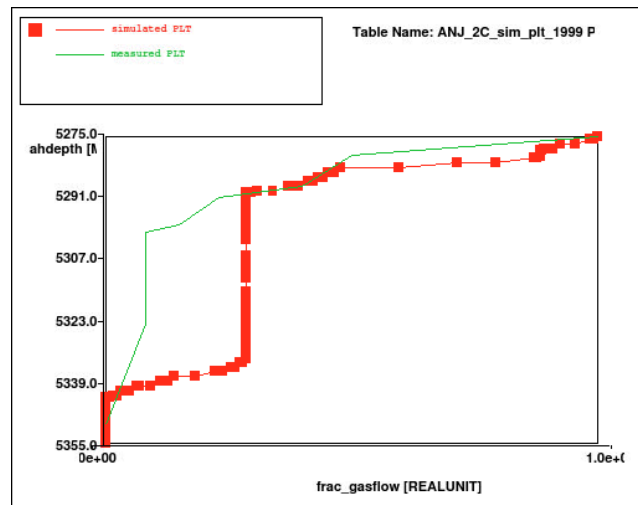


Figure 43 Simulated (red line + squares) and measured (green line) PLT in ANJ-2C in 1999 with original perforations from 1994 closed and new perforations from 1997 added. Base case realisation.

On top of these modifications, high permeable layers in the bottom units were modelled as 1m thick and were therefore reduced in magnitude by a factor 10 as is indicated in Table 23. This is in line with the historical well performance as is shown in Figure 44. The permeability modifications seem to properly represent the historical well production.

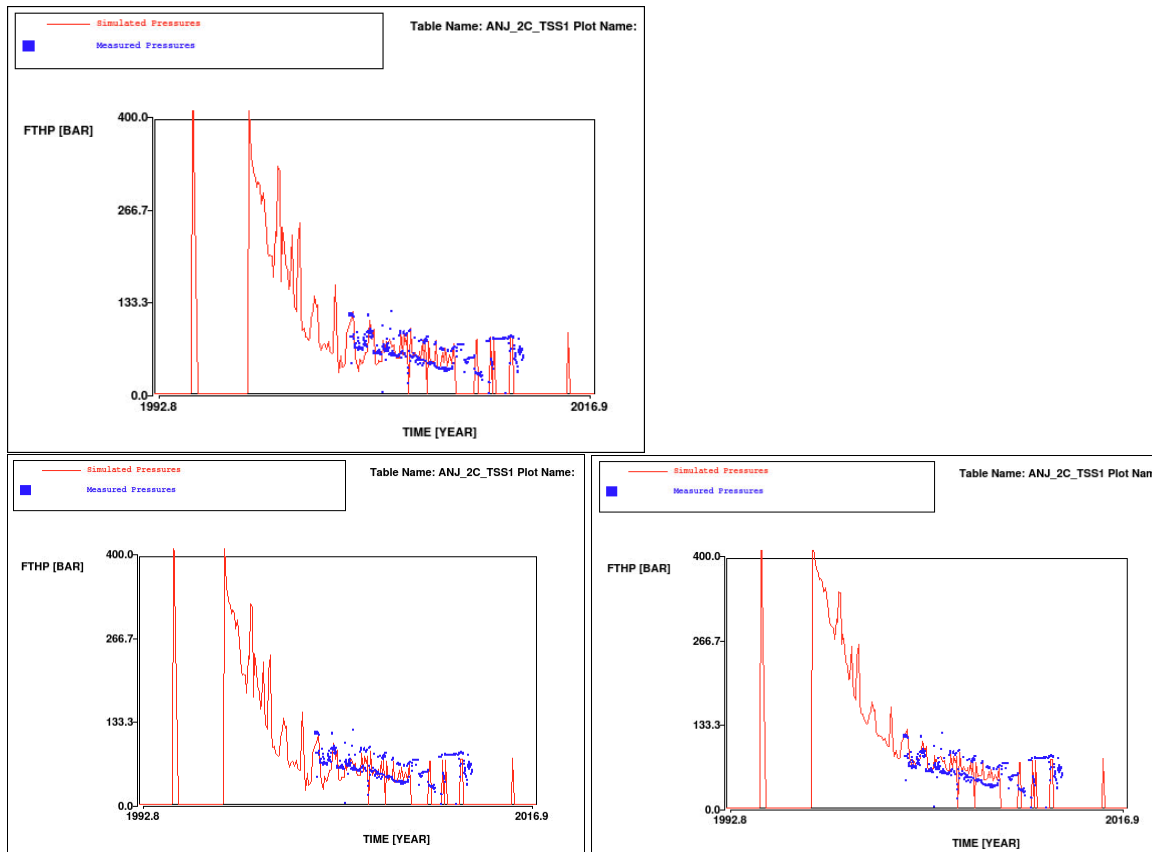


Figure 44 Simulated (red line) and measured (blue squares) flowing tubing head pressures in ANJ-2C. Top: base case. Left: low case. Right: high case.

The downhole pressure match is shown in Figure 45. The cause of the pressure build-up in the recent years is believed to be the aquifer influx.

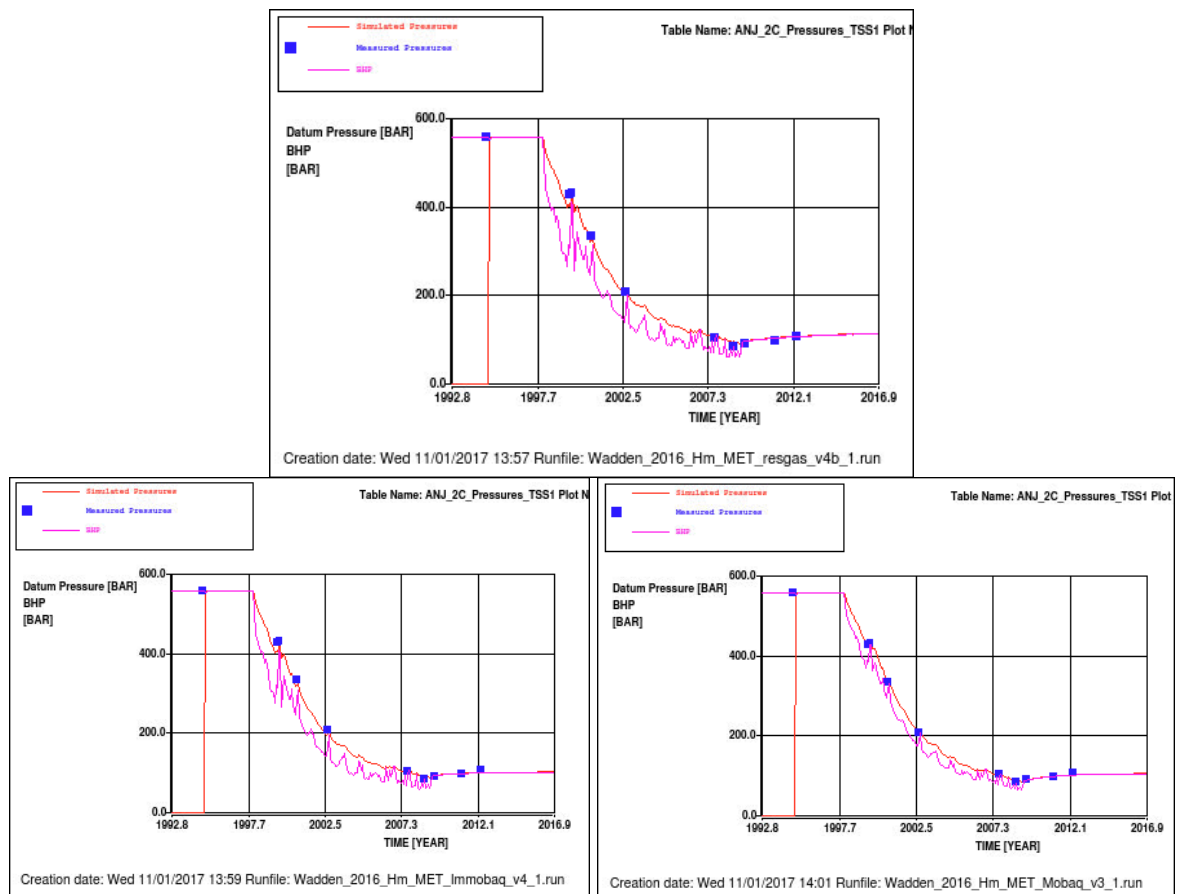


Figure 45 Simulated reservoir pressure (red line) and measured (blue squares) downhole pressure data in ANJ-2C. Top: base case. Left: low case. Right: high case.

Like Anjum, Metslawier is a mature field that can be used for calibrating compaction coefficients. Little depletion of the aquifer results in higher compaction coefficients and vice versa. Core measurements suggest high compaction coefficients for this area. To match with subsidence measurements, aquifer depletion is expected to be limited. This residual gas below FWL reservoir realisation supports this subsidence model, where aquifer depletion is hampered by gas in the water leg.

The parameters used for history matching for field development and for the M&R cycle are shown in Table 24. The base case (residual gas below FWL) model has been based on the immobile aquifer model, with a modified aquifer. This model makes water influx more natural, since the aquifer expands more when depleted. Where an immobile aquifer requires a relatively high water relative permeability end-point (0.2), the base case value can be used (0.1) when assuming gas below FWL.

Table 24 History matching parameters used for the Meet & Regel cycle for Metslawier.

Parameter	Static	Low M&R2016 ²⁸	Base M&R2016 ²⁹	High M&R2016 ³⁰	Low M&R2015 ³¹	Base M&R2015 ³¹ Error! B ookmark not defined.	High M&R2015 ³¹
Residual gas below FWL	0.09	0	0.08	0	0	0.08	0
GBV multiplier	1	1.07	1.05	1.02	1.07	1.07	1.00
k_h multiplier	1	0.85	0.85	1.0	0.85	0.85	1.0
k_v multiplier	N/A	$8.5 \cdot 10^{-3}$	$8.5 \cdot 10^{-3}$	0.010	$8.5 \cdot 10^{-3}$	$8.5 \cdot 10^{-3}$	0.010
GWC (m TVNAP)	3728	3728	3728	3728	3728	3728	3728
k_h multiplier aquifer	N/A	$1 \cdot 10^{-4}$	0.10	1	$1 \cdot 10^{-4}$	0.10	1
k_v multiplier aquifer	N/A	$1 \cdot 10^{-4}$	0.10	1	$1 \cdot 10^{-4}$	0.10	1
Residual gas	0.3	0.30	0.20	0.25	0.30	0.20	0.25
$k_w@S_{rg}$	0.1	0.20	0.10	0.1	0.20	0.10	0.1

6.1.6.2 Meet & Regel cycle 2015 vs 2016 model comparison

The Metslawier immobile aquifer model of M&R2015 had fast aquifer layers, since the low permeability multiplier was not honoured in certain layers. This has now been changed such that aquifer permeability multipliers equally affect high- as well as low permeability zones. This has resulted in a more natural depletion curve for the low case realisation. This modelling change cannot be reflected in a single parameter and hence it is not visible in Table 24.

The change in permeability modelling has a slight effect on GBV multiplier, also of the base and high case models.

6.1.6.3 Water production

The well ANJ-2C has observed water breakthrough. This is seen in the salinity of water samples in 2005, the foam lifting required since 2006, the liquid rise in the well bore and the salt scaling over the perforations (Figure 46). Water movement was extensively modelled in 2013 and 2014 and was concluded to be encroaching from the west, where the structure dips into the water. The water is could have entered the well via high permeable streaks (Figure 47) and subsequently have cross-flowed into the top reservoir units (Figure 48). Some stranded gas pockets could have driven water into the well via these streaks.

²⁸ Input deck: Wadden_2016_MET_Immobaq_v4.INP

²⁹ Input deck: Wadden_2016_MET_resgas_v4b.INP

³⁰ Input deck: Wadden_2016_MET_Mobaq_v3.INP

³¹ Input deck: Wadden_2015_MET_MRN_v3.INP

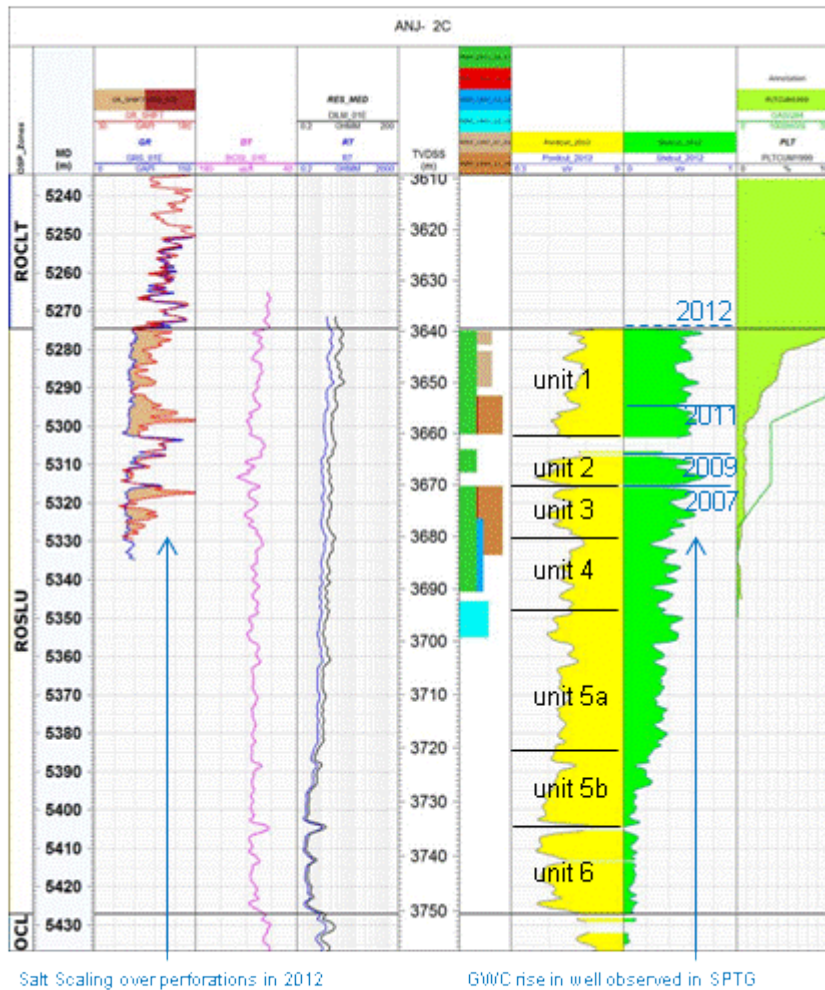


Figure 46 Log of ANJ-2C showing the salt scaling with the gamma ray log in the left panel and the liquid rise from SPTG in the right panel.

Date	Density (kg/L)	Cl (mg/L)
11/07/2005	1.18	161000
12/07/2005	1.17	149000
13/07/2005	1.15	131000
14/07/2005	1.14	126000

Table 25 Water sample data from ANJ-2C in 2005

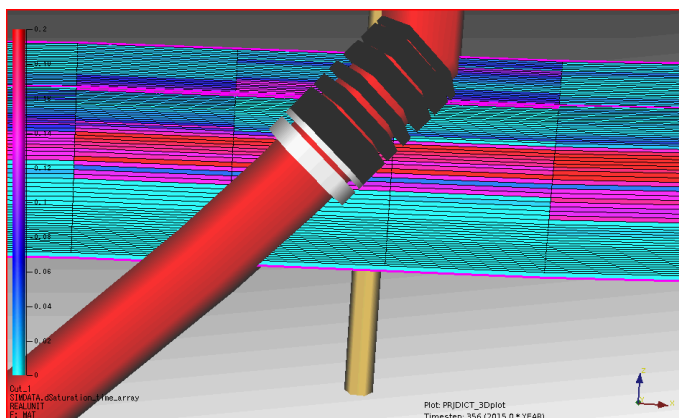


Figure 47 Cross section of the water saturation change around ANJ-2C with in red the water entering via high permeable streaks and cross flowing at the top (blue is no change in saturation).

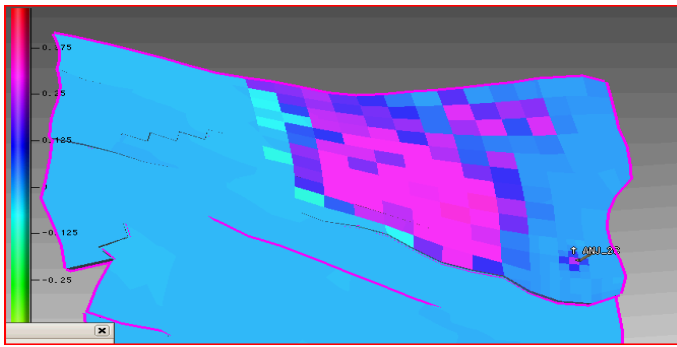


Figure 48 Water saturation change in unit 1, with in red the water encroaching from the west (blue is no change in saturation), and around the well the cross-flow.

The simulation indicates lower WGRs than observed at surface. This could indeed indicate that this model misses an extra drive mechanism. For subsidence calculations however, the model suffices. Pressures have been matched to the well and a large uncertainty range in the aquifer pressure has been used.

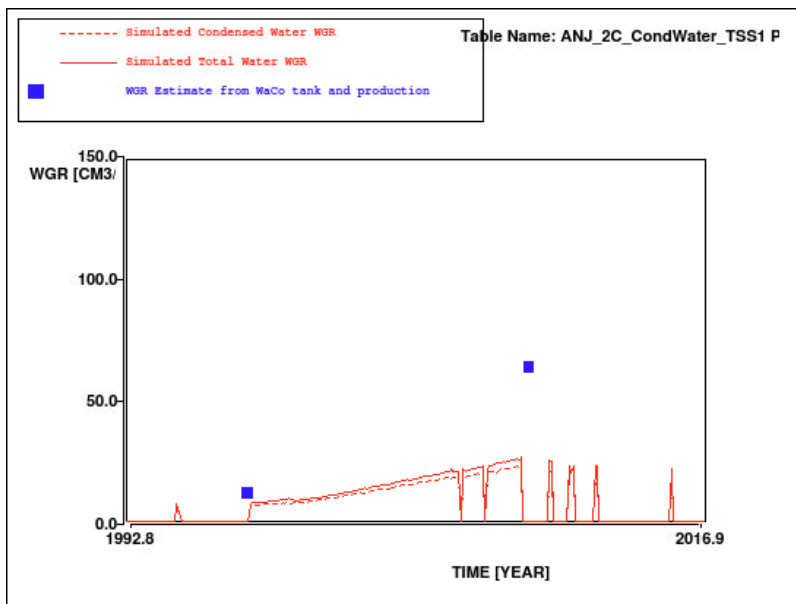


Figure 49 Simulated total WGR (red solid line), simulated condensed WGR (red dashed line) and estimated WGR from production and WaCo tank observations (blue squares) for ANJ-2C

6.1.7 Moddergat

The Moddergat field (Figure 50) is located in the eastern Waddenzee section of the Noord Friesland Concession (NE-Netherlands). It was discovered by the well MGT-1B in 1995 and found virgin pressures at 567 bar, which is significantly overpressured (datum level equals 3860mTVDNAP). Wet gas is evacuated to the Anjum plant facilities as of February 2007. Its P/z plot is shown in Figure 51.

The Moddergat field is contained in the Upper Slochteren Sandstone Member (ROSLU) of the Rotliegend Formation. It consists of Aeolian and fluvial/lacustrine sediments deposited in a desert environment. The thickness of the ROSLU in MGT-1 is 108 m, of which approximately 78 mTV (gross) is gas bearing. The Moddergat gas field is mainly a fault closed structure at Base Zechstein (Rotliegend) level.

Seismic indicates a fault in the E-W direction that separates the field in a northern and a southern part. The single well only sees the northern section. It is difficult to judge whether

this fault is (partly) sealing. The small fault block, named Nes North, is likely in communication with the field and is included in the modelling.

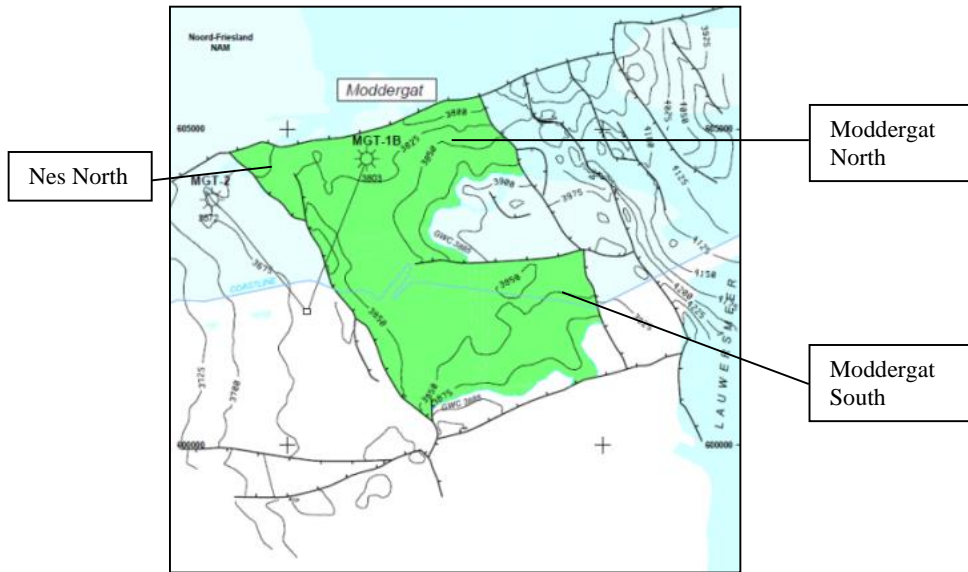


Figure 50 Moddergat ARPR top ROSL map

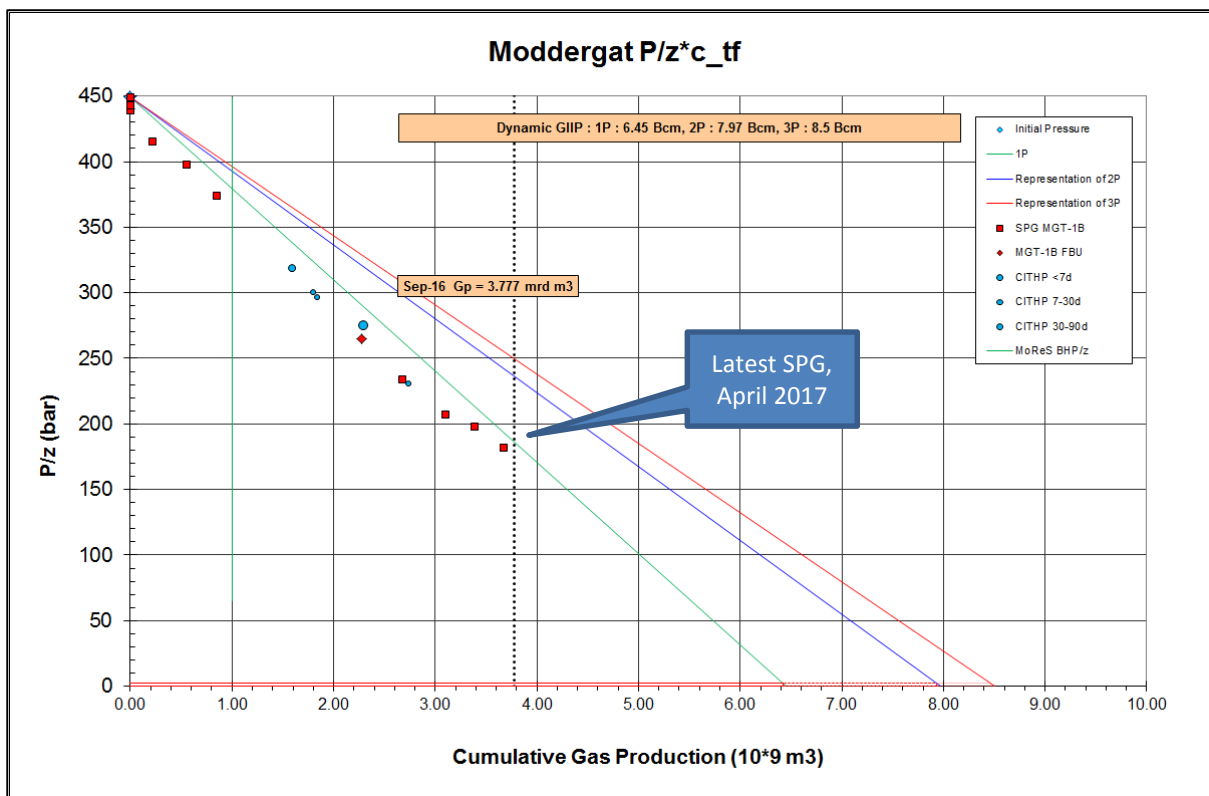


Figure 51 P/z plot for MGT-1B.

Due to its high initial pressures, P/z has been corrected for rock compressibility (c_f).

6.1.7.1 Reservoir model

This field was extensively modelled in 2015, in preparation of a potential infill well targeting the southern block of the field. A critical look at the permeability model, backed by core data from MGT-1B, suggested that connectivity throughout the field is probably poorer than previously thought. It hence seems likely that, irrespective of fault sealing behaviour, pressures in the southern half of the field are lagging the reservoir pressure around MGT-1B (see Figure 52).

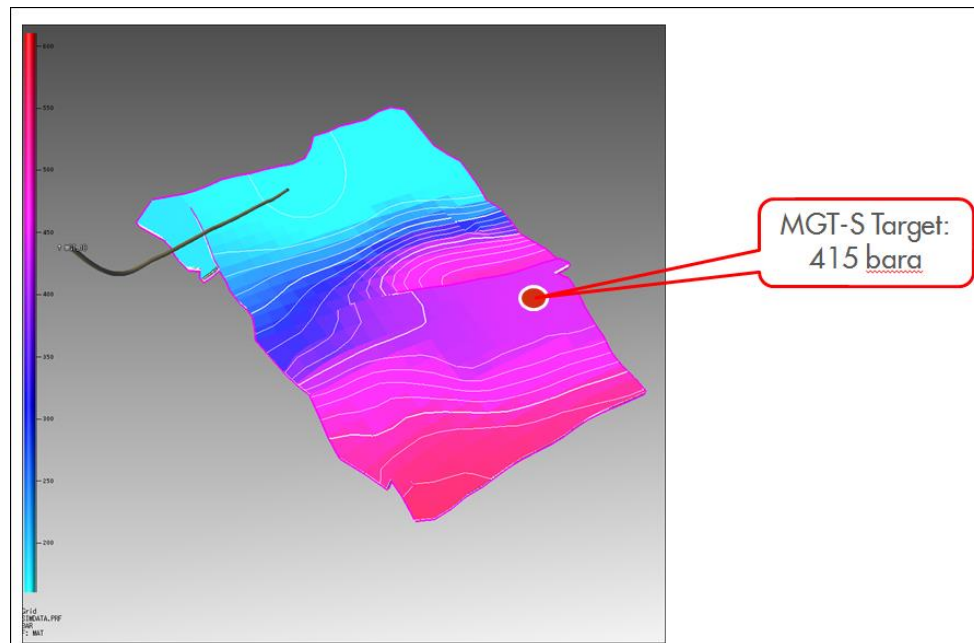


Figure 52 Base case pressure profile in the Moddergat field in 2015.

The history match on downhole pressure is shown in Figure 53 and the flowing THP match is shown in Figure 54. Although the matches are good, history matching has proved a challenge. The two-phase model predicts water encroachment to MGT-1B, impacting relative permeability and hence expecting that lower FTHPs are needed to fit production rates. Currently this is overcome with a very low k_{rw} end point (not outside the k_{rw} uncertainty range described in Section 5.1.3, but on the low end).

Furthermore, modelling has revealed that, with the given static model, some extra pressure support must exist to fit the base case GIIP with dynamic data. Residual gas below FWL can actually give this pressure support and this is precisely what was used in the base case model.

Alternatively, the model can be matched with a much higher GIIP and with a radiating southern half the field through a baffling fault. But to follow the base case GIIP as much as possible, and to avoid underestimating subsidence due south of the east-west intra-field fault and pressure drop in general, the former option with a base case GIIP was preferred for the base case subsidence match (Table 26). For the low and high case subsidence models, where residual gas below FWL is absent, this higher GIIP and baffling fault combination *has* been used.

The initial PLT was well matched indicating that the modelled permeability contrasts are in line with the well performance (Figure 55).

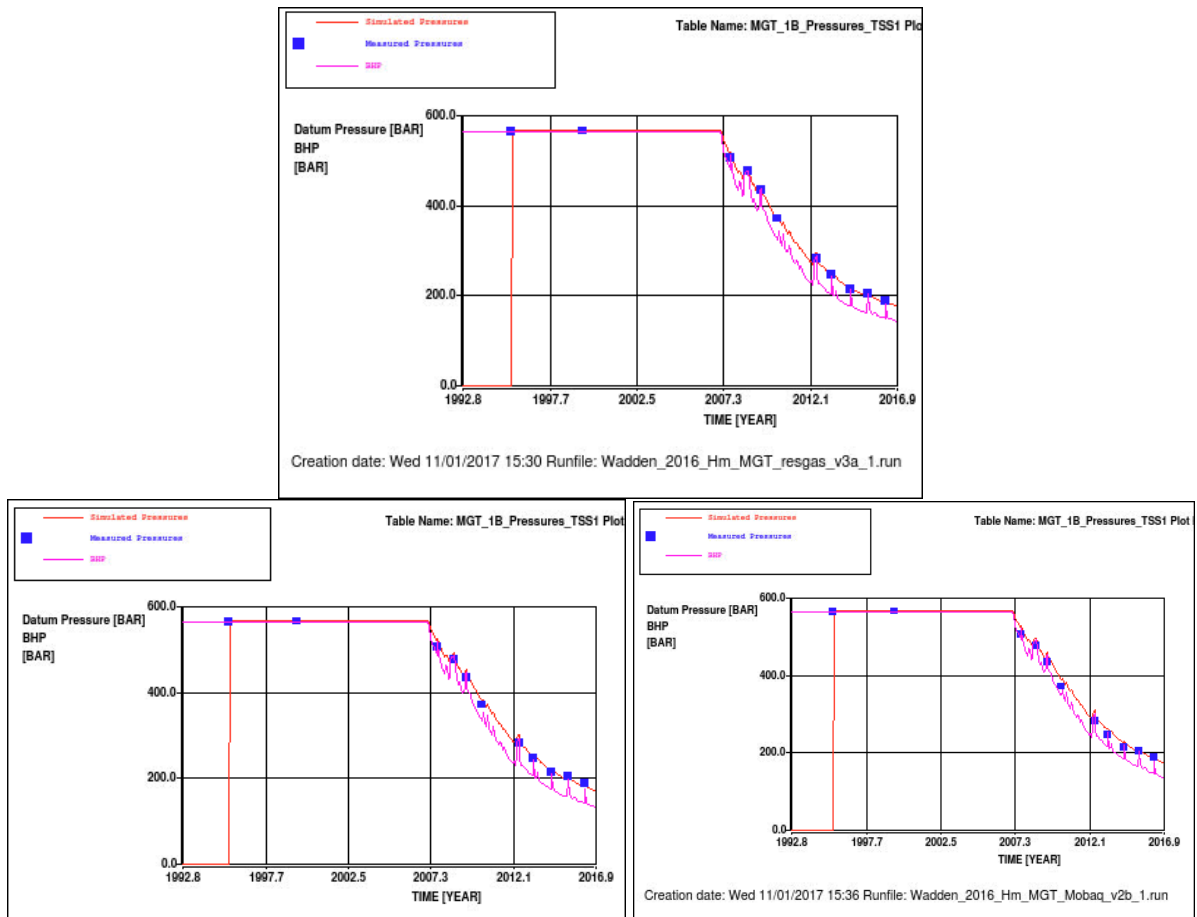


Figure 53 Simulated reservoir pressure (red line), simulated BHP (violet line) and measured (blue squares) downhole pressure data in MGT-1B. Top: base case. Left: low case. Right: high case.

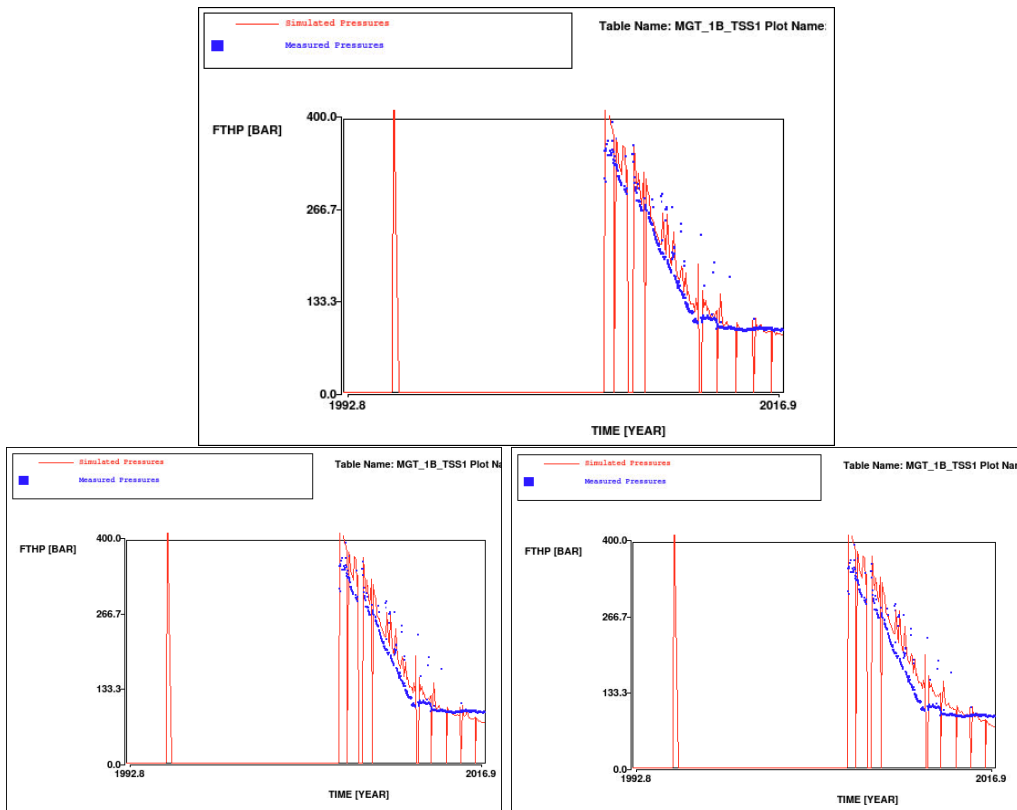


Figure 54 Simulated (red line) and measured (blue squares) flowing tubing head pressures in MGT-1B. Top: base case. Left: low case. Right: high case.

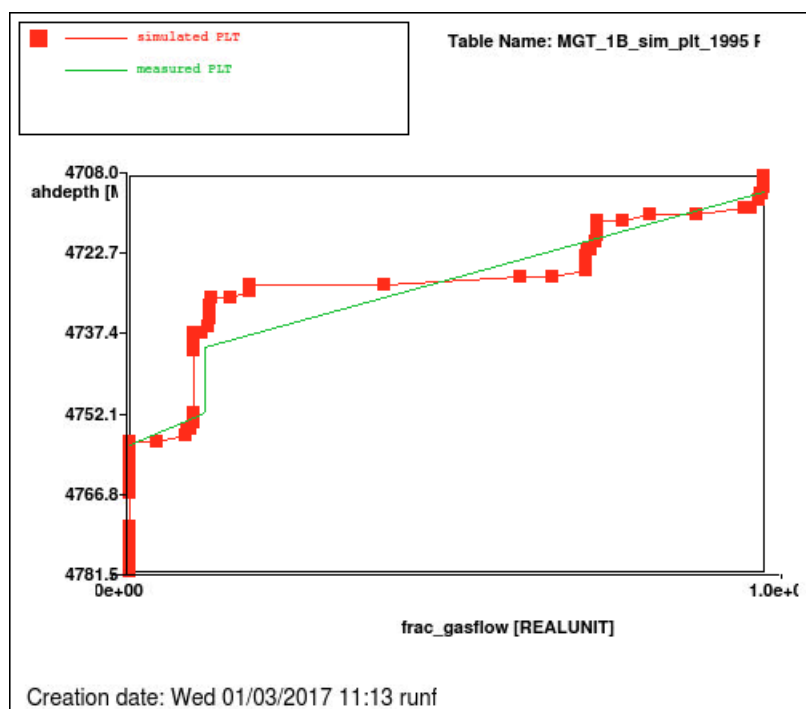


Figure 55 Simulated (red line + squares) and measured (green line) PLT in MGT-1B in 1995

Table 26 History matching parameters used for the Meet & Regel cycle for Moddergat

Parameter	Static	Low M&R2016 ³²	Base M&R2016 ³³	High M&R2016 ³⁴	Low M&R2015 ³⁵	Base M&R2015 ³⁵	High M&R2015 ³⁶
Residual gas sat. below FWL	0.20	0	0.20	0	0	0.20	0
GBV multiplier	1.0	1.3	1.0	1.25	1.3	1.0	1.2
GIIP (BNCM) above FWL.	6.8	8.9	6.8	8.2	8.9	6.8	8.2
E-W Fault Seal (east)	N/A	0.01	1	0.01	0.01	1	0.01
E-W Fault Seal (west)	N/A	0.01	1	0.01	0.01	1	0.01
k_h multiplier ³⁷	1	2.0	2.0	2.0	2.0	2.0	2.0
k_v multiplier ³⁷	N/A	0.10	0.10	0.10	0.10	0.10	0.10
GWC (m TVNAP)	3885	3885	3885	3885	3885	3885	3885
k_h multiplier aquifer	N/A	1 10⁻⁴	0.32	1	1 10 ⁻⁴	0.32	1
k_v multiplier aquifer	N/A	1 10⁻⁴	0.32	1	1 10 ⁻⁴	0.32	1
Residual gas	0.3	0.25	0.23	0.15	0.25	0.23	0.15
$k_w@S_{rg}$	0.1	0.01	0.01	0.01	0.01	0.01	0.01

³² Input deck: Wadden_2016_MGT_Immobaq_v2b_MGTS.INP

³³ Input deck: Wadden_2016_MGT_resgas_v3a_MGTS.INP

³⁴ Input deck: Wadden_2016_MGT_Mobaq_v2b_MGTS.INP

³⁵ Input deck: Wadden_2015_MGT_MRN_v2

³⁶ Input deck: Wadden_2015_MGT_MRN_v3

³⁷ Due to the (absolute) permeability model update, the two M&R cycles are incomparable.

6.1.7.2 Meet & Regel cycle 2016 vs 2015 model comparison

A new SPG measurement was performed in April 2016. This pressure showed a little less pressure decline than straight extrapolation from initial pressure (Figure 51). This was as expected for the base case, residual gas model. For the mobile aquifer model (high case) a slightly higher GIIP was required to accommodate for this: GBV multiplier was modified from 1.20 to 1.25.

6.1.7.3 Water production

The water production for MGT-1B is given in Figure 56. The WGR measurements have quite some uncertainty, although with MGT-1B being a significant well in the system we know that it cannot be an excessive water producer.

Analogue wells perforating ROSLU3 (MGT-2 in Nes, ANJ-2C in Metslawier) have shown water extensive water influx from this zone, so this risk also applies to MGT-1B. There is however a possibility to set a plug to block off ROSLU3 perforations if deemed required. For now, the model suggests that very little formation is being produced, which is in line with observations.

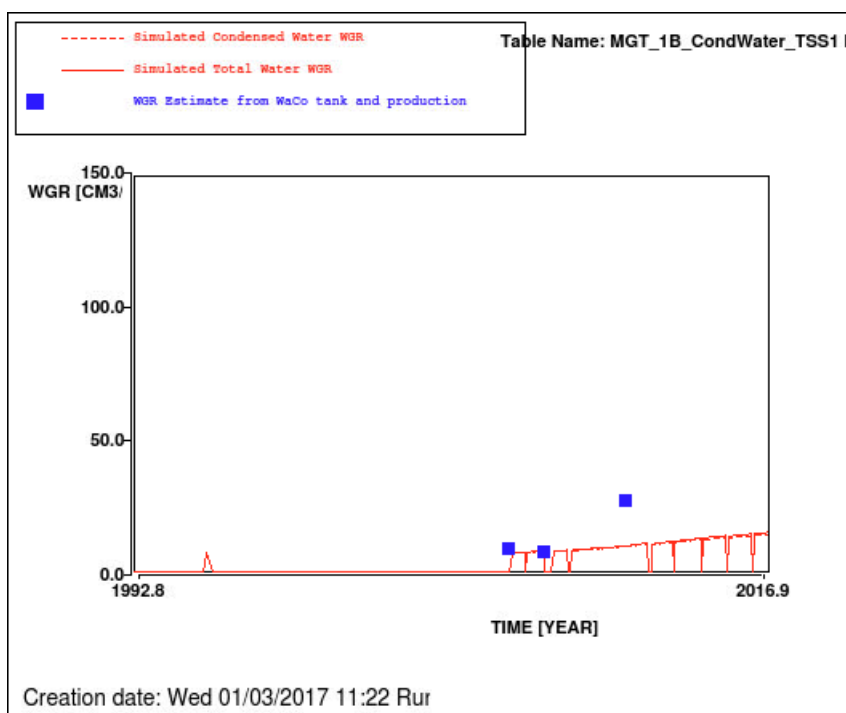


Figure 56 Simulated total WGR (red solid line), simulated condensed WGR (red dashed line) and estimated WGR from production and WaCo tank observations (blue squares) for MGT-1B. Base case realisation.

6.1.8 Nes

The Nes field (Figure 58) is located in the eastern Waddenzee part of the Noord Friesland Concession (NE-Netherlands). It was discovered by the well MGT-2 in April 1995. Wet gas is evacuated to the Anjum plant facilities as of February 2007. Its P/z plot can be found in Figure 59.

The Nes field is contained in the Upper Slochteren Sandstone Member (ROSLU) of the Rotliegend formation. It consists of Aeolian and fluvial/lacustrine sediments deposited in a desert environment. The thickness of the ROSLU in MGT-2 is 112 m, of which

approximately 60 mTV (gross) is gas bearing. The Nes gas field is a low-relief fault-closed structure.

In 2012, large amounts of water were being produced from MGT-2. PLT results showed water influx from the bottom perforations (Ref 8). A bridge plug was set on the shale layer between units 1 and 3 in October 2012, after which water production stopped. In 2012 MGT-3 was also drilled. Its top came in 22 m TV deeper than prognosis, and therefore only unit 1 was gas bearing. RFT results showed a pressure lag between unit 1 and unit 3 of around 100 bar (Ref 9). Units below unit 3 were also depleted, showing only minor pressure differentials compared to unit 3. This indicates that the shale layer (unit 2) between unit 1 and 3 is at least partially sealing and that the water bearing layers are relatively well connected. Currently, only unit 1 is being produced from.

In Q4 2015, an infill well was drilled, MGT-4A, which targeted the units 3-6 in the west of the field. However, it found the reservoir 26 metres deeper than prognosis and only found unit 1 gas-bearing. This resulted in the decision to drill a second well, MGT-5, in the south of the field. Also MGT-5 came in deep: 46 metres deeper than prognosis. It had found the GWC in ROSLU1 approximately at the same level as that of ROSLU3 in MGT-2. This suggests that the Nes field has the same original contact for both units. MGT-5 well found 5 metres of gas-bearing sands in ROSLU3 with a different contact in ROSLU3, at 3758mTV, 27 metres deeper than the original GWC at 3731mTV in ROSLU3. This difference could be explained by a movement of water from the MGT-5 area (south) to the MGT-2 area (north) via a U-tubing effect, see Figure 57.

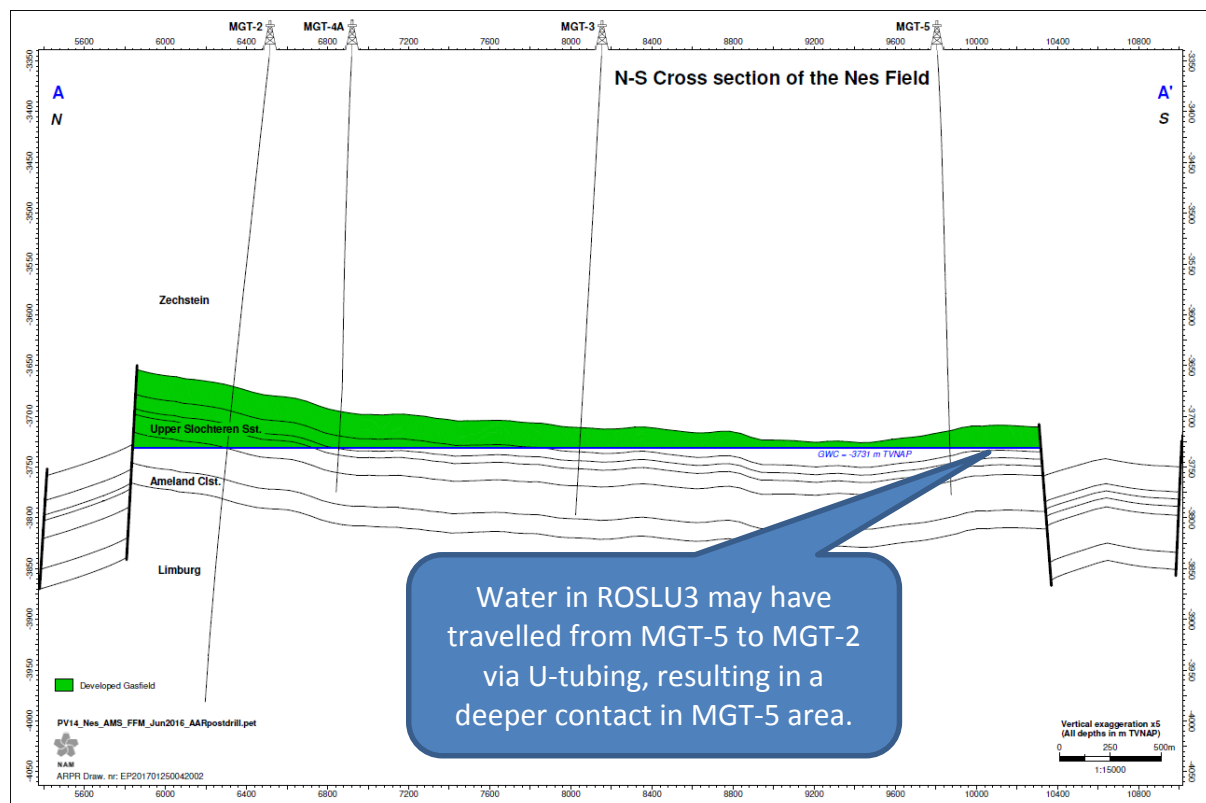


Figure 57 Cross section of Nes field.

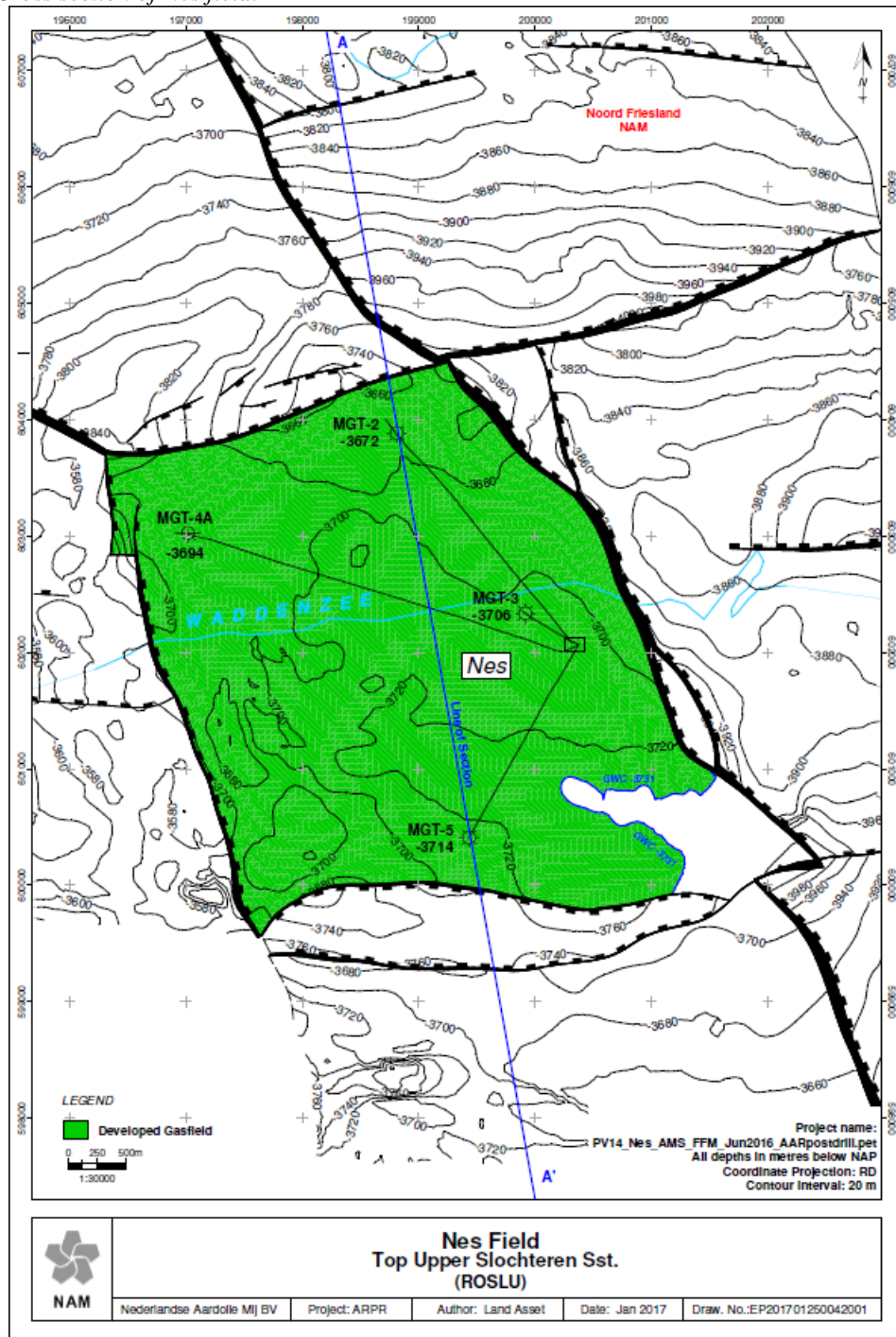


Figure 58 NES ARPR top ROSL map

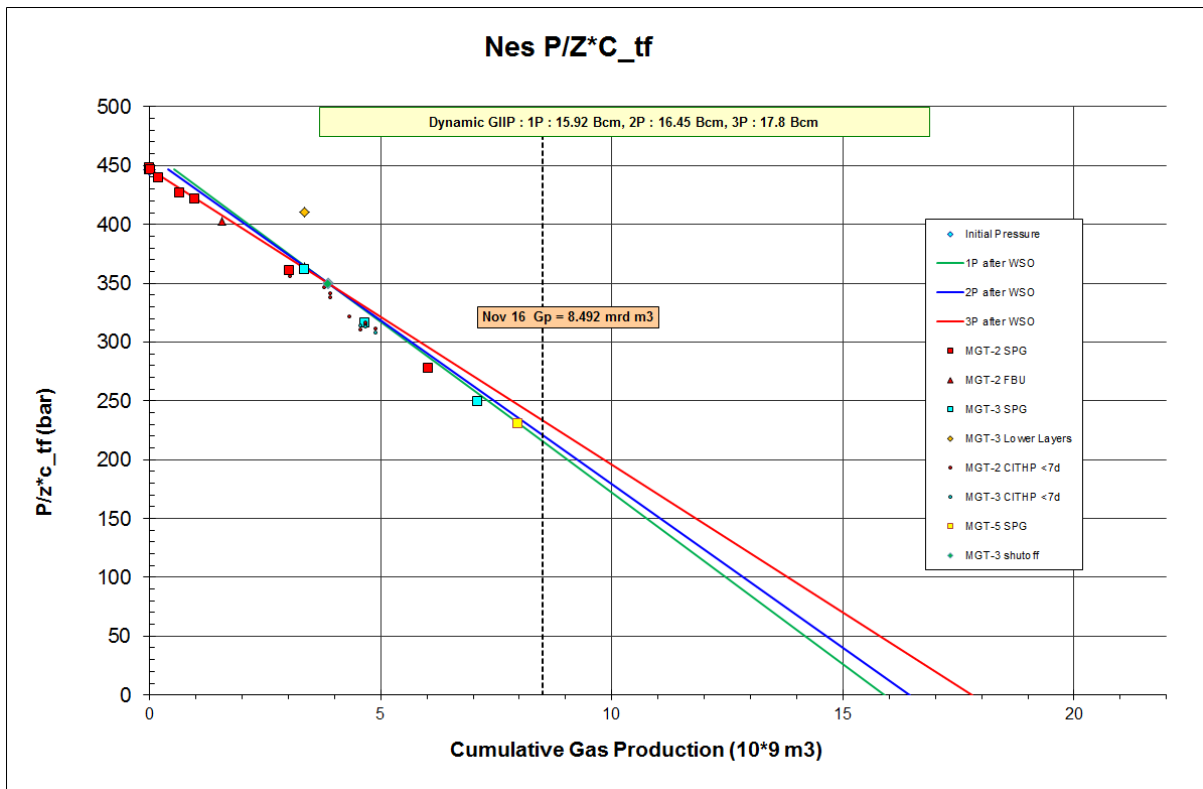


Figure 59 P/z plot for MGT-2 and MGT-3. Due to the high initial pressures, P/z has been corrected for rock compressibility (c_{if}).

6.1.8.1 Reservoir model

The static model was revised after the MGT-4A and MGT-5 wells were drilled, co-kriging the top structure to the new well tops. With the wells coming in much deeper than expected, production coming from ROSLU1 only since 2012, and with ROSLU3 pressures considerably higher than in ROSLU1, the ROSLU1 dynamic volume (15 bcm) was much higher than post-drill static volumes initially suggested (~bcm). Subsequently the porosity was increased (based on MGT-4A and MGT-5 log data) and the gas saturation height function was modified from the MGT-2 to the MGT-3 function, giving greater hydrocarbon volumes. After these changes, the pressure history could be properly matched.

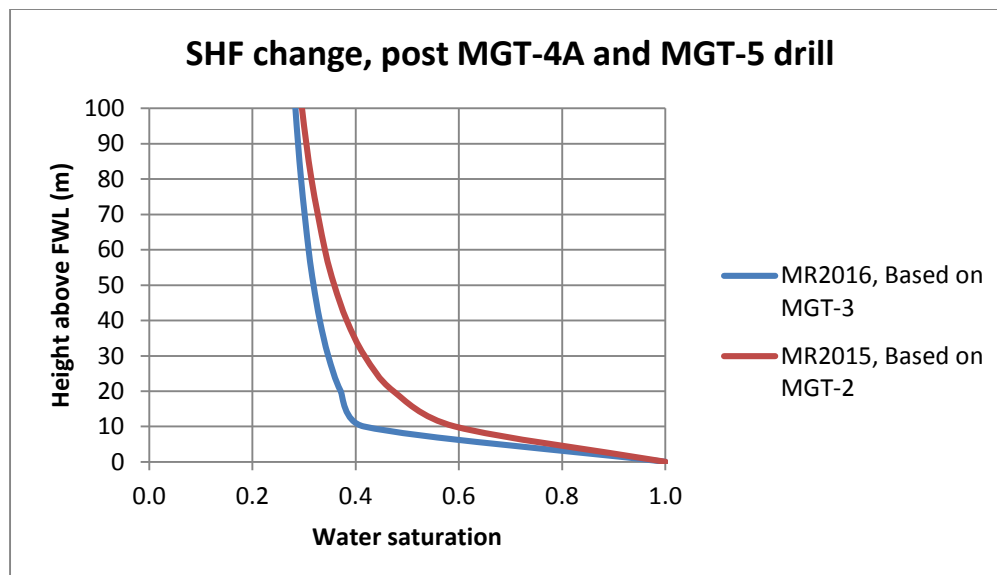


Figure 60 Saturation-Height function (SHF) modification after MGT-4A and MGT-5 well drilling and logging results.

The reservoir model for Nes is approached from a slightly different angle to that of the other fields. Nes has multiple wells drilled into the reservoir (MGT-3, -4A, -5) where an RFT was performed after part of the field was depleted.

To match the RFT on water pressures, the aquifer mobility has to be non-zero, ruling out a completely immobile aquifer. This results in a different approach to defining the low, base and high case subsidence realisations. With the aquifer pressure anchored at certain pressures at certain points in time, its mobility is not recognised as the key subsurface uncertainty.

The parameter currently seen as the largest uncertainty is vertical permeability. With RFTs mainly measuring the shallow part of the water leg, the degree of pressure depletion towards the deeper part of the reservoir is an unknown and relevant to subsidence forecasting. The low case model has a low k_v , the high case model has a high k_v .

Figure 61 shows the RFT match of the base case M&R2016 model for MGT-3, -4A and -5. Figure 62 also shows the MGT-3 RFT for the low and high case models. The match deteriorates, but is nevertheless used since the match on MGT-5 (not depicted) is still good.

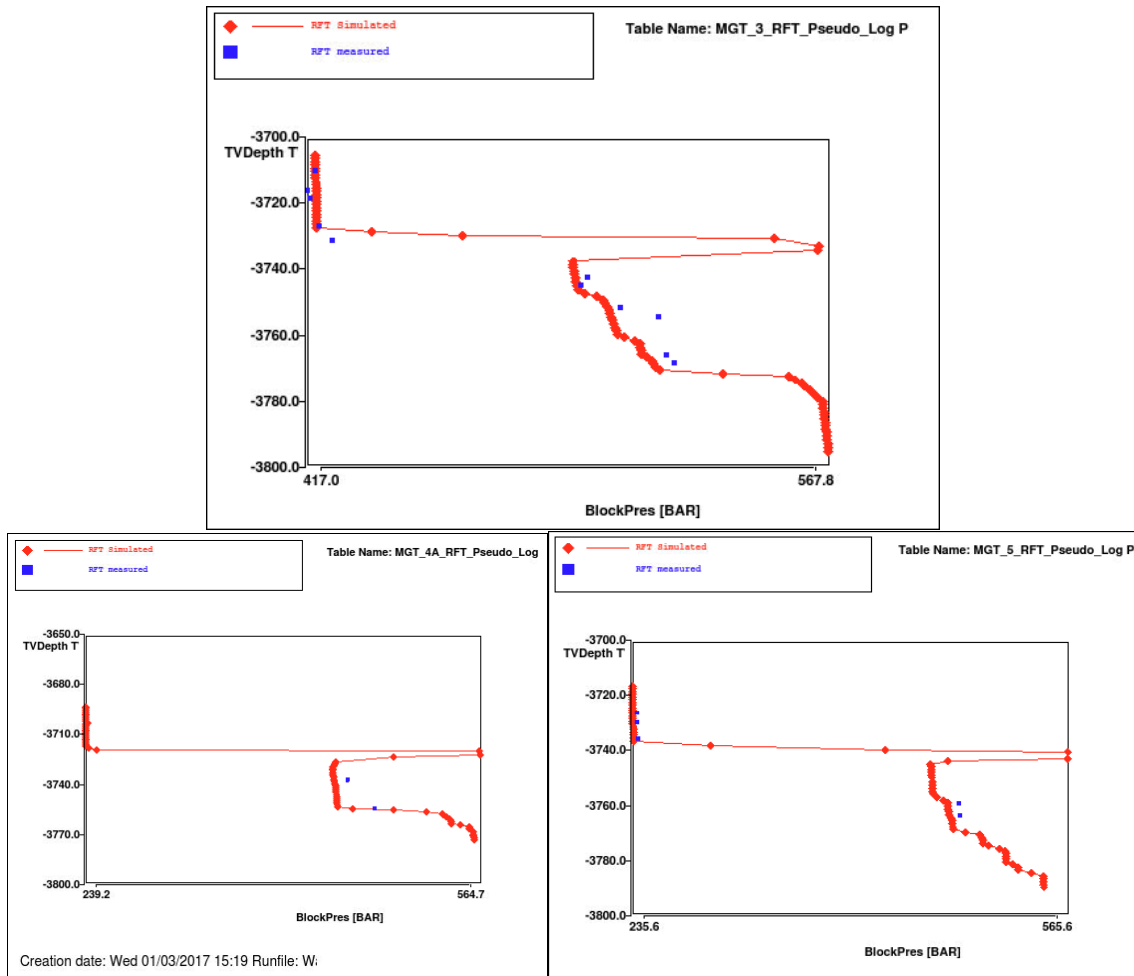


Figure 61 Simulated (red line and squares) and measured RFT pressure data (blue squares) for MGT-3. Top: MGT-3. Left: MGT-4A. Right: MGT-5.

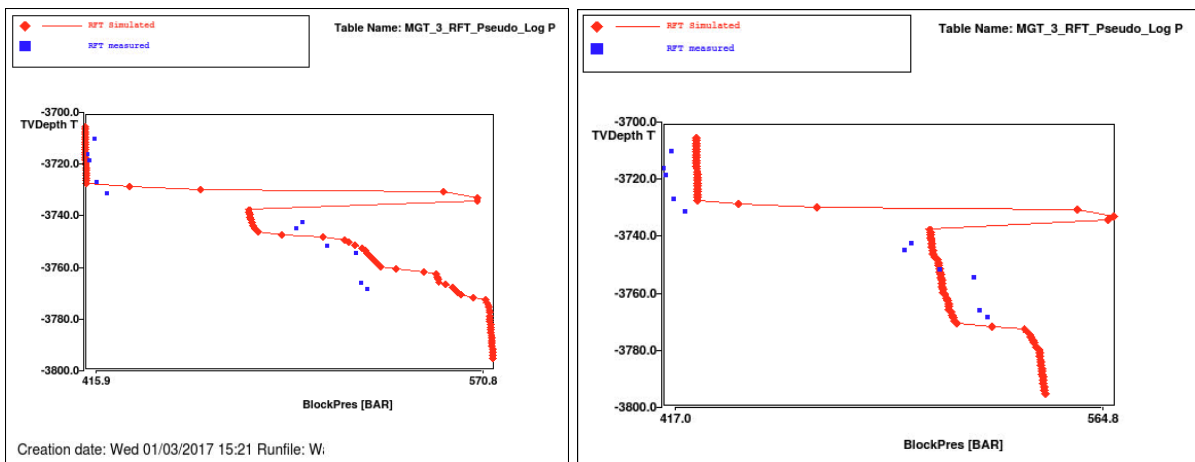


Figure 62 Simulated (red line and squares) and measured RFT pressure data (blue squares) for MGT-3. Left: Low-case (low k_v) model. Right: High-case (high k_v) model.

Figure 63, Figure 64 and Figure 65 show the downhole pressure match of MGT-2, MGT-3 and MGT-5 respectively. Figure 66 and Figure 67 show the tubing head pressure match for MGT-2 and MGT-3 respectively.

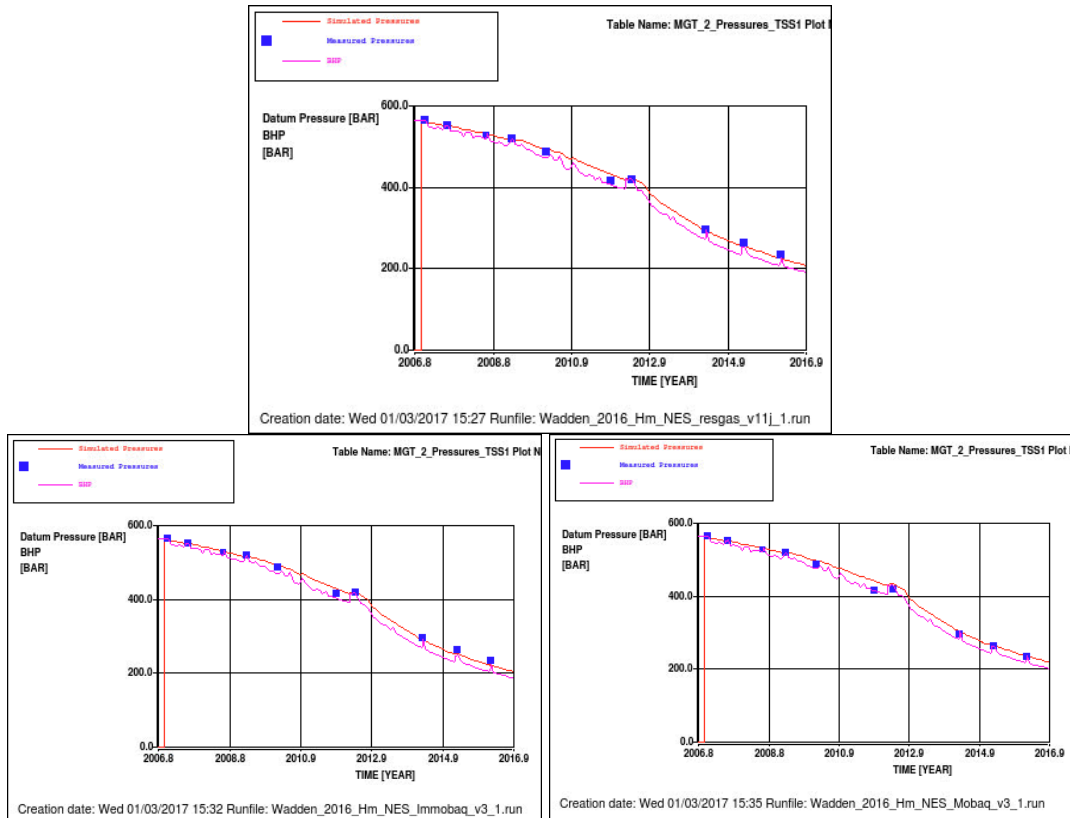


Figure 63 Simulated reservoir pressure (red line), BHP (violet line) and measured (blue squares) downhole pressure data in MGT-2. Top: Base case. Left: low case. Right: high case.

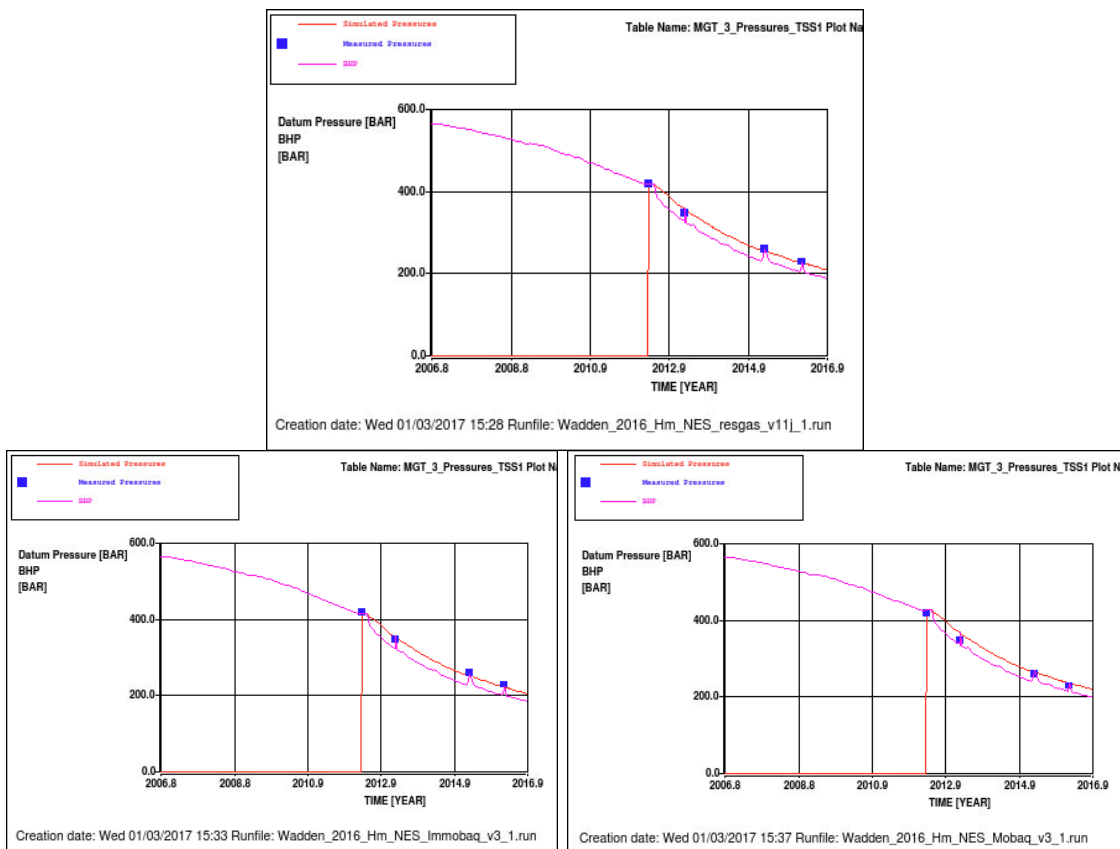


Figure 64 Simulated reservoir pressure (red line), BHP (violet line) and measured (blue squares) downhole pressure data in MGT-3. Top: Base case. Left: low case. Right: high case.

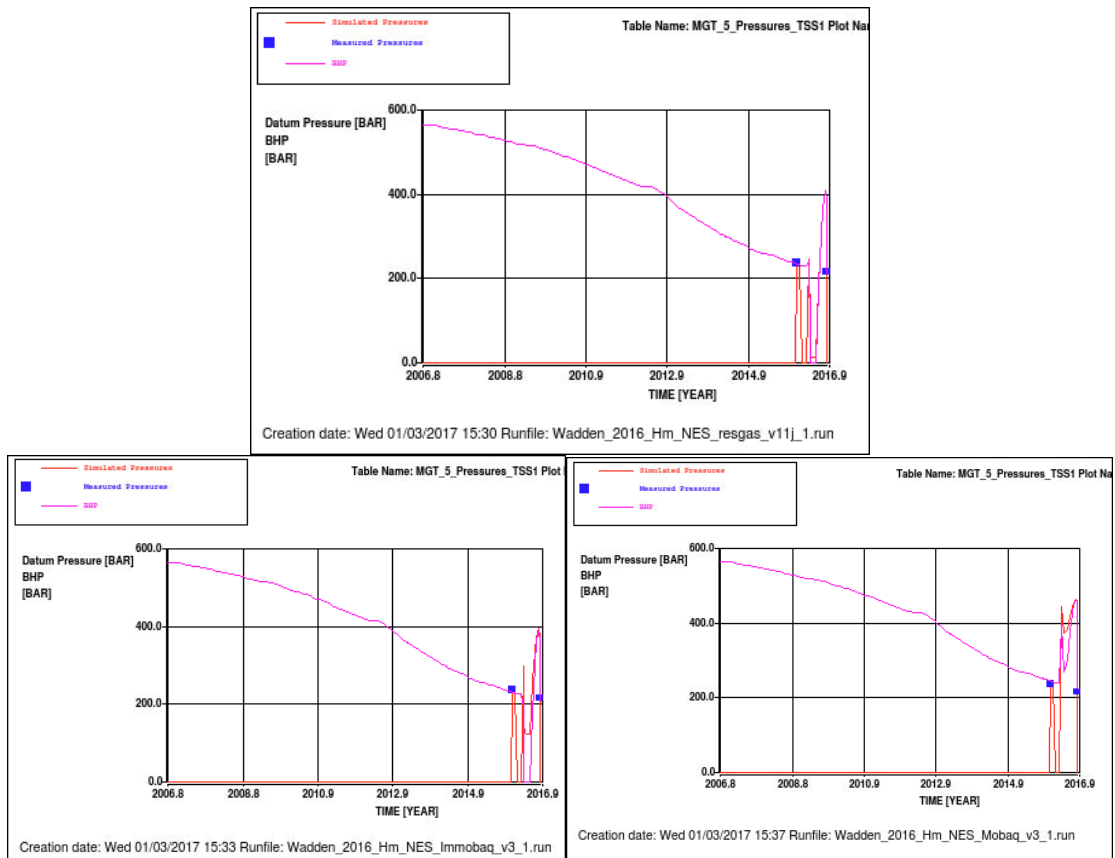


Figure 65 Simulated reservoir pressure (red line), BHP (violet line) and measured (blue squares) downhole pressure data in MGT-5 ROSSLU1. Top: Base case. Left: low case. Right: high case.

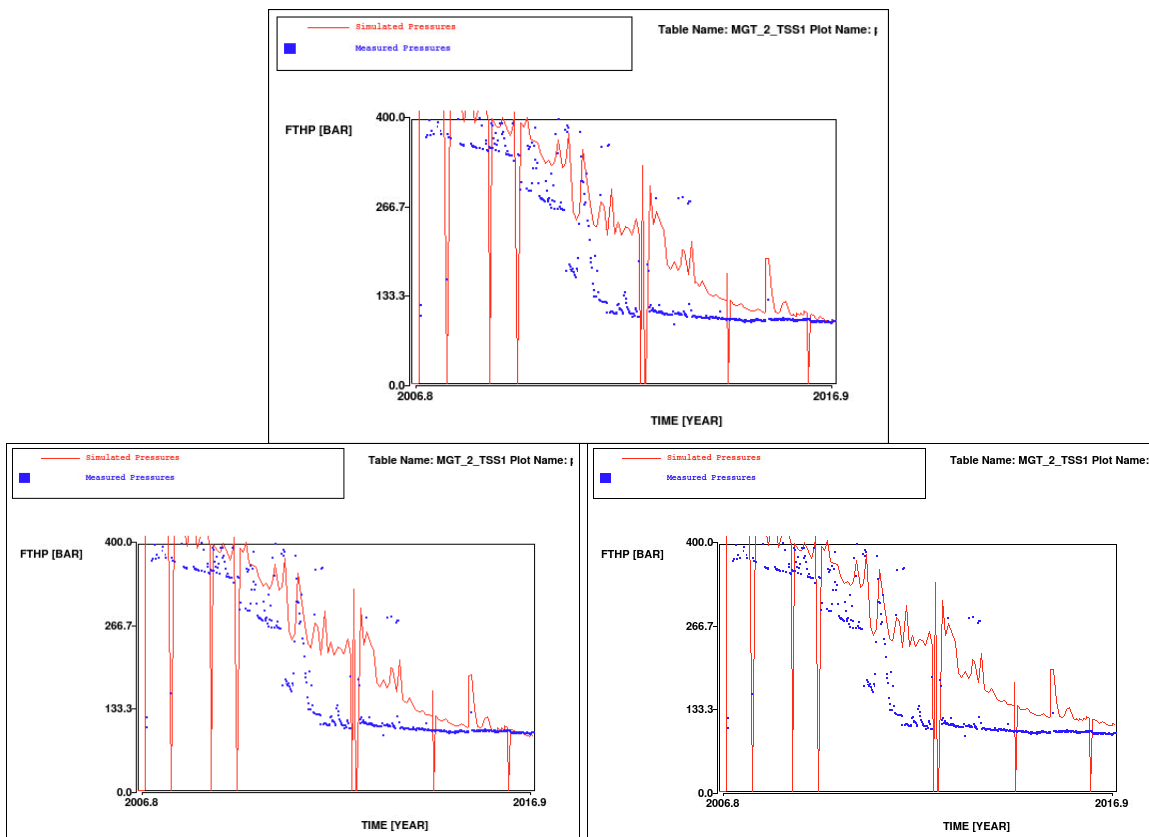


Figure 66 Simulated (red line) and measured (blue squares) flowing tubing head pressures in MGT-2. Top: Base case. Left: low case. Right: high case.

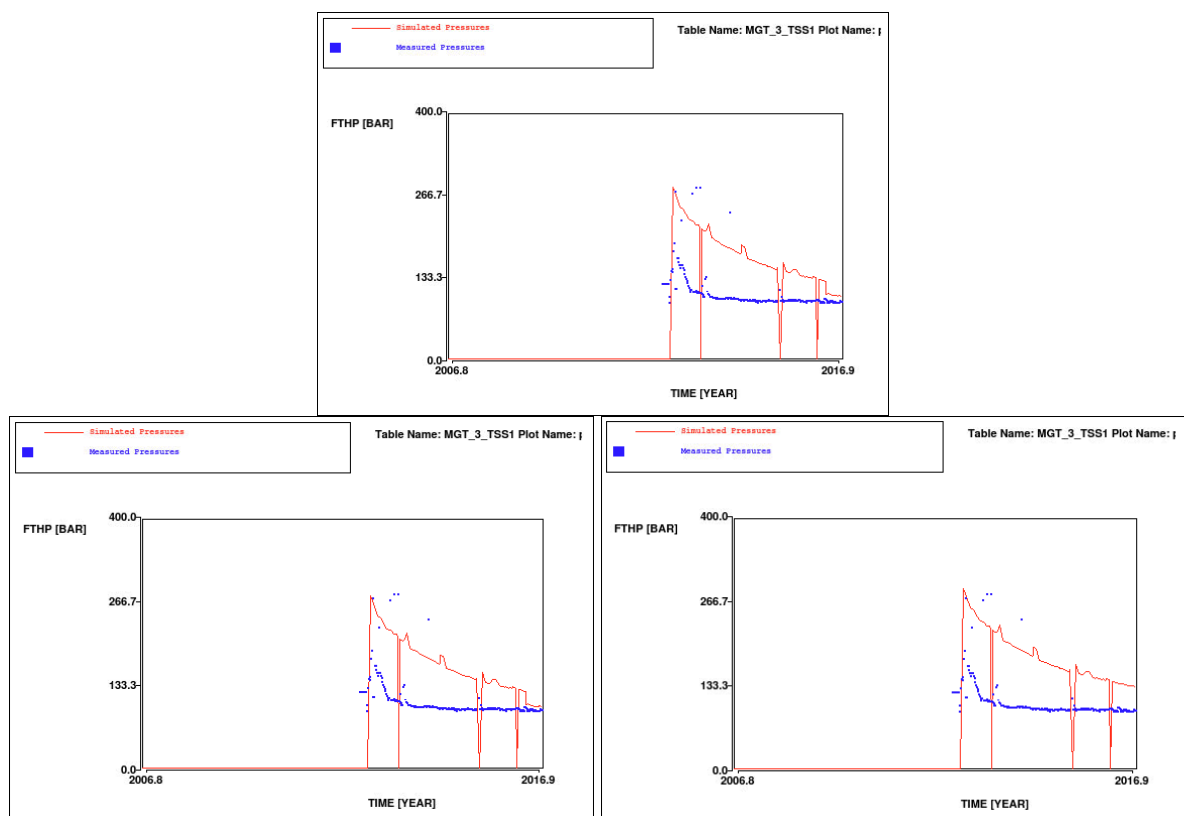


Figure 67 Simulated (red line) and measured (blue squares) flowing tubing head pressures in MGT-2. Top: Base case. Left: low case. Right: high case.

The pressure matches in general sense work well. Only the FTHP matches are somewhat off. As described in Section 4.3.6, the THP match is considered of secondary importance after downhole pressure matches. With RFTs and SPGs nicely matched, the models are considered fit-for-purpose for pressure forecasting for subsidence.

6.1.8.2 Meet & Regel cycle 2016 vs 2015 model comparison

With information coming from new wells, the dynamic realisation build was modified compared to M&R2015. Last year, the transmissibility of the ROLSU2 shale was taken as key subsurface uncertainty to subsidence modelling. Since then, MGT-4A and MGT-5 RFTs have been taken and found ROSLU3 (gas and water) at high (450-480 bara) pressure, almost 240 bar higher than ROSLU1 gas pressures. This has given valuable insight that the ROSLU2 is (almost) sealing on production timescales. Hence this can no longer be carried as key subsurface uncertainty.

This gave reason to re-define the realisation for the Nes field as shown in Table 27.

Table 27 Overview of dynamic realizations Nes M&R 2015 vs 2016

	Base structure	Residual gas below FWL	Vertical permeability in ROSLU3	GIIP [BNCM] above FWL	Unit 2 shale transmissibility
<i>M&R2015</i>					
1 – Low	pre- MGT4A,-5	x	Base	21.7	sealing
2 – Base	pre- MGT4A,-5	x	Base	19.4	large baffle
3 – High	pre- MGT4A,-5	x	Base	17.2	small baffle
<i>2016</i>					
1 – Low	post- MGT4A,-5	x	Low	16.7	sealing
2 – Base	post- MGT4A,-5	x	Base	16.7	sealing
3 – High	post- MGT4A,-5	x	High	16.7	sealing

Table 28 shows the parameters used for each realisation. The horizontal and vertical permeability multipliers have been split per unit (Top Unit 1, Bottom Unit 1, Unit 2 and Unit3-6) to be able to match on the PLTs and RFTs.

Table 28 History matching parameters used for the Meet & Regel cycle for Nes

Parameter	Static	Low M&R2016 ³⁸	Base M&R2016 ³⁹	High M&R2016 ⁴⁰	Low M&R2015 ⁴¹	Base M&R2015 ⁴¹	High M&R2015 ⁴¹
Residual gas sat. below FWL	0.16	0.16	0.16	0.16	0.15	0.15	0.15
Connected GIIP (Bcm)	16.7	16.7	16.7	16.7	21.7	19.4	17.2
Top structure		Post-MGT-4A,MGT-5			Pre-MGT-4A,MGT-5		
Average ROSLU1 porosity	0.15	0.156	0.156	0.156	0.136	0.136	0.136
GBV multiplier	1	1.0	1.0	1.0	1.20	1.05	0.93
k_h multiplier (TU1/BU1/U2/U3-6)	1	0.35 / 1.15 / 1 / 2.0	0.35 / 1.15 / 1 / 2.0	0.35 / 1.15 / 1 / 2.0	1.5 / 1.5 / 1.5 / 3.2	1.1 / 2.2 / 1 / 2.2	1 / 2.8 / 1 / 0.5
k_v multiplier (TU1/BU1/U2/U3-6)	N/A	1 / 1 / 0.001 / 0.03	1 / 1 / 0.001 / 0.3	1 / 1 / 0.001 / 1.0	0.01 / 0.01 / 1.9 10 ⁻⁴ / 0.01	1 / 1 / 0.03 / 0.02	1 / 1 / 3.2 / 0.02
GWC (m TVNAP)	3731	3731	3731	3731	3731	3731	3731
k_h multiplier aquifer	N/A	0.3	0.3	1.0	0.70	0.32	1
k_v multiplier aquifer	N/A	0.3	0.3	1.0	1	1	1
Residual gas	0.3	0.28	0.28	0.28	0.34	0.28	0.28
$k_w@S_{rg}$	0.1	0.1	0.1	0.1	0.1	0.1	0.1

The key differences in bold are related to the static GIIP changing. Furthermore, with the porosities in the static model changing, the permeability was also modified. The changes in permeability multiplier do not represent a modification of absolute permeability, since the permeability models themselves have changed. The varying k_v for the different cases has also been reflected in bold. For the high case, the aquifer was made extra mobile by equating the aquifer multiplier to unity.

6.1.8.3 Water production

Well MGT-2 experienced water breakthrough in 2012. This has been observed in increase in water production Figure 68 and PLT (Ref 8). The PLT showed that the lowest perforations were producing water. These were shut off with a plug. It is uncertain whether the water encroached vertically or horizontally. The lowest perforations are relatively close to the GWC, which makes vertical encroachment possible. The exact water encroachment behaviour is difficult to model.

³⁸ Input deck: Wadden_2016_NES_Immobaq_v3.INP

³⁹ Input deck: Wadden_2016_NES_resgas_v11j.INP

⁴⁰ Input deck: Wadden_2016_NES_Mobaq_v3.INP

⁴¹ Input deck: Wadden_2015_NES_MRN_v7.INP

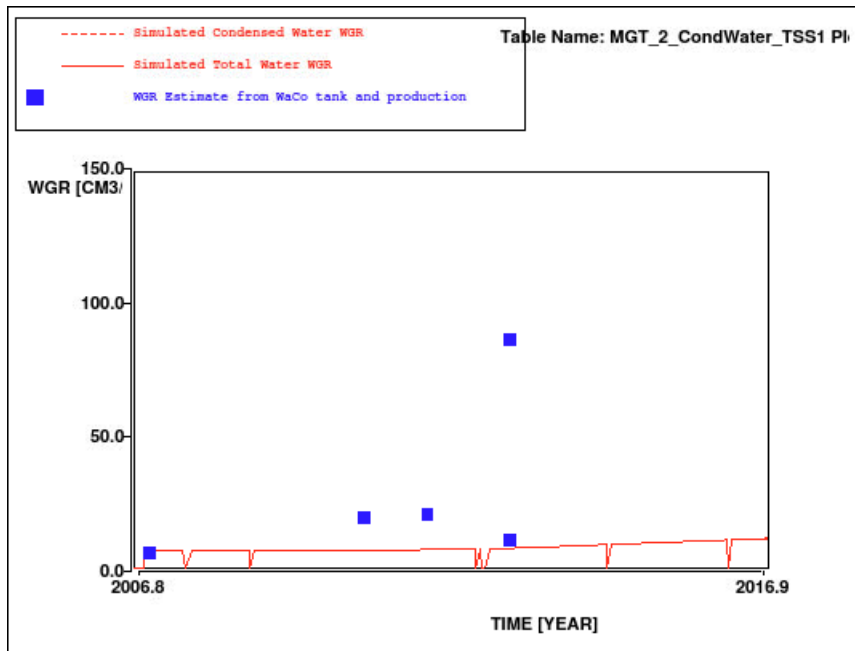


Figure 68 Simulated total WGR (red solid line), simulated condensed WGR (red dashed line) and estimated WGR from production and WaCo tank observations (blue squares) for MGT-2 [$s\ m^3/E6N\ m^3$].

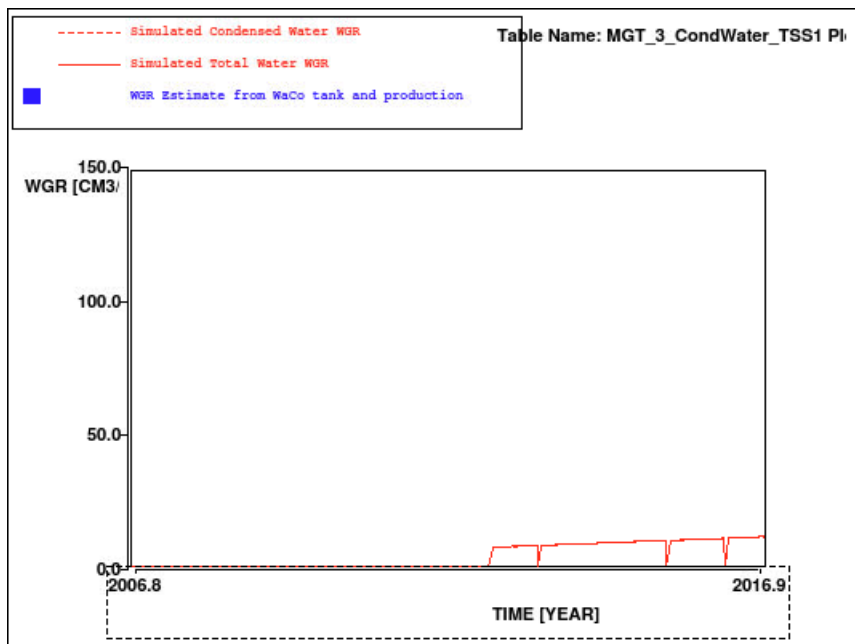


Figure 69 Simulated total WGR (red solid line), simulated condensed WGR (red dashed line) and estimated WGR from production and WaCo tank observations (blue squares) for MGT-3 [$s\ m^3/E6N\ m^3$].

6.1.9 Vierhuizen

The Vierhuizen field (Figure 70) is located approximately 5 km to the north of the Munnekezipl field. The field was discovered by VHN-1 in 1994, which confirmed economic gas productivity from the Upper Slochteren formation. The western lobe of the field (discovered by VHN-3 well, but economic development has not been proven) is almost completely contained in the Noord Friesland concession (and reported in the Vierhuizen West entry). The South Block in the eastern lobe of the field (discovered by VHN-1) lies almost fully in the Groningen concession. The area between the western and eastern lobe lies in the De Marne concession. As GIIP in the De Marne concession is minor it is reported together with the North Friesland volumes. The eastern lobe is bounded to the North by an East-West running fault.

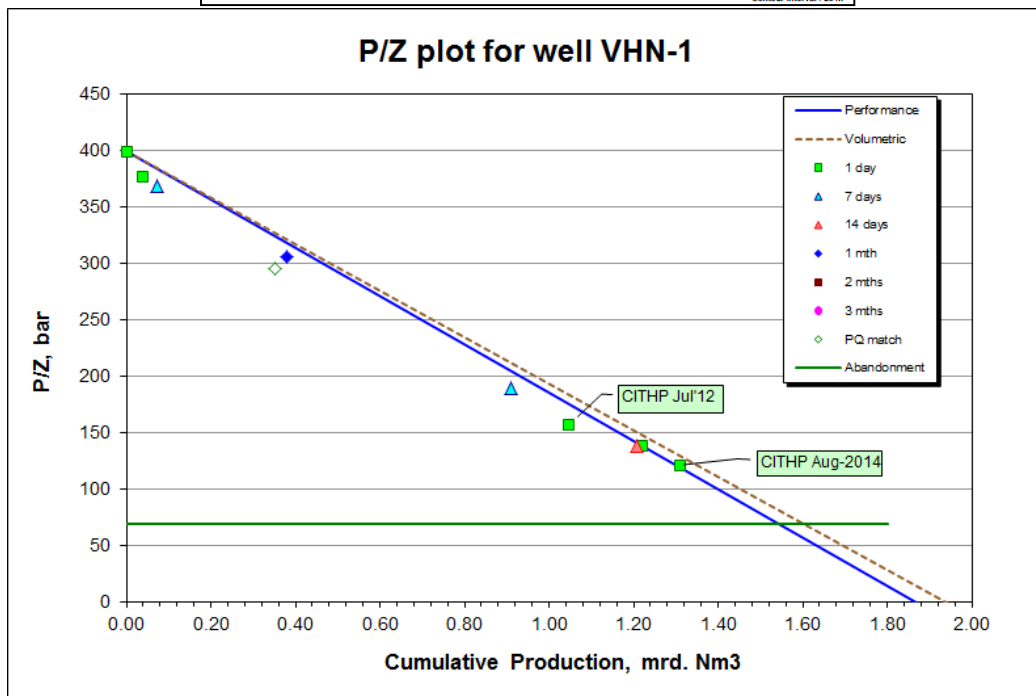
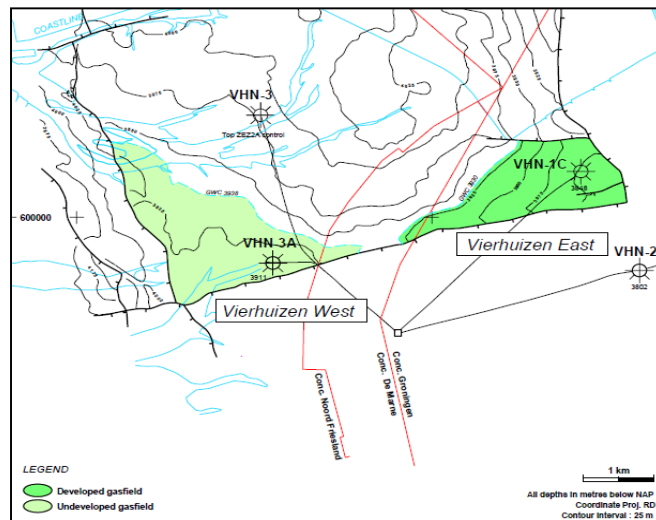


Figure 70 ARPR Top ROSLU map for Vierhuizen-East and P/z plot for VHN-1C.

6.1.9.1 Reservoir model

The Vierhuizen reservoir is connected to a relatively large aquifer compared to the size of the gas field. Because of this, the model expects strong water influx from the aquifer if this is assumed fully mobile. The P/z plot in Figure 70 shows some extra pressure support in late

field-life. Due to the small size of the field and large aquifer behind it, it is suspected that aquifer support plays a role here. Also the reservoir model supports this view.

The gas below FWL realisation indeed generates pressure support. But at the same time, aquifer pressures stay very high – almost virgin. An immobile aquifer realisation cannot mimic the pressure behaviour described, without modifying certain parameters to unrealistic values. Because of this, it was decided during M&R2015 to define a single realisation for both low and base case: the paleo-gas below FWL realisation. The mobile aquifer realisation has also been constructed. No changes have been made to this modelling strategy. An overview of the realisations is given in Table 29.

Table 29. Overview of dynamic realizations during M&R 2015 for Vierhuizen

	Base structure	Immobile aquifer	Paleo-residual gas below FWL	Mobile aquifer	Base dynamic GIIP
1 – Low/ Base	x		x		x
2 – High	x			x	x

The downhole pressures matches are shown in Figure 71. The base case model shows a good match with the data. The mobile aquifer realisation does not very well, since the model expects water encroachment, reducing the effective permeability around the well, or increasing drawdown. Nevertheless, the model is used as a high case subsidence sensitivity.

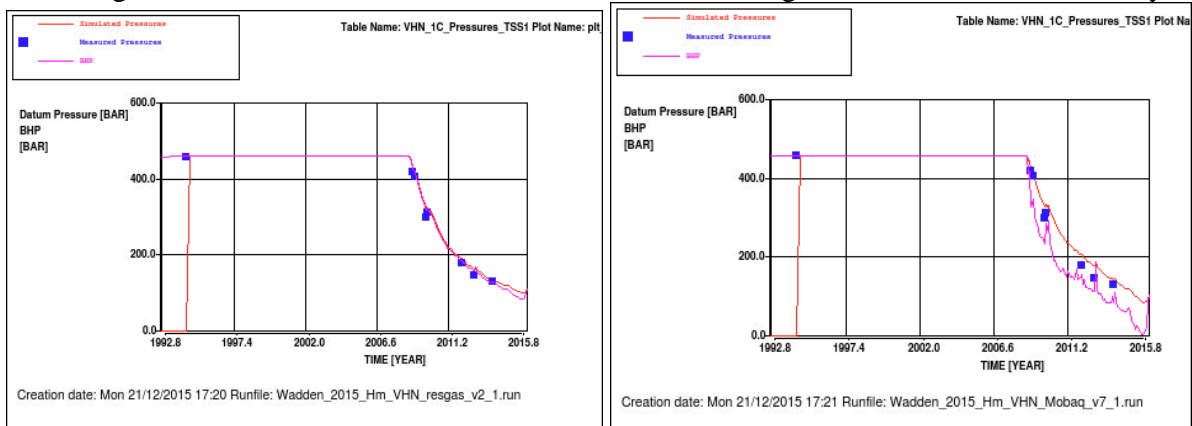


Figure 71 Simulated reservoir pressure (red line), BHP (violet line) and measured (blue squares) downhole pressure data in MGT-3. Left: low/base case. Right: high case.

Figure 72 shows the FTHP match of the two models.

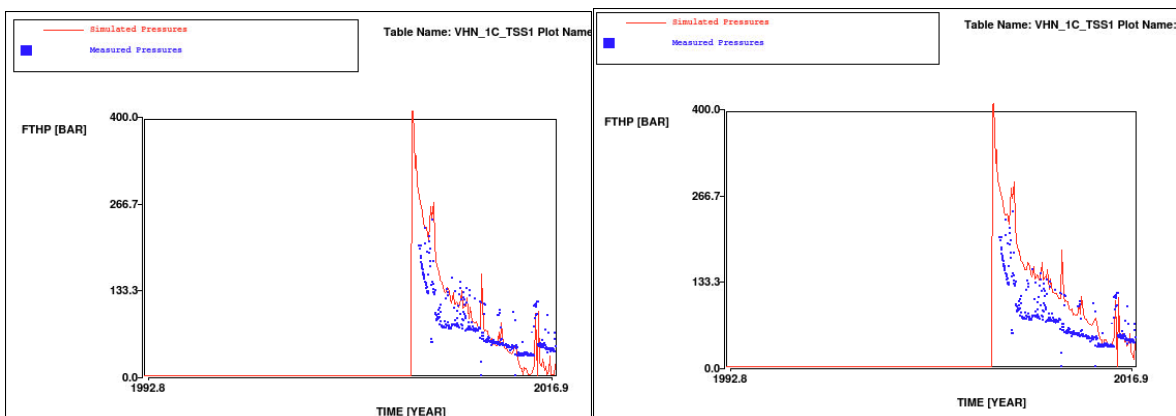


Figure 72 Simulated (red line) and measured (blue squares) flowing tubing head pressures in VHN-1C. Left: low/base case. Right: high case.

Table 30 History matching parameters used for the Meet & Regel cycle for Vierhuizen.

Parameter	Static	Low/Base M&R2016 ⁴²	High M&R2016 ⁴³	Low/Base M&R2015 ⁴⁴	High M&R2015 ⁴⁴
Residual gas sat. below FWL	0.16	0.16	0	0.16	0
GBV multiplier	2.3	1.0	1.10	1.0	1.05
k_h multiplier	1	2.3	0.058	2.3	0.058
k_v multiplier	N/A	0.058	0.99	0.058	0.99
GWC (m TVNAP)	3930	3930	3937	3930	3937
k_h multiplier aquifer	N/A	0.32	1	0.32	1
k_v multiplier aquifer	N/A	0.32	1	0.32	1
Residual gas	0.3	0.18	0.10	0.18	0.10
$k_w@S_{rg}$	0.1	0.16	0.1	0.16	0.1
K*h multiplier VHN-1C	1	0.03	1	1	1

6.1.9.2 Meet & Regel cycle 2016 vs 2015 model comparison

Little has changed compared to the models in M&R2016. However, with production steadily continuing from VHN-1C without watering out, the mobile aquifer model needs more volume. For the paleo-residual gas model, the M&R2015 model was not fine-tuned to the measured FTHP. This fit has now been improved, by imposing a k_h -multiplier on the well. This is somewhat undesired, and it is proposed to (statically and dynamically) redefine this field in the M&R2017.

6.1.9.3 Water production

The Grijpskerk system to which Vierhuizen is flowing connects over 20 wells and the WGR allocation uncertainty is very high. Therefore, no WGR matching was performed for this field.

⁴² Input deck: Wadden_2016_VHN_resgas_v3.INP

⁴³ Input deck: Wadden_2016_VHN_Mobaq_v3a.INP

⁴⁴ Input deck: Wadden_2015_VHN_MRN_v2.INP

6.2 Forecasting

6.2.1 Forecasting Assumptions

As described in Section 4.7, the models are constrained to the Business Plan 2016 gas production figures. The figures deviate from Business Plan 2015, which was used for M&R2015. An overview of the production changes are given in Table 31.

Table 31 Changes to production (M&R2016 – M&R2015), in E6N m³/y.

	ANJ-1	ANJ-4	ANJ-2	ANJ-3	LWO-1	LWOO Infill	LWO-2	LWO-3	MGT-1	MGT Infill	MGT-2	MGT-3	4 (Nes)	5 (Nes)	VHN-1
2015	0	4	0	5	0	1	0	-7	5	0	12	7	0	0	-8
2016	0	8	0	-24	10	0	-3	6	14	0	30	17	-184	-138	20
2017	0	-10	0	5	39	0	-5	19	24	0	38	22	-236	-137	66
2018	0	0	0	0	20	-216	3	11	7	-75	25	10	-202	-96	49
2019	0	-4	0	22	3	-161	6	-9	-8	-216	21	4	-160	-75	11
2020	0	-8	0	25	-3	-31	0	-15	-11	-84	-14	-21	-124	-65	0
2021	0	-2	0	13	28	53	0	3	6	-43	-2	-13	-104	-50	0
2022	0	-33	0	0	20	69	0	-4	7	237	-9	-24	-84	-40	0
2023	0	3	0	0	19	62	0	1	5	51	4	-16	-68	-28	0
2024	0	4	0	0	17	59	0	0	-1	22	7	-13	-53	-22	0
2025	0	4	0	0	13	54	0	0	78	-48	7	-12	-40	-16	0
2026	0	6	0	0	12	48	0	3	21	0	11	-9	-23	-8	0
2027	0	7	0	0	8	46	0	1	11	0	20	-2	-16	-4	0
2028	0	10	0	0	0	0	0	0	13	0	37	14	-6	15	0
2029	0	47	0	0	0	0	0	0	79	0	123	56	0	6	0
2030	0	45	0	0	0	0	0	0	73	0	117	51	0	0	0
2031	0	42	0	0	0	0	0	0	66	0	108	44	0	0	0
2032	0	40	0	0	0	0	0	0	60	0	101	29	0	0	0
2033	0	38	0	0	0	0	0	0	56	0	96	13	0	0	0
2034	0	36	0	0	0	0	0	0	52	0	94	8	0	0	0
2035	0	34	0	0	0	0	0	0	49	0	92	0	0	0	0
Sum	0	271	0	46	186	-17	2	9	607	-157	918	165	-1299	-657	161

Major changes to forecasting are discussed on a field-by-field basis in this section. An overview of all production figures is given in Appendix A (see also Ref 10).

6.2.2 Forecasting results

This section discusses the outcome of the forecasting and the impact it has had on the subsidence prognosis. Figure 73 and Figure 74 show the differences between M&R2016 reservoir models that feed into subsidence calculations versus M&R2015 for the base case. Differences are generally small, except for the Nes field, which is covered in Subsection 6.2.2.6. Also the Lauwersoog-C change looks large at first sight, but the inflated vertical axis is somewhat misleading. Slight changes to average virgin pressure (as also evident from Lauwersoog-C in Figure 74) have to do with water density change, described in Section 4.2.5.

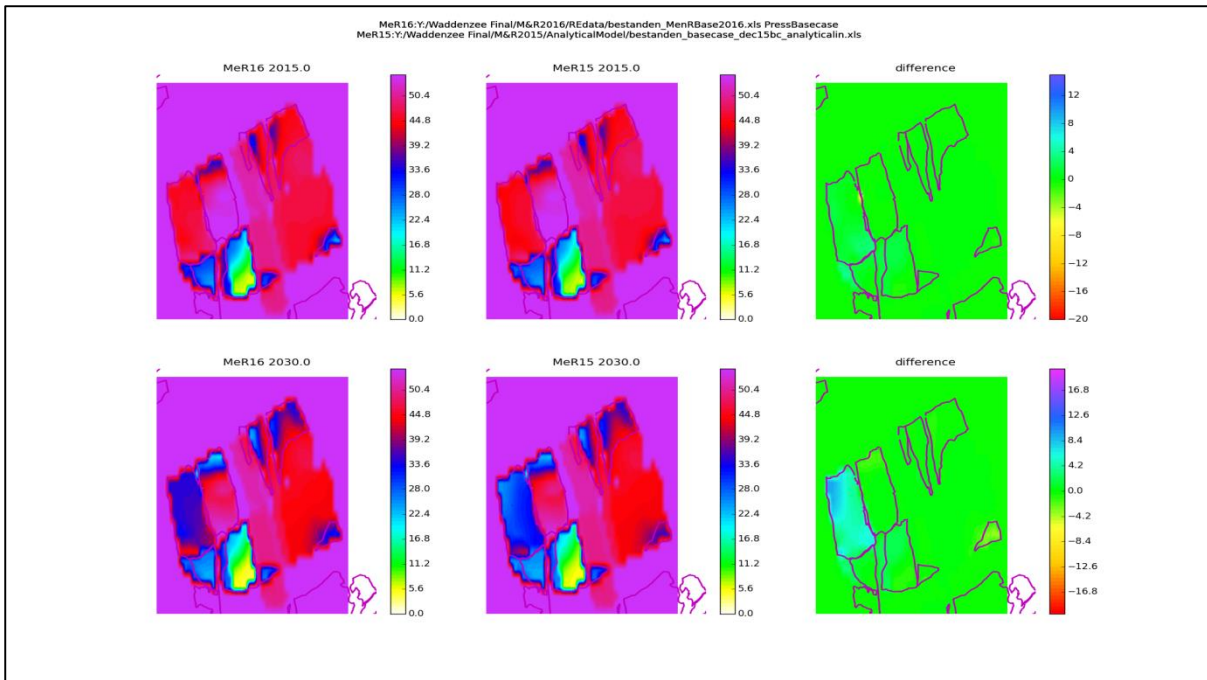


Figure 73 Modelled average reservoir pressure (MPa) of Waddenzee area (base case). Left column: M&R2015. Middle column: M&R2016. Right column: difference plot. Top 2015, bottom 2030.

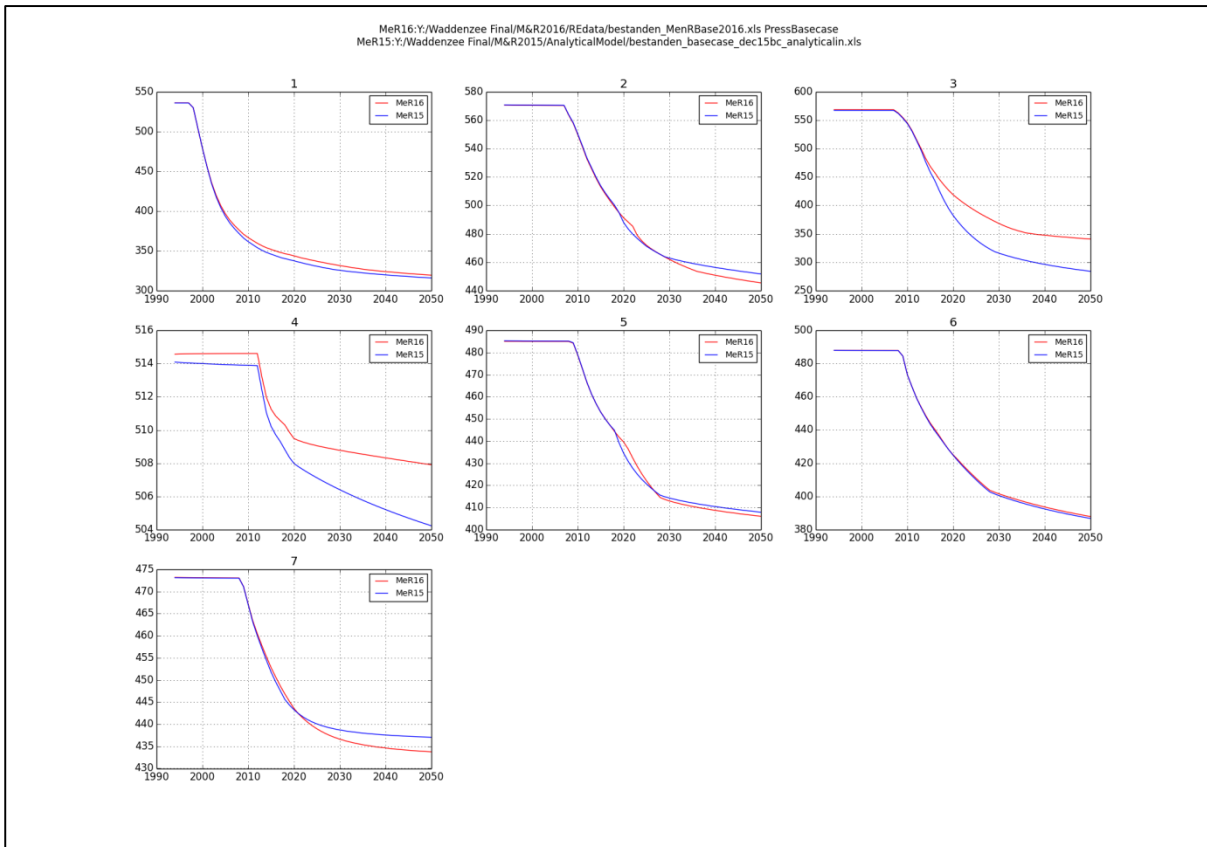


Figure 74 Average reservoir pressures per (set of) field(s), base case. Red: M&R2016, blue: M&R2015. 1 = Anjum, Ezumazijl, Metslawier, 2 = Moddergat, 3 = Nes, 4 = Lauwersoog Central, 5 = Lauwersoog East, 6 = Lauwersoog West, 7 = Vierhuizen.

6.2.2.1 Anjum, Ezumazijl, Metslawier

Since Anjum, Ezumazijl and Metslawier (non-Waddenzee fields) are the fields that act as a calibration for the subsidence prognosis for the other fields, these fields are analysed together. Therefore, the depletion is depicted in terms of today (2016) and not in the future.

A changes occurred to Anjum (ANJ-4) production forecast. The projected end-of-field-life of Anjum has been extended from 2028 to 2035, since the potentially newly drilled TRN-2 well is incorporated in the system forecast, resulting in longer system life. But being a calibration field, changes to forecasting of the Anjum fields are irrelevant to Waddenzee subsidence.

Anjum is the most important ‘calibration field’ of the area. The water pressures of this field are shown in Figure 75 along with the models of M&R2015. There are no significant changes to the pressure prognosis of Anjum.

In the other two fields, the changes are also small. Only Metslawier had an update, where the high permeability streaks in ROSLU5B and ROSLU6 were modelled differently. This has caused the low- and base-case depletion model to be modified.

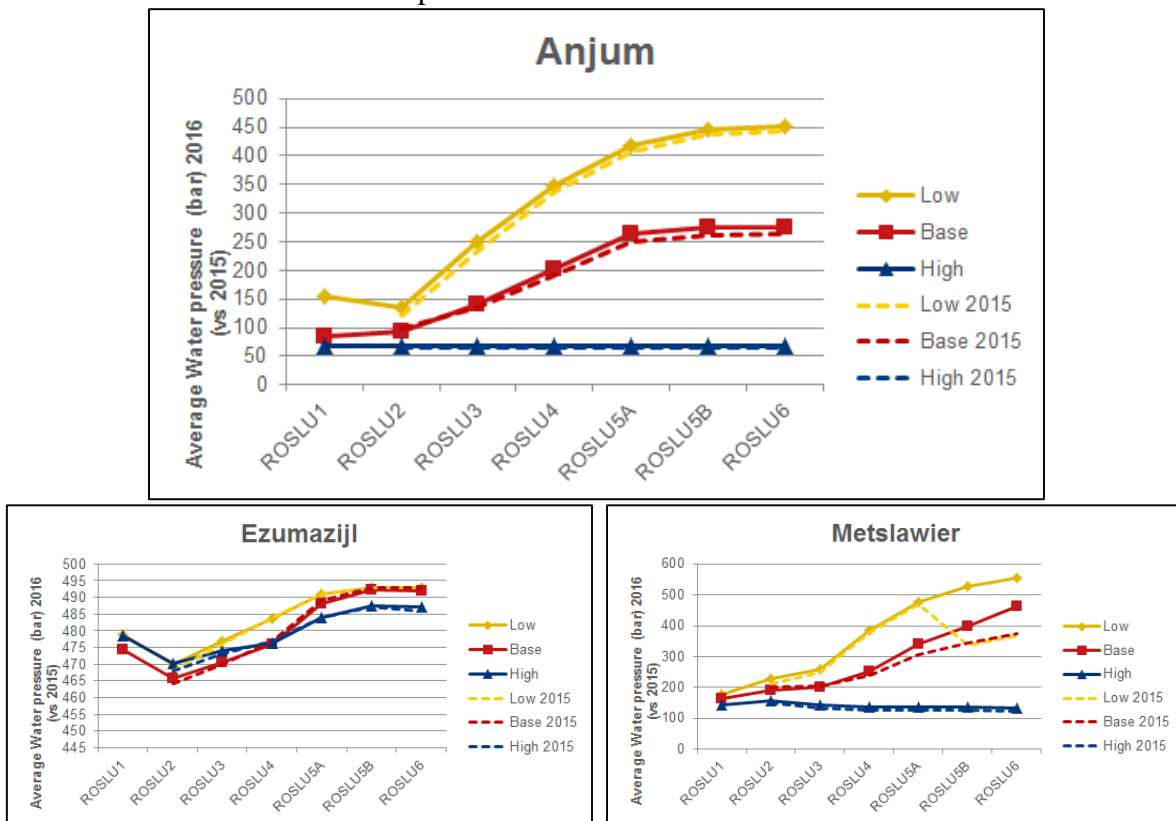


Figure 75 Water pressures in 2016, per zone for fields Anjum, Ezumazijl and Metslawier. Comparison with M&R2015, at 2015.

6.2.2.2 Lauwersoog Central

With a small lowering of production forecast, the low and base case have less pressure depletion than the previous year. But average depletion in Lauwersoog-C is by any means marginal (initial pressure at datum equals 500bara).

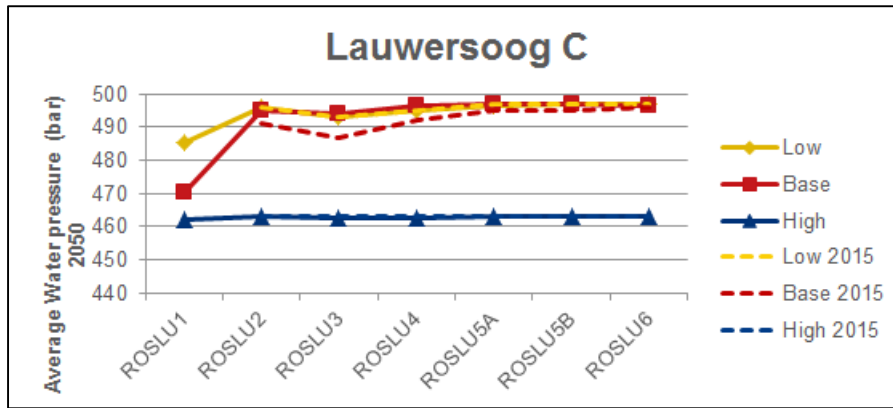


Figure 76 Water pressures in 2050, per zone for Lauwersoog C.

6.2.2.3 **Lauwersoog East**

In Business Plan 2016, 0.17 BNCM more is forecast to produce from Lauwersoog-Oost than in 2015. This modification comes from the field model update performed in Q4 2015, during the maturation of the Lauwersoog East infill project. The revision has led to a slight increase of the water pressure drop in the high case. One would expect this effect also to be visible for the base case, but this is compensated by the lowering of k_v in the base case model. For the low case, water pressures have stayed unaffected. Of course gas pressures do modify accordingly.

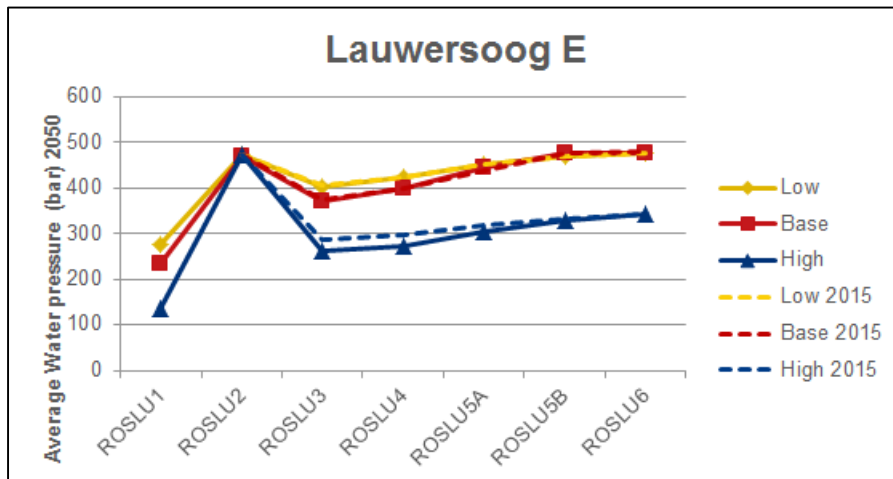


Figure 77 Water pressures in 2050, per zone for Lauwersoog East.

6.2.2.4 **Lauwersoog West**

For Lauwersoog West, changes are very limited. A higher k_v was modelled for the high case (see Section 6.1.5.2), impacting the pressures in the deeper layers.

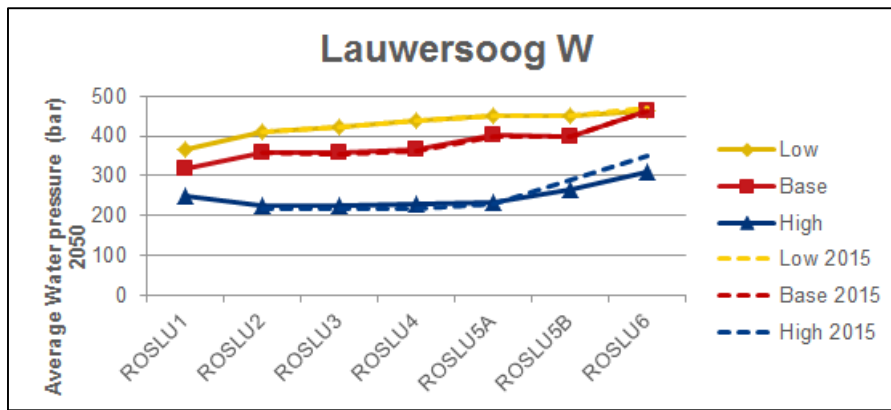


Figure 78 Water pressures in 2050, per zone for Lauwersoog West

6.2.2.5 **Moddergat**

The models of Moddergat have remained largely unchanged. The high case model had a modification to the GBV (see Section 6.1.7.2) and hence the average pressure has somewhat decreased.

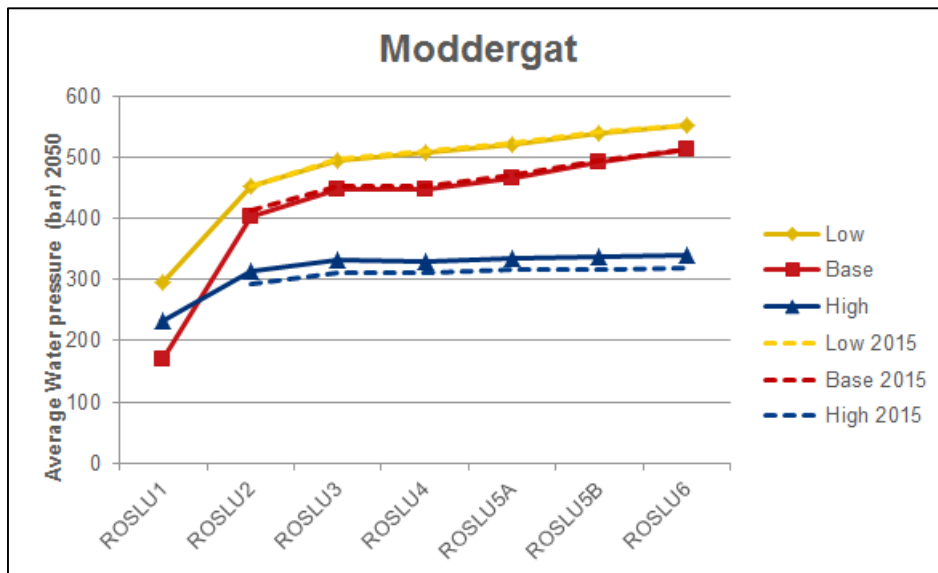


Figure 79 Water pressures in 2050, per zone for Moddergat.

6.2.2.6 **Nes**

The Nes model has substantially changed as discussed in Section 6.1.8. The two newly drilled wells MGT-4A and MGT-5 have given new insights that the ROSLU2 shale is at least strongly baffling. As a result the pressure forecast has also changed, with depletion in the lower layers being much less than previously modelled. The updated range lies almost entirely above the old pressure range. This may have significant impact on the subsidence forecast of the Nes area.

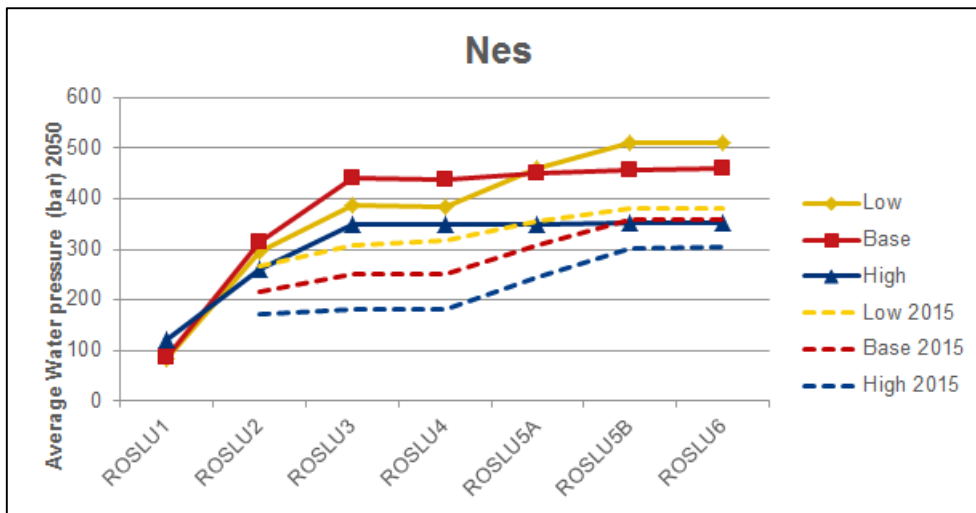


Figure 80 Water pressures in 2050, per zone for Nes

6.2.2.7 Vierhuizen

In Vierhuizen, the Business Plan update revealed that production is likely to continue until 2019, whereas last year, production was expected to stop in 2017. This has caused downward revision of high case depletion pressures. Nevertheless, average pressure for the Vierhuizen field remains relatively high and as a result the predicted subsidence remains limited.

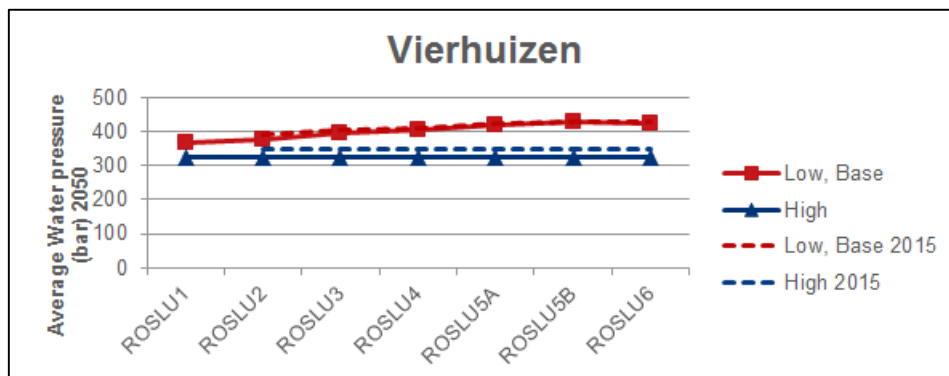


Figure 81 Water pressures in 2050, per zone for Vierhuizen.

6.2.3 Subsidence scenarios

The subsidence calculation method is beyond the scope of this report and is described thoroughly in Ref 11. However it is worth noting here in what way the different realisations have been used for subsidence calculations.

Subsidence is calculated by combining the pressure drop in the reservoir model with overburden compaction characteristics. A probabilistic method has been used to determine a realistic low-base-high subsidence scenario. Geomechanical parameters as well as the subsurface realisations presented in this document were used as input uncertainties to these calculations.

Deterministic subsidence scenarios have subsequently been defined to align with the P90, P50 and P10 subsidence outcomes. This was done by combining multiple realisations of different fields.

Table 32 Subsidence scenarios.

	Low case subsidence scenario	Base case subsidence scenario	High case subsidence scenario
Anjum Fields			
Anjum	<i>High realisation</i>	<i>Base realisation</i>	<i>Base realisation</i>
Ezumazijl	<i>High realisation</i>	<i>Base realisation</i>	<i>Base realisation</i>
Metslawier	<i>Base realisation</i>	<i>Base realisation</i>	<i>Base realisation</i>
Waddenzee Fields			
Lauwersoog Central	<i>Low realisation</i>	<i>Base realisation</i>	<i>High realisation</i>
Lauwersoog East	<i>Low realisation</i>	<i>Base realisation</i>	<i>High realisation</i>
Lauwersoog West	<i>Low realisation</i>	<i>Base realisation</i>	<i>High realisation</i>
Moddergat	<i>Low realisation</i>	<i>Base realisation</i>	<i>High realisation</i>
Nes	<i>Low realisation</i>	<i>Base realisation</i>	<i>High realisation</i>
Vierhuizen East	<i>Low/Base realisation</i>	<i>Low/Base realisation</i>	<i>High realisation</i>

Table 32 shows which subsurface realisation is used for which subsidence scenario. The only change to M&R2015 is marked in bold: Metslawier Base realisation used in the low case subsidence scenario.

The table may read a little difficult and is illustrated by an example in the paragraph below.

*The high case subsidence scenario for the entire Waddenzee area is created in three steps. **The first step** involves calibrating the base pressure-drop realisations of the Anjum fields to the existing subsidence measurements above these fields. **The second step** is to determine the overburden compaction properties that are required to match the measured subsidence. In **the third step** these overburden compaction parameters are then used in combination with the high pressure-drop realisations of the Waddenzee fields to determine the subsidence forecast for the Waddenzee.*

Since Anjum, Ezumazijl and Metslawier have a calibration function, combining their high depletion realisation with the low realisation of the Waddenzee Fields will result in a low subsidence scenario and vice versa. However, the combination of a low depletion realisation of the Anjum fields with the high depletion realisation of the Waddenzee fields could not be matched with subsidence measurements. Hence the base realisation was used for the Anjum fields in the high subsidence scenario. The same holds for combining a high depletion realisation of Metslawier with low cases of Waddenzee fields. Thus effectively, the low realisation of Anjum, Ezumazijl and Metslawier as well as the high case of Metslawier are not used in any deterministic subsidence scenario.

6.2.4 General forecasting conclusion

In general, the depletion forecast of the Anjum and Waddenzee fields have not changed by a large degree. Existing uncertainties on aquifer depletion have remained the same. There was therefore no change to the methodology of realisation building.

An exception to the previous paragraph is the Nes field. The two wells MGT-4A and MGT-5 have generated valuable insights in that the ROSLU2 shale is at least strongly baffling. This has resulted into a much lower degree of depletion for the deeper layers.

Furthermore, the sealing capacity of ROSLU2 confirms what is believed to be the case in other fields (e.g. Lauwersoog) too. Therefore the learnings of Nes did not lead to any modification of the other fields: the ROSLU2 in many fields was already sealing.

The inclusion of Ternaard Infill well to the total Waddenzee production forecast has led to a longer production tail of the system. This affects Anjum and Moddergat, and also Nes. On Nes these changes are added to the changes caused by including the information from the new wells.

REFERENCES

Ref 1 J. Seubring & R.G. Hakvoort, Petrophysical evaluation of the Rotliegend in the North-Friesland Waddenzee area, 2004, EP200412271228

Ref 2 F.C. Seeberger, Methodology of predicting gas- and aquifer pressures in the proposed Waddenzee development area. EP200512206995

Ref 3 Shell Production Handbook

*Ref 4 Ron Peterson. DEPLETION OF ROTLIEGEND GAS AQUIFERS- PART2 (draft18).
\\europe.shell.com\tcs\ams\ui.nam\field\epe_re_02\wadden\mores_2013\Reports\11_MR2015\...*

Ref 5 A.M. Tichler, SCAL inventory Land North 29-12-2015. EP201512253848

Ref 6 R. Gray, Advanced rock properties study for NAM BV; Well: Anjum-1, 1994, NAM 26.914

Ref 7 Ezumazijl North Development Well ANJ-5B, Summary of the ANJ-5B well, 2003, NAM200302001936

Ref 8 J. Seubring, MGT-2 PLT results (September, 2012), 2012, EP201209216710

Ref 9 M. Schenkel, Petrophysical Evaluation of MGT-3, June 2012, EP201205214774

Ref 10 Winningsplan Profiles.

\\europe.shell.com\tcs\ams\ui.nam\field\epe_re_02\wadden\mores_2013\99_Include\10_Forecast\MR2016_Forecasts\Winningsplan+Actual_BP16.xlsx, tab Base_Forecasts_MR2016

Ref 11 Gaswinning vanaf de locaties Moddergat, Lauwersoog en Vierhuizen. Resultaten uitvoering Meet- en regelcyclus 2016

FIGURES

Figure 1 Map of the Waddenzee area	9
Figure 2 Histogram of Nes permeability (M&R2016: Orange filled, M&R2015: green dotted line)	14
Figure 3 Porosity-Permeability relationship (M&R 2016: green, M&R2015: red)	14
Figure 4 Core plug permeability data for gas and aquifer leg.....	20
Figure 5 Residual gas saturation as a function of the connate water saturation	27
Figure 6 Relative water permeability at residual gas saturation as a function of the residual gas saturation.	27
Figure 7 ARPR top ROSL map of Anjum field	30
Figure 8 P/z plot Anjum-1 and Anjum-4 combined	30
Figure 9 Simulated pressure (red line), simulated BHP (violet line) and measured down hole pressure (blue squares) for base case. Left: ANJ-1, Right: ANJ-4B.	32
Figure 10 Simulated pressure (red line), simulated BHP (violet line) and measured down hole pressure (blue squares) for low case. Left: ANJ-1, Right: ANJ-4B.	32
Figure 11 Simulated pressure (red line), simulated BHP (violet line) and measured down hole pressure (blue squares) for high case. Left: ANJ-1, Right: ANJ-4B.	32
Figure 12 Simulated (red line) and measured (blue squares) FTHP data in ANJ-4B. Top: base case. Left: low case. Right: high case.	33
Figure 13 Simulated (red line + squares) and measured (green line) PLT in ANJ-1. Base case model.	34
Figure 14 Simulated total WGR (red solid line), simulated condensed WGR (red dashed line) and estimated WGR from production and WaCo tank observations (blue squares) for ANJ-4B. Base case realisation.	35
Figure 15 Ezumazijl ARPR top ROSL map.....	37
Figure 16 P/z plot ANJ-3.....	37
Figure 17 Simulated pressure (red line), simulated BHP (violet line) and measured (blue squares) downhole pressure data in ANJ-3. Top: base case. Left: low case. Right: high case.	38
Figure 18 Simulated (red line) and measured (blue squares) flowing tubing head pressures in ANJ-3. Top: Base case. Left: Low case. Right: High case.	39
Figure 19 Simulated (red line + squares) and measured (green line) PLT in ANJ-3.....	39
Figure 20. Simulated total WGR (red solid line), simulated condensed WGR (red dashed line) and estimated WGR from production and WaCo tank observations (blue squares) for ANJ-3. Base case realisation.	41
Figure 21 Lauwersoog-Central ARPR top ROSL map	41
Figure 22 P/z plot for LWO-2.	42
Figure 23 Simulated pressure (red line), simulated BHP (violet line) and measured (blue squares) downhole pressure data in LWO-2. Top: base case. Left: low case. Right: high case.	43
Figure 24 Simulated (red line) and measured (blue squares) flowing tubing head pressures in LWO-2. Top: base case. Left: low case. Right: high case.	43
Figure 25 Simulated total WGR (red solid line), simulated condensed WGR (red dashed line) and estimated WGR from production and WaCo tank observations (blue squares) for LWO-2. Base case realisation.	45
Figure 26 Lauwersoog-Oost ARPR top ROSL map	46
Figure 27 P/z plot for LWO-1B.....	46
Figure 28 Simulated (red line + squares) and measured (green line) PLT in LWO-1B. Left: 1997, pre-production. Right: 2014. Base case realisation.	47
Figure 29 Simulated reservoir pressure (red line), flowing bottom hole pressure (violet line) and measured (blue squares) downhole pressure data in LWO-1B. Top: base case. Left: low case. Right: high case.	48
Figure 30 Simulated (red line) and measured (blue squares) flowing tubing head pressures in LWO-1B. Top: base case. Left: low case. Right: high case.	49
Figure 31 Simulated total WGR (red solid line), simulated condensed WGR (red dashed line) and estimated WGR from production and WaCo tank observations (blue squares) for LWO-1B.....	50
Figure 32 Lauwersoog-West ARPR top ROSL map.....	51
Figure 33 P/z plot LWO-3.....	51
Figure 34 Simulated (red line and squares) and measured RFT pressure data (blue squares) for LWO-3.....	52
Figure 35 Simulated (red line + squares) and measured (green line) PLT in LWO-3. Base case realisation.....	52

Figure 36 Simulated reservoir pressure (red line), flowing bottom hole pressure (violet line) and measured (blue squares) downhole pressure data in LWO-3. Top: Base case Left: low case. Right: high case.	53
Figure 37 Faults in the MoReS simulation model.	54
Figure 38 Simulated (red line) and measured (blue squares) flowing tubing head pressures in LWO-3. Top: base case. Left: low case. Right: high case.	54
Figure 39 Simulated total WGR (red solid line), simulated condensed WGR (red dashed line) and estimated WGR from production and WaCo tank observations (blue squares) for LWO-3. Base case realisation.	56
Figure 40 Metslawier ARPR top ROSL map.....	57
Figure 41 P/z plot for ANJ-2C.	57
Figure 42 Simulated (red line + squares) and measured (green line) PLT in ANJ-2C with original perforations in 1994. Base case realisation.	58
Figure 43 Simulated (red line + squares) and measured (green line) PLT in ANJ-2C in 1999 with original perforations from 1994 closed and new perforations from 1997 added. Base case realisation.	59
Figure 44 Simulated (red line) and measured (blue squares) flowing tubing head pressures in ANJ-2C. Top: base case. Left: low case. Right: high case.	60
Figure 45 Simulated reservoir pressure (red line) and measured (blue squares) downhole pressure data in ANJ-2C. Top: base case. Left: low case. Right: high case.	61
Figure 46 Log of ANJ-2C showing the salt scaling with the gamma ray log in the left panel and the liquid rise from SPTG in the right panel.	63
Figure 47 Cross section of the water saturation change around ANJ-2C with in red the water entering via high permeable streaks and cross flowing at the top (blue is no change in saturation).	63
Figure 48 Water saturation change in unit 1, with in red the water encroaching from the west (blue is no change in saturation), and around the well the cross-flow.	64
Figure 49 Simulated total WGR (red solid line), simulated condensed WGR (red dashed line) and estimated WGR from production and WaCo tank observations (blue squares) for ANJ-2C.....	64
Figure 50 Moddergat ARPR top ROSL map.....	65
Figure 51 P/z plot for MGT-1B. Due to its high initial pressures, P/z has been corrected for rock compressibility (C_{tr}).	65
Figure 52 Base case pressure profile in the Moddergat field in 2015.	66
Figure 53 Simulated reservoir pressure (red line), simulated BHP (violet line) and measured (blue squares) downhole pressure data in MGT-1B. Top: base case. Left: low case. Right: high case.	67
Figure 54 Simulated (red line) and measured (blue squares) flowing tubing head pressures in MGT-1B. Top: base case. Left: low case. Right: high case.	67
Figure 55 Simulated (red line + squares) and measured (green line) PLT in MGT-1B in 1995.....	68
Figure 56 Simulated total WGR (red solid line), simulated condensed WGR (red dashed line) and estimated WGR from production and WaCo tank observations (blue squares) for MGT-1B. Base case realisation.	69
Figure 57 Cross section of Nes field.	71
Figure 58 NES ARPR top ROSL map.....	71
Figure 59 P/z plot for MGT-2 and MGT-3. Due to the high initial pressures, P/z has been corrected for rock compressibility (C_{tr}).	72
Figure 60 Saturation-Height function (SHF) modification after MGT-4A and MGT-5 well drilling and logging results.	73
Figure 61 Simulated (red line and squares) and measured RFT pressure data (blue squares) for MGT-3. Top: MGT-3. Left: MGT-4A. Right: MGT-5.	74
Figure 62 Simulated (red line and squares) and measured RFT pressure data (blue squares) for MGT-3. Left: Low-case (low k_v) model. Right: High-case (high k_v) model.	74
Figure 63 Simulated reservoir pressure (red line), BHP (violet line) and measured (blue squares) downhole pressure data in MGT-2. Top: Base case. Left: low case. Right: high case.	75
Figure 64 Simulated reservoir pressure (red line), BHP (violet line) and measured (blue squares) downhole pressure data in MGT-3. Top: Base case. Left: low case. Right: high case.	75
Figure 65 Simulated reservoir pressure (red line), BHP (violet line) and measured (blue squares) downhole pressure data in MGT-5 ROSLU1. Top: Base case. Left: low case. Right: high case.	76
Figure 66 Simulated (red line) and measured (blue squares) flowing tubing head pressures in MGT-2. Top: Base case. Left: low case. Right: high case.	76
Figure 67 Simulated (red line) and measured (blue squares) flowing tubing head pressures in MGT-2. Top: Base case. Left: low case. Right: high case.	77

Figure 68 Simulated total WGR (red solid line), simulated condensed WGR (red dashed line) and estimated WGR from production and WaCo tank observations (blue squares) for MGT-2 [$\text{s m}^3/\text{E6N m}^3$].	79
Figure 69 Simulated total WGR (red solid line), simulated condensed WGR (red dashed line) and estimated WGR from production and WaCo tank observations (blue squares) for MGT-3 [$\text{s m}^3/\text{E6N m}^3$].	79
Figure 70 ARPR Top ROSLU map for Vierhuizen-East and P/z plot for VHN-1C.	80
Figure 71 Simulated reservoir pressure (red line), BHP (violet line) and measured (blue squares) downhole pressure data in MGT-3. Left: low/base case. Right: high case.	81
Figure 72 Simulated (red line) and measured (blue squares) flowing tubing head pressures in VHN-1C. Left: low/base case. Right: high case.	81
Figure 73 Modelled average reservoir pressure (MPa) of Waddenzee area (base case). Left column: M&R2015. Middle column: M&R2016. Right column: difference plot. Top 2015, bottom 2030.	84
Figure 74 Average reservoir pressures per (set of) field(s), base case. Red: M&R2016, blue: M&R2015.	84
Figure 75 Water pressures in 2016, per zone for fields Anjum, Ezumazijl and Metslawier. Comparison with M&R2015, at 2015.	85
Figure 76 Water pressures in 2050, per zone for Lauwersoog C.	86
Figure 77 Water pressures in 2050, per zone for Lauwersoog East.	86
Figure 78 Water pressures in 2050, per zone for Lauwersoog West	87
Figure 79 Water pressures in 2050, per zone for Moddergat.	87
Figure 80 Water pressures in 2050, per zone for Nes	88
Figure 81 Water pressures in 2050, per zone for Vierhuizen.	88

TABLES

Table 1. Overview of dynamic realisations (all fields except Nes and Vierhuizen).....	6
Table 2. Overview of dynamic realisations (Nes).....	6
Table 3. Overview of dynamic realisations (Vierhuizen).	7
Table 4 Rock compressibility per field	12
Table 5 Static gas initially in place (GIIP) above FWL.....	13
Table 6. Overview wells in Waddenzee area.....	16
Table 7. SPG measurements since M&R2015.	17
Table 8. Converted CITHPs since M&R2015.	17
Table 9. RFT measurements since M&R2015.....	18
Table 10: Average of gas saturation measurements in aquifer and the weighted average resulting in expected field averages for residual gas saturation below FWL (encircled in green). This saturation was used as a starting point and was only modified if an insufficient history match could be made.	20
Table 11. Overview of dynamic realizations. Cases 1-6 apply to all fields. The high structure cases were applied to Moddergat and Nes only.	22
Table 12. Overview of dynamic realizations. Cases 1-2 apply to all fields. The high structure cases were applied to Moddergat and Nes only.	22
Table 13. Overview of dynamic realizations during M&R 2016 for all Waddenzee fields except Nes and Vierhuizen.	23
Table 14. Overview of dynamic realizations during M&R 2016 for Vierhuizen.....	23
Table 15 Overview of dynamic realizations during M&R 2015 for Nes.	23
Table 16 Gas initially in place, BNCM.....	25
Table 17 Relative permeability uncertainty range.....	26
Table 18 History matching parameters used for the Meet & Regel cycle for Anjum.	34
Table 19 History matching parameters used for the Meet & Regel cycle for Ezumazijl.	40
Table 20 History matching parameters used for the Meet & Regel cycle for Lauwersoog C.	44
Table 21 History matching parameters used for the Meet & Regel cycle for Lauwersoog East.	49
Table 22 History matching parameters used for the Meet & Regel cycle for Lauwersoog West	55
Table 23 Permeability thickness and modifications compared to permeability thickness obtained from FBU data. Black squares indicate that these zones did not participate in the kh of the FBU.	58
Table 24 History matching parameters used for the Meet & Regel cycle for Metslawier.	62
Table 25 Water sample data from ANJ-2C in 2005.....	63
Table 26 History matching parameters used for the Meet & Regel cycle for Moddergat.....	68
Table 27 Overview of dynamic realizations Nes M&R 2015 vs 2016.....	77
Table 28 History matching parameters used for the Meet & Regel cycle for Nes.....	78
Table 29. Overview of dynamic realizations during M&R 2015 for Vierhuizen.....	81
Table 30 History matching parameters used for the Meet & Regel cycle for Vierhuizen.	82
Table 31 Changes to production (M&R2016 – M&R2015), in E6N m ³ /y.	83
Table 32 Subsidence scenarios.....	89
Table 33 Historical production (italic) + M&R 2016 Forecast volumes (E6N m ³ /y) – Normal profile....	96

APPENDIX A: IMPOSED FORECASTS BY WELL.

Table 33 Historical production (*italic*) + M&R 2016 Forecast volumes (E6N m³/y) – Normal profile

	ANJ-1	ANJ-4	ANJ-2	ANJ-3	LWO-1	LWOO Infill	LWO-2	LWO-3	MGT-1	MGT Infill	MGT-2	MGT-3	MGT-4	MGT-5	VHN-1
1997	352	293	18	0	0	0	0	0	0	0	0	0	0	0	0
1998	332	1769	532	0	0	0	0	0	0	0	0	0	0	0	0
1999	722	1223	577	76	0	0	0	0	0	0	0	0	0	0	0
2000	720	948	751	104	0	0	0	0	0	0	0	0	0	0	0
2001	784	862	664	154	0	0	0	0	0	0	0	0	0	0	0
2002	583	813	493	70	0	0	0	0	0	0	0	0	0	0	0
2003	480	651	366	65	0	0	0	0	0	0	0	0	0	0	0
2004	370	512	278	60	0	0	0	0	0	0	0	0	0	0	0
2005	272	395	209	32	0	0	0	0	0	0	0	0	0	0	0
2006	196	285	124	42	0	0	0	0	0	0	0	0	0	0	0
2007	168	218	130	53	0	0	0	0	382	0	340	0	0	0	0
2008	147	264	125	29	42	0	0	85	312	0	485	0	0	0	168
2009	89	188	18	40	271	0	0	300	454	0	540	0	0	0	309
2010	96	169	0	11	295	0	0	185	479	0	768	0	0	0	292
2011	111	137	0	44	315	0	0	187	518	0	983	0	0	0	190
2012	52	113	0	39	261	0	40	135	392	0	718	333	0	0	154
2013	0	117	0	31	215	0	37	122	406	0	813	614	0	0	132
2014	0	57	0	0	185	0	20	109	354	0	708	513	0	0	114
2015	0	68	0	21	146	1	10	82	280	0	538	392	0	0	75
2016	0	78	0	2	138	0	5	88	257	0	493	348	0	46	79
2017	0	20	0	5	143	0	6	106	254	0	441	307	0	99	80
2018	0	0	0	0	134	0	14	95	234	0	384	259	0	106	66
2019	0	44	0	22	103	0	12	68	200	0	321	206	0	85	49
2020	0	72	0	25	83	76	0	56	152	0	229	141	0	59	11
2021	0	73	0	13	107	134	0	70	154	0	220	130	0	54	0
2022	0	37	0	0	90	130	0	59	133	265	184	101	0	44	0
2023	0	67	0	0	82	110	0	60	125	74	171	91	0	40	0
2024	0	63	0	0	73	95	0	56	115	40	154	78	0	31	0
2025	0	59	0	0	65	84	0	54	108	0	143	70	0	24	0
2026	0	56	0	0	59	75	0	52	98	0	133	62	0	15	0
2027	0	52	0	0	49	68	0	44	86	0	126	56	0	12	0
2028	0	50	0	0	0	0	0	0	86	0	130	61	0	21	0
2029	0	47	0	0	0	0	0	0	79	0	123	56	0	6	0
2030	0	45	0	0	0	0	0	0	73	0	117	51	0	0	0
2031	0	42	0	0	0	0	0	0	66	0	108	44	0	0	0
2032	0	40	0	0	0	0	0	0	60	0	101	29	0	0	0
2033	0	38	0	0	0	0	0	0	56	0	96	13	0	0	0
2034	0	36	0	0	0	0	0	0	52	0	94	8	0	0	0
2035	0	34	0	0	0	0	0	0	49	0	92	0	0	0	0